Czech Technical University in Prague
Faculty of Electrical Engineering
Department of Control Engineering

Modelling and control of walking robots

Doctoral Thesis

Milan Anderle

Prague, August 2015

Ph.D. Programme: Electrical Engineering and Information Technology
Branch of study: Control Engineering and Robotics

Supervisor: Prof. RNDr. Sergej Čelikovský, CSc.

To my parents

Declaration

This doctoral thesis is submitted in partial fulfillment of the requirements for the degree of doctor (Ph.D.). The work submitted in this dissertation is the result of my own investigation, except where otherwise stated. I declare that I worked out this thesis independently and I quoted all used sources of information in accord with Methodical instructions about ethical principles for writing academic thesis. Moreover, I declare that it has not already been accepted for any degree and is also not being concurrently submitted for any other degree.

Prague, August 2015

Milan Anderle

Acknowledgements

I would like to thank, first and foremost, my supervisor, prof. Sergej Čelikovský, for his guidance and support throughout my doctoral studies and during completion of this thesis. I would also like to thank my colleagues at the Department of Control Engineering of the Faculty of Electrical Engineering at Czech Technical University in Prague and at the Department of Control Theory of the Institute of Information Theory and Automation of the Czech Academy of Sciences. Finally, I would like to express the gratitude to my parents and my girlfriend Jana for their love and patience not only during the time of my studies.

Prague, August 2015 Milan Anderle

Contents

Goals and Objectives

Topic of the thesis is the modelling and control of the underactuated walking robots. More specifically, the goals of the thesis are as follows:

1. To find mathematical models of both the continuous-time swing phase and the impulsive impact phase for Acrobot and 4-link being the simplest representatives of underactuated walking robots.

2. To design control methods for Acrobot walking including state feedback controllers and reference trajectory design based on partially linear form of Acrobot. Further, to develop methods for observer design to replace unmeasured states of Acrobot.

3. To verify stability of the newly developed tracking algorithms in the application of the feedback tracking of the reference trajectory during more steps to demonstrate the ability of Acrobot walking during a priori unlimited number of steps.

4. To extend the developed results for Acrobot, i.e. the state feedback controller, the reference trajectory and the observer design, to 4-link being a more realistic walking model.

Abstract

This thesis is focused on the design of novel methods for underactuated walking robot control in a way resembling a human walk. The methods are based on partially linear form of Acrobot as the representative of a class of underactuated walking robots. Indeed, Acrobot is the simplest underactuated walking robot theoretically able to walk. Later on, a general method is proposed enabling to extend directly results for Acrobot to any general planar n-link chain underactuated at its pivot point. This technique is referred to as the so-called generalized Acrobot embedding. By virtue of the partial linearization property it is possible to transform the original nonlinear representation of Acrobot into its partially linear form having a one-dimensional nonlinear component only. The newly obtained results include design methods for Acrobot walking, i.e. state feedback controllers, observers and planning of walking-like reference trajectories to be tracked. To be more specific, state feedback controllers are based on the knowledge of time varying entries resulting from approximate linearization of the mentioned nonlinear component along selected Acrobot walking-like reference trajectory. In one particular case of the controller design only bounds of these time varying entries are taken into the account. Alternatively, information about time varying entries including time derivative of the entries up to the order four is used. As already noted, reference trajectory design methods belong to the thesis original results as well. To accommodate the impact effect, the developed reference trajectory is also using the idea that the angular velocities at the end of the previous step and at the beginning of the next step have to be in a ratio determined by the impact properties. Next, due to the absence of the actuator at the pivot point, it is not easy to directly measure all states of Acrobot. Therefore, two algorithms to observe unmeasurable states of Acrobot were developed here based on particular knowledge of angular positions and velocities. Finally, due to its simple geometry, Acrobot is able to walk only theoretically, as it would always hit the ground by its swing leg. Therefore, the results developed for Acrobot are extended to the so-called 4-link using the above mentioned embedding method. As a matter of fact, 4-link may serve as a reasonable model of pair of legs with knees thereby providing a more realistic walking model, though without a torso.

Chapter 1

Introduction

The aim of this thesis is the design of the control strategies for the simplest underactuated walking robot, called in the literature as the Acrobot or the Compass gait biped and some extensions of these strategies to more complex walking models. Acrobot has two degrees of freedom, namely, two rigid links, and one actuator placed between them. Underactuated walking robots form a subclass of bipedal robots, however, they are usually footless. As a consequence, the angle between the ground and the leg which is in a contact with the ground is not directly actuated. One can simply imagine the locomotion of the underactuated walking robot like a walk of a human on his/her stilts.

Underactuated walking robots present a particular case of underactuated mechanical systems, which are, in general, mechanical systems with actuators having less actuators than the number of degrees of freedom. An efficient control of underactuated mechanical systems is a challenging task of last decades by virtue of their broad application domain in real-life systems including robotics, e.g. mobile or walking robots, aerospace vehicles like aircrafts, spacecrafts, helicopters or satellites, marine vehicles like submarines or swimming robots, see [104, 115]. In the literature, one can find various examples of underactuated mechanical systems. Among the simplest ones are e.g. cart pole system, Furuta pendulum, convey-crane system, Pendubot, Acrobot, reaction wheel pendulum, ball and beam system etc., for details see [39].

As already noted, the typical representatives of the underactuated mechanical systems are Acrobot and Pendubot. Despite the fact that the representative systems feature, indeed, the elementary design, they possess nonlinearities which implicate their effective control as a challenging task of recent decades. Among the first results in this field are McGeer's passive walker [85], Fukuda's brachiation robot [107, 108], Acrobot [21, 89] or Pendubot [2, 40, 121]. Of course, it is not enough to develop an efficient control of representatives systems or systems mentioned above only, however, occasionally it is possible to convert a real system under some assumptions, simplifications or embedding

methods into already mentioned underactuated systems or similar systems. That is why their efficient control is worth studying.

Recently, numerous works have addressed the stabilization of Acrobot inverted position and extending its domain of attraction, see [21, 89]. However, slightly more challenging task is a swing up control, i.e. to move Acrobot from its downward stable position, or stable equilibrium, to its upward unstable position, or unstable equilibrium, and control Acrobot in its upward position. The first results in this field were demonstrated using inverted pendulum [43, 132] whereas the swing up control of Acrobot was done in [118, 119]. It was shown in [114] that the fully actuated robots are exact feedback linearizable whereas it was shown in [116, 117] that the method of partial feedback linearization [59] is applicable for Acrobot control.

Indeed, the partial feedback linearization method based on a change of coordinates that transforms the original nonlinear system into a partially linear system appears convenient for underactuated mechanical systems control. In the literature [116, 117], one can find two application examples of partial feedback linearization applied to Acrobot. The first one, called collocated linearization, is based on the output equation related to the actuated angle, whereas the second one, called non-collocated linearization, is based on the output equation related to the underactuated angle. The non-collocated linearization is possible under a special condition on a inertia matrix called strong inertia coupling, see [115, 116].

The related non-collocated linearization property is valid only for a restricted class of underactuated systems, therefore, a classification of underactuated mechanical systems into classes with identical properties were introduced. By virtue of the classification, a control technique developed for a system within one class can be simply adapted to any other system which belongs to the same class. It was shown in [95, 96], that underactuated mechanical systems can be divided into eight classes based on stabilization. In [81, 135] one can find different classification based on a full linearizability. Another classification based on mechanical properties is given in [78].

1.1 State of the art

In this section, a brief introduction into history of bipedal robots is presented at first to show that walking robots research topic has been of deep interest for quite some time. Secondly, the current state of the art in control of underactuated walking robot is presented.

1.1.1 Brief history of robotic in walking

From the historical point of view, the first reference to a legged locomotion was done by Aristotle 350 B.C. in his work *Progression of Animals* [16]. One of the first researchers who focused on the design of various robotic systems and actually enhanced robotics into science was Leonardo do Vinci. Nevertheless, the first actual legged mechanisms are the *Mechanical Horse* patented in 1893 by L.A. Ryggs [106, 111] and the *Steam Man*, a biped machine, proposed in 1893 by Georges Moore, see [111]. Moreover, the Steam Man is probably the first really constructed biped able to walk. In [93] one can find a detailed description of historical evolution of walking robotic systems. Since the Mechanical Horse or the Steam Man the research on legged robot locomotion has grown into a multidisciplinary field involving physiology, classical mechanics, computer science, control theory and general robotics. To give a short introduction to this field, a few of pioneering legged robot prototypes will be described. For more extensive and more detailed list see [93, 111, 130].

One of the earliest legged machine able to walk is the quadrupedal *General Electric Walking Truck*, also know as the *General Electric Quadruped*, constructed by Mosher [77] in the 1960s. This vehicle was over 3 m by 3 m in its size and weighted 1400 Kg. It required an external power source to drive its hydraulic actuators. It carried a single operator who was responsible for controlling each of twelve servo loops that controlled legs. It was capable of a top speed of 2.2 m/s and could carry 220 kg payload. The General Electric Quadruped has demonstrated capabilities of walking machines, i.e. easy overcoming of obstacles or good movement in a terrain. Nevertheless, it was clear that automatic control system instead of an operator is essential for such legged machine control. The first four leg walking robot, called as *Phony Pony*, fully controlled by an automatic control system was built by McGhee and Frank in 1966, see [112].

The first biped able to walk called *WAP-1* was developed by Kato in 1969. Kato continued in the research and in 1970 he developed *WAP-2*. A movement of WAP-2 was significantly faster than movement of WAP-1. Moreover, in 1971 Kato developed *WAP-3*. WAP-3 was able to move in the three-dimensional way as the first biped in the world at all.

In addition to these pioneering machines, there have been a lot of other prototypes developed in recent years. Many prototypes of bipedal walking robots differing in structure, degrees of freedom, walking capabilities or control and analysis of bipedal gaits were built. For more complete treatments of legged machine history see [19, 34, 70, 93, 103, 105, 112, 125, 127].

Among others, the most word-wide famous bipeds to-date are *ASIMO* developed by the Honda Corporation [36, 55], *Robonaut 2*, designed jointly by NASA's Johnson Space

Center and General Motors [37], *Atlas* - The Agile Anthropomorphic Robot developed by Boston Dynamics, *WABIAN-2* of Waseda University [53, 94] or Humanoid robot *HRP-4* developed by the National Institute of Advanced Industrial Science and Technology (AIST) [65]. These robots are capable of walking, running at certain speeds and moving in a rough terrain. Moreover, they can use their hands to manipulate objects.

However, only a few prototypes were built in the field of the underactuated walking robots. Probably the first underactuated biped able to walk down the slope was a passive walker constructed by McGeer [85]. He showed that a simple planar mechanism with two legs could be made to steadily walk down a slight slope with no other energy input or control. This system acts like two coupled pendulums. The stance leg acts like an inverted pendulum and the swing leg acts like a free downward pendulum attached to the stance leg at the hip. With sufficient mass at the hip the system has a stable limit cycle, that is, a nominal trajectory that repeats itself and returns to this trajectory even if slightly perturbed. A natural extension of the two-segment passive walker includes knees, which provide natural ground clearance without need for any additional mechanisms. It is shown in [86] that even with knees the system has a stable limit cycle. As a matter of fact, McGeer built a four-link planar passive walker. This mechanism featured locking knees to prevent leg collapse and circular feet to give a rolling ground contact. It weighted 3.5 Kg, was 0.5 m tall and could stably walk down the 1.4 degree slope at about 0.4 m/s. The McGeer's mechanism was duplicated in [44] and detailed analysis of its dynamics was performed together with dynamics of several passive walkers with similar morphologies. It is shown in [47] that a two-link planar passive walker with prismatic legs can also exhibit stable gaits. By adding a torque acting between legs and adding a control to regulate the biped's total energy, it is possible to increase the set of initial conditions from which solutions converge to the stable gait.

A two-legged passive walker in 3-D is analyzed in [71]. This system is similar to the McGeer's original walker, except that it has an extra degree-of-freedom allowing for side-to-side rocking. There is no stable limit cycle, although the stability of its planar motion is preserved. The instability is in a single mode, similar to an inverted pendulum unstable mode. A three-dimensional version of the McGeer's passive walker is presented in [35]. This passive walker weighted 4.8 Kg and measured 0.85 m in height. With carefully designed feet and pendular arms, it was able to walk down the 3.1 degree slope at about 0.5 m/s.

Last but not least, the so-called *Rabbit* and *MABEL* are listed here as the most famous examples of the current prototypes of the underactuated walking robots. Rabbit is the five-link planar bipedal walker constructed in 1999 by a group of several French research laboratories and the University of Michigan, see [130]. MABEL is a planar bipedal robot

comprised of five links assembled to form a torso and two legs terminated in point feet with knees, see [50]. MABEL was constructed in 2008 as a result of collaboration of the University of Michigan and the Robotic Institute of Carnegie Mellon University. Main difference between the Rabbit and the MABEL consists in the location of the actuators. MABEL's actuators are located in the torso, and, moreover, actuated degrees of freedom of each leg are not equivalent to angles in knees or in the hip, see [50]. The brand new construction of the MABEL facilitates not only a stable walking but also a running.

1.1.2 Control of biped robot locomotion

The control of a biped robot locomotion has been studied over few decades and yet it is not satisfactory solved by now. A detailed survey of an initial research on the biped robot locomotion topic can be found e.g. in [127, 128]. One of the common approaches of the biped robot control consists in a tracking of a precomputed reference trajectory. Nevertheless, many studies corresponding to a ballistic motion of the robot based on pointwise ground contact were published, see e.g. [45, 47, 85]. The reference trajectory to be tracked can be determined in various ways, e.g. to be equivalent to a reference system, like a human or a passive system able to move in a desired way [124, 126]. Moreover, the reference trajectory can be found as a result of optimization of some cost criterion, see e.g. [32, 33, 38, 52]. By virtue of the reference trajectory, standard tracking methods can be used. A tracking via a PID controller was proposed in [1, 42, 99] whereas a computed torque method or a sliding mode control were proposed e.g. in [31, 66, 82, 99, 102].

In contrast to a common approach based on a reference trajectory tracking a completely different approach based on building in desired system's dynamics via a set of constraining functions with desired dynamics is widely used in walking robot control. This idea was for the first time presented in [103] and expanded by Koditschek in [25, 26, 91, 110] later on. This approach was exploited e.g. in [41, 57, 60, 62, 90] as well.

An alternative biped control technique to a reference trajectory tracking is a technique based on total energy control or angular momentum control demonstrated e.g. in [47, 57, 58, 61, 97, 98, 100, 101, 109]. This control mode is the first stage of the control approach based on constraining functions with desired dynamics.

However, it was not possible to obtain any rigorous stability proof of biped control using the above cited control approaches. Therefore, in [49] a new control strategy based on virtual constraints approach was designed in such a way that facilitates application of the method of Poincaré sections. Exponentially stable controllers for biped robots were designed in [131] by virtue of newly defined concept of hybrid zero dynamics. The hybrid zero dynamics is an extension of the well-known zero dynamics [59] taking into

the account the impact map. The zero dynamics of the swing phase modelled by ordinary differential equations was studied e.g. in [18, 84, 119].

It was shown in [123] that biped dynamics can be represented by a partially linear model by virtue of suitable choice of coordinates. In [27] a construction of scalar functions depending on configuration variables with appropriate relative degrees was shown, moreover, the functions were used to control an underactuated biped in single support phase. This result was extended in [51] where it was shown that if the generalized momentum conjugate to the cyclic variable is not conserved (as it is the case of Acrobot) then there exists a set of outputs that define one-dimensional exponentially stable zero dynamics. The change of coordinates defined in [29, 30, 136] which results in a partial feedback form of Acrobot is extension of results in [27, 51, 96]. The partially linear form of Acrobot presented in [29, 30, 136] is the crucial one for new results presented in this thesis later on.

Control approaches briefly compiled in the previous paragraphs are based on the measurements of all necessary robot's states. However, this assumption is rarely fulfilled in real applications of the underactuated biped walking. Due to that fact, some research has been done to cope with this problem, namely, the observer design for estimation of angular positions and angular velocities from available measurement. However, there are very few results in the field of the observer design in contrast to the field of the biped walking control, especially in the area of observers based on nonlinear techniques. Kalman filter was designed for angular velocities estimation from angular positions measurement in [87]. A high gain observer [20], that estimates the absolute angular positions and velocities of a biped robot using a measurement of the actuated relative angular positions only is suggested in [72]. An observer based on the second order sliding mode approach is suggested in [74] to determine absolute angular positions and velocities based on relative angular positions measurements only. Furthermore, the observer based on the step-by-step higher order sliding mode approach [22] is suggested in [73, 75, 76]. Last but not least, observers for the biped robot based both on fuzzy and on disturbance alternation approach can be found in the literature as well.

Despite the fact that many results were published in the field of reliable and economic walking or running of bipeds, no complete solution has been found yet. Therefore, the underactuated biped control topics are worth further wider and deeper research.

1.2 Goals of the thesis and methods to achieve them

The main goal of the thesis is to study the novel methods of the underactuated walking robots control using intrinsically nonlinear techniques in order to improve the existing

control approaches. More specifically, a movement of Acrobot in a way resembling a human walk based on partially exact feedback linearized form of Acrobot will be analyzed. In this sense, the thesis will continue in a research initiated in [30, 133, 134, 136] where the exact partial feedback linearization of order 3 of Acrobot was introduced. For the purpose of Acrobot movement, the feedback controller and the walking trajectory to be tracked will be design based on partially linear form of Acrobot as well. Moreover, an observer for unmeasured states of Acrobot will be designed in order to apply the developed results on a real model of an underactuated walking robot in the future. Acrobot is able to walk theoretically only because his leg would stumble upon the ground during the step. Therefore, "knees" will be added into "legs" and results developed for Acrobot will be extended to the so-called 4-link.

These goals will be achieved using both theoretical analysis of nonlinear control methods and systematic and extensive numerical simulations and experiments.

1.3 The main contribution of the thesis

The main contribution of the thesis aims to develop the novel techniques of the feedback tracking of the reference trajectory to move Acrobot in a way resembling a human walk. By virtue of the partial linearization property of Acrobot it is possible to transform the nonlinear representation of Acrobot into its partially linear form with a one-dimensional nonlinear component only. The newly developed state feedback controllers are based on a more or less deeper knowledge of time varying entries resulting from approximate linearization of the mentioned nonlinear component along selected Acrobot reference trajectory. The developed reference trajectory uses the idea that the angular velocities at the end of the previous step and at the beginning of the next step have to be in a ratio determined by the impact properties. The control approach based on the reference trajectory tracking using the developed feedback controller minimizes errors arisen from some tenuous inaccuracies during the step. In contrast to another control methods based on a numerical approach where the robot is "pushed forward" from previously exactly computed initial conditions in order to finish the step in desired time and configuration, our methods using the feedback controllers during the swing phase are more robust against disturbances and, moreover, these methods are simpler when extended to more complicated walking structures. Finally, the developed feedback controllers and walking trajectories are supplemented by the estimator in order to apply the control approach to a real laboratory model of walking robot with point feet in the future. Acrobot is able to walk only theoretically due to its simple geometry. As a matter of fact, it would always hit the ground by its swing leg. Therefore, the results originally developed for Acrobot

are extended to a more realistic model of walking robot, to the so-called 4-link which resembles pair of legs with knees and without a body or even a torso.

1.4 Organization of the thesis

The rest of the thesis is organized as follows. Chapter 2 introduces some preliminary knowledge about modelling of walking robots. Chapter 3 presents the exact partial feedback linearization method and introduces the partially linear form of Acrobot. It also introduces the concept of the embedding of the so-called generalized Acrobot into 4-link. Chapters 4 to 7 presents the novel contribution of the thesis. More specifically, Chapter 4 presents the trajectory design for Acrobot, while Chapter 5 presents various state feedback controllers exponentially tracking Acrobot target trajectory based on the partial feedback linearization approach. Extension of these results to the 4-link case using the mentioned embedding technique is provided as well. Two nonlinear observers for Acrobot are presented in Chapter 6. In Chapter 7 stability tests of Acrobot walking controlled by feedback controllers from Chapter 5 combined with the impact effect during many steps are provided. Finally, thesis results are summarized in Chapter 8 together with the outlooks for future research.

Chapter 2

Modelling of the n-link underactuated mechanical systems

Mathematical models of two underactuated walking robot structures are derived in this chapter. These models include both the so-called swing phase and the impact map of angular velocities at the impact moment. One can find many models of underactuated mechanical systems in the literature, see e.g. in [54, 124] for survey. Some information is repeated here in order to keep the thesis self-contained.

More specifically, the so-called Acrobot and 4-link are considered here, see Figures 2.1a, 2.1b. These mechanical systems have similar structures. They are special cases of the n-link chain with $n-1$ actuators between them supported at one of its ends at a pivot point on a flat surface. Acrobot is the 2-link with two degrees of freedom (DOF) and with one actuator placed between these links, therefore, it is perhaps the simplest underactuated mechanical system. The 4-link is, roughly speaking, Acrobot with knees. It consists of four links with three actuators between them. In both cases the point where these structures touch the ground is not actuated. In other words, both of them belong to the class of underactuated walking robots.

Both Acrobot and 4-link are typical representatives of the so-called Lagrangian hybrid systems, i.e. mechanical systems, described by the Lagrangian approach, with a collision or, in other words, with an impact, which causes a discontinuous change in angular velocities while angular positions remain continuous. Indeed, both mechanical systems have continuous-time and discrete-time phases of their dynamics. The continuous-time phase is described by the system of differential equations whereas the discrete-time phase is described by the algebraic map. Both dynamics are covered by the general hybrid

system model in the following form

$$\dot{x} = F(x,u), \qquad x \in C(x), \tag{2.1}$$

$$x^+ = G(x^-,u), \qquad x \in D(x), \tag{2.2}$$

where $x \in \mathbb{R}^n$, $F(x)$ and $G(x)$ are smooth functions, $C(x)$ and $D(x)$ are subsets of $\mathbb{R}^n$ and u is an input. Moreover, $C(x) \cup D(x) = \mathbb{R}^n$ and x^-, x^+ stand for the system state just before and just after the impact, respectively. Trajectory of the model (2.1), (2.2) starting from the initial condition $x(t_0) = x_0 \in C(x)$ is determined as follows: for $x(t) \in C(x(t))$ it is a solution of the ordinary differential equation (2.1). When $x(\bar{t}\,) \in D(x(\bar{t}\,))$, for some $\bar{t}$, it continues as another solution of (2.1) denoted $\tilde{x}(t)$, $t \geq \bar{t}$, having the "re-set" initial condition $\tilde{x}(\bar{t}\,) = G(x(\bar{t}\,),u)$. General hybrid model (2.1), (2.2) describes wide variety of systems. In addition to mechanical systems with collision, one can mention e.g. switching systems, hybrid system automata, discrete events in biological systems etc.

Acrobot depicted in Figure 2.1a has two "legs" with only one actuator placed between them. 4-link depicted in Figure 2.1b has two "legs" as well, moreover, both legs have a "knee". Acrobot or 4-link walking consists of the continuous part, i.e. when one leg, usually called *swing leg* is in the air and of the impulsive part which occurs when the swing leg hits the ground. For the sake of completeness, the second leg which is in contact with the ground during the step is usually called as the *stance leg*.

The continuous part, when the swing leg is in the air, is modelled by the well-known Lagrangian approach and it is usually called in the literature as the swing-phase. During the swing-phase the configuration of Acrobot or 4-link is described by generalized coordinates q and it is bounded by an one-sided constraint as two solid bodies cannot penetrate each other. In our case, that limitation means that the swing leg cannot go under the ground, i.e. the height of the swing leg's end-point has to be $h_{endpoin}(q) \geq 0$. The next section will present the derivation of the dynamical model for Acrobot and 4-link in detail.

When the swing leg hits the ground, i.e. $h_{endpoint}(q) = 0$, the so-called impact occurs. The result of this event is an instantaneous jump of angular velocities $\dot{q}$ while angular positions q remain continuous. The impact is modelled as a contact between two rigid bodies. To derive the impact mapping, the so-called extended inertia matrix $D_e(q_e)$ plays a crucial role. Detailed derivation of the impact model for Acrobot and for 4-link will be presented in the second part of this chapter. The event when the swing leg touches the ground is in the literature usually referred to as the so-called double-phase.

Integration of continuous-time and discrete-time phases into the general model of hybrid systems (2.1), (2.2) is surveyed e.g. in [10, 49, 131].

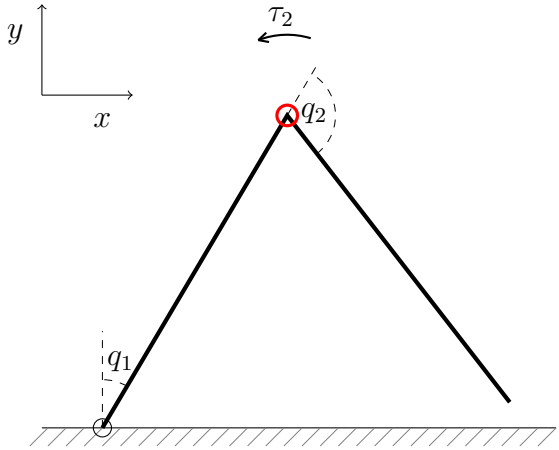

Figure 2.1a. Acrobot

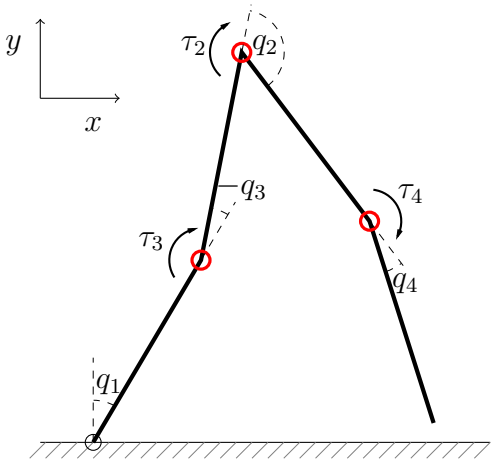

Figure 2.1b. 4-link

2.1 Dynamical model of the 2-link and the 4-link mechanical system

The well-known Euler-Lagrangian approach, see [39, 48, 113] will be used here. First, define Lagrangian $\mathcal{L}(q, \dot{q})$ given by the difference between kinetic $\mathcal{K}$ and potential $\mathcal{P}$ energy of the modelled mechanical system

$$\mathcal{L}(q, \dot{q}) = \mathcal{K} - \mathcal{P}. \tag{2.3}$$

Kinetic energy $\mathcal{K}$ of a rigid link can be computed as the sum of kinetic energy of the rotation movements and kinetic energy of the translation movements. For the purpose of simplification, the entire mass of the rigid link is supposed to be concentrated in the center of mass of the link. In this case, kinetic energy of the rigid link is expressed as follows

$$\mathcal{K} = \frac{1}{2} m v^{\mathrm{T}} v + \frac{1}{2} \omega^{\mathrm{T}} \mathcal{I} \omega, \tag{2.4}$$

where m is total mass of the rigid link, v and ω are linear and angular velocity vectors, respectively, and $\mathcal{I}$ is the symmetric 3×3 and positive definite inertia matrix. Linear and angular velocity vectors and the inertia matrix are expressed with respect to a predefined inertia frame. Potential energy $\mathcal{P}$ of a rigid link can be computed as follows

$$\mathcal{P} = mgh, \tag{2.5}$$

where h is height of the center of mass of the link.

A general set of differential equations describing the time evolution of Acrobot or 4-link is obtained as follows. Let the underactuated angle at the pivot point be denoted as q_1, then the Euler-Lagrange equations give

$$\begin{bmatrix} \frac{d}{dt}\frac{\partial \mathcal{L}}{\partial \dot{q}_1} - \frac{\partial \mathcal{L}}{\partial q_1} \\ \frac{d}{dt}\frac{\partial \mathcal{L}}{\partial \dot{q}_2} - \frac{\partial \mathcal{L}}{\partial q_2} \\ \vdots \\ \frac{d}{dt}\frac{\partial \mathcal{L}}{\partial \dot{q}_n} - \frac{\partial \mathcal{L}}{\partial q_n} \end{bmatrix} = u = \begin{bmatrix} 0 \\ \tau_2 \\ \vdots \\ \tau_n \end{bmatrix}, \tag{2.6}$$

where u stands for the vector of the external controlled forces. System (2.6) is the so-called underactuated mechanical system having the degree of the underactuation equal to one. Equation (2.6) leads to the dynamical equation in the form

$$D(q)\ddot{q} + C(q,\dot{q})\dot{q} + G(q) = u, \tag{2.7}$$

where $D(q)$ is the inertia matrix, $D(q) = D(q)^{\mathrm{T}} > 0$, $C(q,\dot{q})$ contains Coriolis and centrifugal terms, $G(q)$ contains gravity terms and u stands for the vector of external forces.

For the simplicity, the dynamical model of the mechanical system with rigid links and without friction is considered here. Moreover, the rigid links are simplified into the massless links with their whole masses placed in the center of mass of the corresponding link. See Figure 2.2 for link's length specifications for Acrobot. Notations and link's length specifications for 4-link are analogous.

The way of acquiring the equations for kinetic and potential energy of Acrobot or 4-link is based on the approach described in [113]. The advantage of that approach consists in its straightforward expandability to the case of general n-link system. In the following subsection, the model of Acrobot is derived in detail, while Subsection 2.1.2 will be focused on the model of 4-link.

2.1.1 Dynamical model of Acrobot

First of all, define the rotational matrices between two frames. The so-called base frame is the frame related to the horizontal and the vertical direction. Rotational matrix between the base frame and the first link orientation is denoted as R_1^0, while the one between the first link orientation and the second link orientation is denoted as R_2^1. One has that:

$$R_1^0 = \begin{bmatrix} \sin q_1 & -\cos q_1 & 0 \\ \cos q_1 & \sin q_1 & 0 \\ 0 & 0 & 1 \end{bmatrix}, \quad R_2^1 = \begin{bmatrix} \cos q_2 & \sin q_2 & 0 \\ -\sin q_2 & \cos q_2 & 0 \\ 0 & 0 & 1 \end{bmatrix}, \tag{2.8}$$

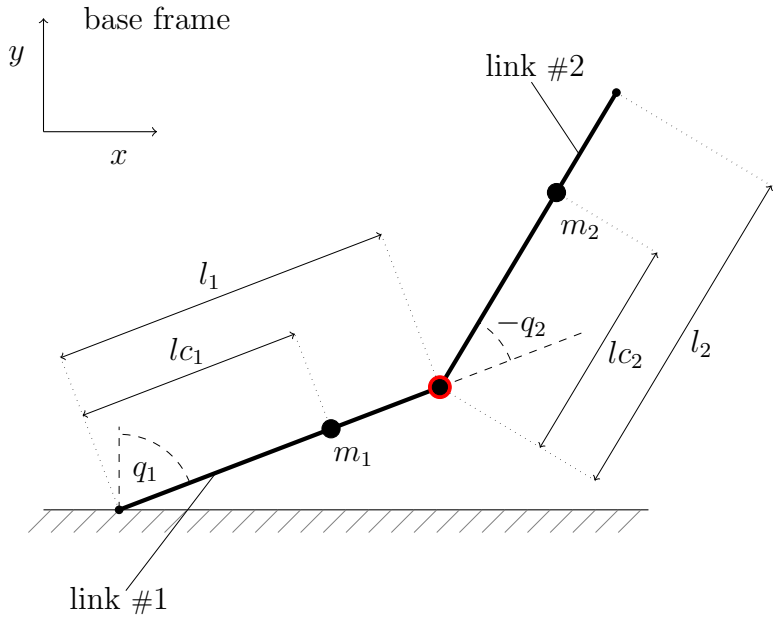

Figure 2.2. Geometry of Acrobot

see Figure 2.2 for the definition of angles q_1 and q_2. The rotational transformation between the base frame and the second link is then given by

$$R_2^0 = R_1^0 \, R_2^1 \,. \tag{2.9}$$

The absolute value of angular velocities between the base frame and the first link and between the first link and the second link are denoted by $\dot{q}_1$ and $\dot{q}_2$, respectively. Vectors of these angular velocities are expressed as follows

$$\omega_{0\,1}^0 = \begin{bmatrix} 0 & 0 & \dot{q}_1 \end{bmatrix}^{\mathrm{T}}, \quad \omega_{1\,2}^1 = \begin{bmatrix} 0 & 0 & \dot{q}_2 \end{bmatrix}^{\mathrm{T}}. \tag{2.10}$$

Here the upper index corresponds to the frame where the angular velocity is defined while the bottom indices represent two frames that rotate each with respect to other. The angular velocity $\omega_{1\,2}^1$ is expressed in the base frame using the rotational matrix R_1^0 as follows

$$\omega_{1\,2}^0 = \omega_{0\,1}^0 + R_1^0 \omega_{1\,2}^1 = \begin{bmatrix} 0 & 0 & \dot{q}_1 + \dot{q}_2 \end{bmatrix}^{\mathrm{T}}. \tag{2.11}$$

The next step is to express the translational velocity of the center of mass of the first link v_{c1}^0 and the translational velocity of the end of the first link v_1^0. Generally, the translational velocity of a point on a rotational link is given by the vector product of the vector of angular velocity of the link ω and radius vector of a point on the link r. Therefore, the translational velocity is given by $v = \omega \times r$. In the case of the first link,

the position vector of the end point r^1_{p1} and the position vector of the center of mass r^1_{c1} are expressed in coordinates of the first link, therefore they have the following form

$$r^1_{p1} = \begin{bmatrix} l_1 & 0 & 0 \end{bmatrix}^{\mathrm{T}}, \quad r^1_{c1} = \begin{bmatrix} l_{c1} & 0 & 0 \end{bmatrix}^{\mathrm{T}}.$$

Using the rotational matrix R^0_1 it is easy to obtain expression of the position vectors in base frame coordinates as follows

$$r^0_{p1} = R^0_1\, r^1_{p1}, \quad r^0_{c1} = R^0_1\, r^1_{c1}.$$

The analogous position vectors can be expressed for the second link

$$r^0_{p2} = R^0_2\, r^2_{p2} = R^0_2 \begin{bmatrix} l_2 & 0 & 0 \end{bmatrix}^{\mathrm{T}}, \quad r^0_{c2} = R^0_2\, r^2_{c2} = R^0_2 \begin{bmatrix} l_{c2} & 0 & 0 \end{bmatrix}^{\mathrm{T}}. \tag{2.12}$$

Finally, the translational velocity v^0_{c1} of the center of mass of the first link can be expressed as follows

$$v^0_{c1} = v^0_1 + \omega^0_{0\,1} \times r^0_{c1}, \tag{2.13}$$

where v^0_1 is equal to zero because it means the velocity of the base frame and the remaining entries $\omega^0_{0\,1}$ and r^0_{c1} were defined earlier. The translational velocity v^0_{c2} of the center of mass of the second link is expressed in the coordinates connected with the base frame as follows

$$v^0_{c2} = v^0_2 + \omega^0_{1\,2} \times r^0_{c2}, \tag{2.14}$$

where v^0_2 is equal to the translational velocity of the initial point of the second link, namely $v^0_2 = \omega^0_{0\,1} \times r^0_{p1}$, and the remaining entries $\omega^0_{1\,2}$ and r^0_{c2} were defined earlier.

In such a way, all necessary parameters for computation of kinetic and potential energy are known. General expression for kinetic and potential energy of the rigid rod is shown in (2.15) and in (2.16). The final expression for the kinetic energy of Acrobot has the following form

$$\mathcal{K} = \frac{1}{2} m_1 (v^0_{c1})^{\mathrm{T}} v^0_{c1} + \frac{1}{2} (\omega^0_{0\,1})^{\mathrm{T}} \mathcal{I}_1 \omega^0_{0\,1} + \frac{1}{2} m_2 (v^0_{c2})^{\mathrm{T}} v^0_{c2} + \frac{1}{2} (\omega^0_{1\,2})^{\mathrm{T}} \mathcal{I}_2 \omega^0_{1\,2} \tag{2.15}$$

and the final expression for the potential energy of Acrobot has the form as follows

$$\mathcal{P} = m_1 g l_{c1} \cos(q_1) + m_2 g \left(l_1 \cos(q_1) + l_{c2} \cos(q_1 + q_2) \right). \tag{2.16}$$

After substitution of equations for kinetic (2.15) and potential energy (2.16) into Lagrangian equation (2.3) it is possible to determine Euler-Lagrangian equations (2.6). The complete first line of Euler-Lagrange equations is as follows

$$\begin{aligned} 0 \;=\; & \left(m_1 l_{c1}^2 + m_2 l_1^2 + I_{1zz} + m_2 l_{c2}^2 + I_{2zz} + 2 m_2 l_1 l_{c2} \cos q_2 \right) \ddot{q}_1 + \\ & \left(m_2 l_{c2}^2 + I_{2zz} + m_2 l_1 l_{c2} \cos q_2 \right) \ddot{q}_2 + 2 m_2 l_1 l_{c2} \sin q_2 \dot{q}_1 \dot{q}_2 + m_2 l_1 l_{c2} \sin q_2 \dot{q}_2^2 - \\ & m_2 l_{c2} g \sin(q_1 + q_2) - (m_2 l_1 + m_1 l_{c1})\, g \sin q_1, \end{aligned} \tag{2.17}$$

where the zero at the left hand side of the equation expresses the absented actuator at the pivot point. The complete second line of Euler-Lagrange equations is as follows

$$\tau_2 = \left(m_2 l_{c2}^2 + I_{2zz} + m_2 l_1 l_{c2} \cos q_2\right) \ddot{q}_1 + \left(m_2 l_{c2}^2 + I_{2zz}\right) \ddot{q}_2 - m_2 l_1 l_{c2} \sin q_2 \dot{q}_1^2 - m_2 l_{c2} g \sin(q_1 + q_2). \tag{2.18}$$

The following material parameter equations to be substituted into (2.17) and (2.18) are introduced in [39]

$$\begin{aligned} \theta_1 &= m_1 l_{c1}^2 + m_2 l_1^2 + I_{1zz}, \quad \theta_2 = m_2 l_{c2}^2 + I_{2zz}, \\ \theta_3 &= m_2 l_1 l_{c2}, \quad \theta_4 = m_1 l_{c1} + m_2 l_1, \quad \theta_5 = m_2 l_{c2}, \end{aligned} \tag{2.19}$$

where m_1, m_2 is the mass of the link #1, #2, respectively, l_1, l_2 is length of the link #1, #2, respectively, l_{c1}, l_{c2} is the distance to the center of mass of the link #1, #2, respectively, I_{1zz}, I_{2zz} is the moment of inertia around z-axes of the link #1, #2, respectively, about its center of mass, g is gravity acceleration, q_1 is the angle that the link #1 makes with the vertical, q_2 is the angle that the link #2 makes with the link #1, τ_2 is torque applied at the joint between links #1 and #2.

Equations (2.17) and (2.18) can be rewritten using the material parameters (2.19) into the following standard matrix form for mechanical systems (2.7), see e.g. [39]

$$D(q)\ddot{q} + C(q, \dot{q})\dot{q} + G(q) = u,$$

where

$$D(q) = \begin{bmatrix} \theta_1 + \theta_2 + 2\theta_3 \cos q_2 & \theta_2 + \theta_3 \cos q_2 \\ \theta_2 + \theta_3 \cos q_2 & \theta_2 \end{bmatrix}, \tag{2.20}$$

$$C(q, \dot{q}) = \begin{bmatrix} -\theta_3 \sin q_2 \dot{q}_2 & -(\dot{q}_1 + \dot{q}_2)\theta_3 \sin q_2 \\ \theta_3 \sin q_2 \dot{q}_1 & 0 \end{bmatrix}, \tag{2.21}$$

$$G(q) = \begin{bmatrix} -\theta_4 g \sin q_1 - \theta_5 g \sin(q_1 + q_2) \\ -\theta_5 g \sin(q_1 + q_2) \end{bmatrix}. \tag{2.22}$$

Recall, that the 2-dimensional configuration vector (q_1, q_2) is defined in Figure 2.1a and it is slightly different that one defined in [39].

For Acrobot these computations lead to the second-order nonholonomic constraint and the kinetic symmetry, i.e. the inertia matrix depends only on the second variable q_2. The kinetic symmetry plays crucial role in the partial exact feedback linearization approach introduced in Subsection 3.1.3 later on.

2.1.2 Dynamical model of 4-link

The approach presented in the previous section can be extended to the 4-link system. As a matter of fact, it is just needed to add rotation matrices between the second and the third link and between the third and the fourth link R_3^2, R_4^3, respectively:

$$R_3^2 = \begin{bmatrix} \cos q_3 & \sin q_3 & 0 \\ -\sin q_3 & \cos q_3 & 0 \\ 0 & 0 & 1 \end{bmatrix}, \quad R_4^3 = \begin{bmatrix} \cos q_4 & \sin q_4 & 0 \\ -\sin q_4 & \cos q_4 & 0 \\ 0 & 0 & 1 \end{bmatrix}, \tag{2.23}$$

where the angles q_3 and q_4 are defined in Figure 2.1b. The rotational transformations between the base frame and the third link and between the base frame and the fourth link are given by

$$R_3^0 = R_1^0\, R_2^1\, R_3^2, \quad \text{and} \quad R_4^0 = R_1^0\, R_2^1\, R_3^2\, R_4^3, \quad \text{respectively.} \tag{2.24}$$

Moreover, it is necessary to define angular velocities between the second and the third link $\omega_{2\,3}^2$ and between the third and the fourth link $\omega_{3\,4}^3$. Their expression in the base frame is done by an equation analogous to (2.11) with the appropriate rotational matrices R_3^0 and R_4^0 instead of R_1^0.

Furthermore, position vectors of the center of mass has to be determined. It means, to define position vectors r_{c3}^3, r_{c4}^4 and their expression in the base frame coordinates, r_{c3}^0, r_{c4}^0 according to equation (2.12) with the appropriate rotational matrices.

The last computation which has to be done to express the Lagrangian is to find translational velocity of the center of mass of appropriate links v_{c3}^0 and v_{c4}^0 according to equations (2.13) or (2.14).

After all previous computations, it is now possible to write down the expression for kinetic energy of 4-link in the following form

$$\begin{aligned} \mathcal{K} = {} & \frac{1}{2} m_1 (v_{c1}^0)^{\mathrm{T}} v_{c1}^0 + \frac{1}{2} (\omega_{0\,1}^0)^{\mathrm{T}} \mathcal{I}_1 \omega_{0\,1}^0 + \frac{1}{2} m_2 (v_{c2}^0)^{\mathrm{T}} v_{c2}^0 + \frac{1}{2} (\omega_{1\,2}^0)^{\mathrm{T}} \mathcal{I}_2 \omega_{1\,2}^0 + \\ & \frac{1}{2} m_3 (v_{c3}^0)^{\mathrm{T}} v_{c3}^0 + \frac{1}{2} (\omega_{0\,3}^0)^{\mathrm{T}} \mathcal{I}_3 \omega_{0\,3}^0 + \frac{1}{2} m_4 (v_{c4}^0)^{\mathrm{T}} v_{c4}^0 + \frac{1}{2} (\omega_{1\,4}^0)^{\mathrm{T}} \mathcal{I}_4 \omega_{1\,4}^0. \end{aligned} \tag{2.25}$$

The final expression for potential energy of 4-link has following form

$$\begin{aligned} \mathcal{V} = {} & m_1 g l_{c1} \cos(q_1) + m_2 g \left(l_1 \cos(q_1) + l_{c2} \cos(q_1 + q_3) \right) + m_3 g l_1 \cos(q_1) + \\ & m_3 g \left(l_2 \cos(q_1 + q_3) + l_{c3} \cos(q_1 + q_3 + q_2) \right) + m_4 g l_1 \cos(q_1) + \\ & m_4 g \left(l_2 \cos(q_1 + q_3) + l_3 \cos(q_1 + q_3 + q_2) + l_{c4} \cos(q_1 + q_3 + q_2 + q_4) \right). \end{aligned} \tag{2.26}$$

After substitution of equations for kinetic energy (2.25) and potential energy (2.27) into Lagrangian equation (2.3) it is possible to determine four Euler-Lagrangian equations (2.6). Nevertheless, for brevity neither their form nor final model matrices $D(q)$, $C(\dot{q}, q)$, $G(q)$ are given here in detail.

2.2 The impact model

The impact occurs when the swing leg hits the walking surface. The impact mapping is important for the design of the multi-step walking reference trajectory because it changes discontinuously angular velocities of the swing and the stance leg at the end of the step while the angular positions remain continuous. The idea of using the impact map during the reference trajectory design is shown in detail in Section 4.2 later on.

The methods to obtain the impact model for Acrobot or for 4-link are similar for both models. Therefore, the description how to obtain the impact model will be given in a general way and detailed illustration will be provided using the Acrobot model. The impact model for 4-link can be derived by a simple and straightforward extension.

For the development of the impact rules, the original dynamical model (2.7), especially $D(q)$ matrix, has to be extended by adding the Cartesian coordinates (z^1, z^2) of the tip of the stance leg. Overall coordinates q_1, q_2, z^1, z^2 represent the general situation of the Acrobot model without any connection to the base frame[1]. Therefore, the previously developed model with, in general, n DOF will have $n + 2$ DOF. In Acrobot case, the extended model will have 4-DOF.

The extended model of the mechanical system, in our case of Acrobot, is easy to obtain by applying the Lagrangian method and steps described in Subsection 2.1.1. In equation (2.13) the translational velocity of the base frame v_1^0 will be equal to the general translational velocity $[\dot{z}_1, \dot{z}_2, 0]$. Moreover, equation for system potential energy (2.16) is extended by y-coordinate represented by z_2 in all entries of potential energy $\mathcal{P}$.

In the case of Acrobot, the forms of the extended matrices $D_e(q)$, $C_e(\dot{q}, q)$ and $G_e(q)$ are as follows

$$D_e = \left[\begin{array}{c|c|c|c} \theta_1+\theta_2+2\theta_3\cos q_2 & \theta_2+\theta_3\cos q_2 & -\theta_4\cos q_1- \theta_5\cos(q_1+q_2) & \theta_4\sin q_1+ \theta_5\sin(q_1+q_2) \\ \hline \theta_2+\theta_3\cos q_2 & \theta_2 & -\theta_5\cos(q_1+q_2) & \theta_5\sin(q_1+q_2) \\ \hline -\theta_4\cos q_1- \theta_5\cos(q_1+q_2) & -\theta_5\cos(q_1+q_2) & m_1+m_2 & 0 \\ \hline \theta_4\sin q_1+ \theta_5\sin(q_1+q_2) & \theta_5\sin(q_1+q_2) & 0 & m_1+m_2 \end{array}\right], \tag{2.27}$$

$$C_e = \begin{bmatrix} -\theta_3\sin q_2\dot{q}_2 & -\theta_3\sin q_2(\dot{q}_1+\dot{q}_2) & 0 & 0 \\ \theta_3\sin q_2\dot{q}_1 & 0 & 0 & 0 \\ \theta_4\sin q_1\dot{q}_1+\theta_5\sin(q_1+q_2)(\dot{q}_1+\dot{q}_2) & \theta_5\sin(q_1+q_2)(\dot{q}_1+\dot{q}_2) & 0 & 0 \\ \theta_4\cos q_1\dot{q}_1+\theta_5\cos(q_1+q_2)(\dot{q}_1+\dot{q}_2) & \theta_5\cos(q_1+q_2)(\dot{q}_1+\dot{q}_2) & 0 & 0 \end{bmatrix}, \tag{2.28}$$

[1]Realize that the developed swing phase model (2.7) is connected to the coordinate origin, i.e. $(z^1, z^2) = (0, 0)$.

$$G_e = \begin{bmatrix} -g\ (\theta_5 \sin(q_1+q_2) + \theta_4 \sin q_1) \\ -g\,\theta_5 \sin(q_1+q_2) \\ 0 \\ g\,(m_1+m_2) \end{bmatrix}. \tag{2.29}$$

The impact between the swing leg and the ground is modelled as a contact between two rigid bodies. There are many different ways in the literature how the impact can be modelled, see [24, 34, 49, 56], nevertheless, most of them are based on results of [23, 67].

During the impact the external impulsive forces F_{ext} have effect on the model, therefore the vector of impulsive external forces has to be taken into account. The extended model with vector of impulsive external forces is as follows

$$D_e(q_e)\ddot{q}_e + C_e(q_e,\dot{q}_e)\dot{q}_e + G_e(q_e) = B_e u + \delta F_{ext}, \tag{2.30}$$

where q_e is the extended coordinates vector $q_e = (q_1, q_2, z^1, z^2)$ and δF_{ext} represents the vector of the impulsive external forces acting on the robot at the contact point during the impact, moreover $F_{ext} = \int_{t^-}^{t+} \delta F_{ext}(\tau) d\tau$.

The impact model introduced in [49] is derived here under the following hypotheses that imply that the total angular momentum is conserved:

H1) the impact is caused by the collision of the swing leg tip with the ground;

H2) the impact is instantaneous;

H3) the impact results in no rebound and no slipping of the swing leg;

H4) at the moment of the impact, the stance leg lifts from the ground without further interactions;

H5) external forces during the impact are represented by impulses;

H6) actuators cannot generate impulses and hence can be ignored during the impact;

H7) impulsive forces may cause the instantaneous change of the robot velocities, but there is no instantaneous change of the robot configuration.

Following an identical development as in [49], the expression relating the velocity of the robot just before to just after the impact may be written as

$$D_e\left[\dot{q}_e^+ - \dot{q}_e^-\right] = F_{ext}, \tag{2.31}$$

where $\dot{q}_e^+$, $\dot{q}_e^-$, are the angular velocities just after and just before the impact, respectively. According to the above assumptions, F_{ext} is the effect of the impulsive forces acting at the tip of the swing leg, namely

$$F_{ext} = E_2(q_e^-)F_2, \tag{2.32}$$

where $F_2 = \begin{bmatrix} F^T & F^N \end{bmatrix}'$ and $E_2(q_e) = \frac{\partial \Upsilon(q_e)}{\partial q_e}$. The variable Υ[2] represents coordinates of the tip point of the swing leg, i.e.

$$\Upsilon = \begin{bmatrix} z_1 + l_1 \sin q_1 + l_2 \sin(q_1 + q_2) \\ z_2 + l_1 \cos q_1 + l_2 \cos(q_1 + q_2) \end{bmatrix}. \tag{2.33}$$

The expression for $E_2(q_2)$ is therefore as follows

$$E_2(q_e) = \begin{bmatrix} l_1 \cos q_1 + l_2 \cos(q_1 + q_2) & l_2 \cos(q_1 + q_2) & 1 & 0 \\ -l_1 \sin q_1 - l_2 \sin(q_1 + q_2) & -l_2 \sin(q_1 + q_2) & 0 & 1 \end{bmatrix}. \tag{2.34}$$

The angular velocity just before the impact $\dot{q}_e^-$ is given by the extended model (2.30) whereas the angular velocity just after the impact $\dot{q}_e^+$ is given as the result of the impact model. As a consequence of the impact model hypotheses H3, the swing leg neither rebound nor slip and therefore the equation (2.31) is accompanied by the equation

$$E_2(q_e^-)\dot{q}_e^+ = 0. \tag{2.35}$$

The angular velocity just after the impact $\dot{q}_e^+$ and forces acting at the tip of the swing leg are given by the set of equations (2.31) and (2.35) as follows

$$\begin{bmatrix} D_e(q_e^-) & -E_2(q_e^-)' \\ E_2(q_e^-) & 0_{2\times 2} \end{bmatrix} \begin{bmatrix} \dot{q}_e^+ \\ F_2 \end{bmatrix} = \begin{bmatrix} D_e(q_e^-)\dot{q}_e^- \\ 0_{2\times 1} \end{bmatrix}. \tag{2.36}$$

During the impact, it is assumed that the swing leg and the stance leg becomes the new stance leg and the new swing leg, respectively, and Acrobot coordinates q_1 and q_2 are relabeled. To do so, consider Figure 2.3 where one can see the relation between Acrobot angles at the end of the previous step, i.e. q_1, q_2, and relabeled Acrobot angles at the beginning of the new step, i.e. $\widetilde{q}_1$, $\widetilde{q}_2$.

Using trigonometric laws, one can immediately see the following dependencies between the angular positions at the end of the old step and the angular positions at the beginning of the new step

$$\widetilde{q}_1 = \pi - q_1 - q_2, \quad \widetilde{q}_2 = 2\pi - q_2. \tag{2.37}$$

Equation (2.37) represents the change of Acrobot coordinates due to its legs relabeling. Furthermore, its time derivative is related as follows

$$\dot{\widetilde{q}}_1 = -\dot{q}_1 - \dot{q}_2, \quad \dot{\widetilde{q}}_2 = -\dot{q}_2, \tag{2.38}$$

[2]The notation Υ was used in [49].

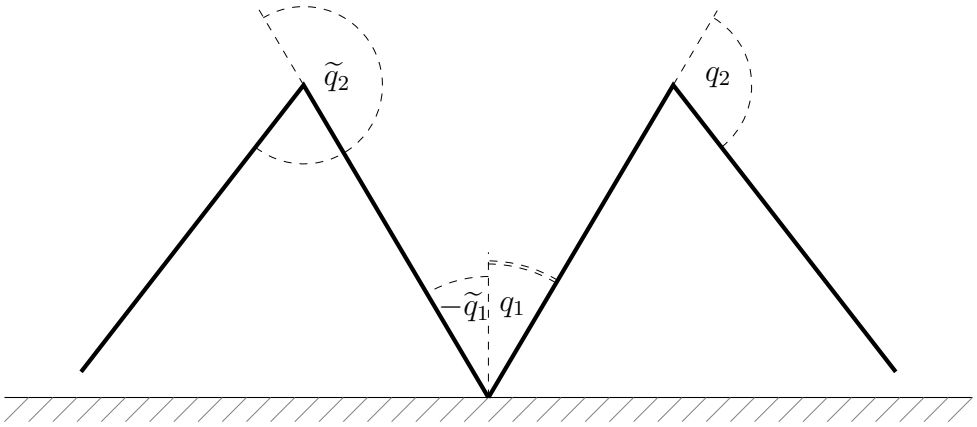

Figure 2.3. The definition of Acrobot angles at the beginning (left side of Figure), and at the end (right side of Figure), of the step.

which represents the change of Acrobot angular velocities $\dot{q}_1$, $\dot{q}_2$ due to legs relabeling. Angular velocities $\dot{q}_1$, $\dot{q}_2$ in (2.38) are given by impact equation (2.36) as a result of the impact at the end of the step.

The final form of the impact matrix $\widetilde{\Phi}_{\mathrm{Ipm}}(q(T))$ is obtained by solving the impact equation (2.36) and implementing the change of legs and their relabeling expressed by equations (2.37), (2.38). Therefore, the definition of the impact matrix of Acrobot is as follows

$$\widetilde{\Phi}_{\mathrm{Imp}}(q(T)) = \begin{bmatrix} \pi \\ 2\pi \\ 0 \\ 0 \end{bmatrix} + \begin{bmatrix} -1 & -1 & 0 & 0 \\ 0 & -1 & 0 & 0 \\ 0 & 0 & -1 & -1 \\ 0 & 0 & 0 & -1 \end{bmatrix} \times \begin{bmatrix} I_{2\mathrm{x}2} & 0_{2\mathrm{x}2} \\ 0_{2\mathrm{x}2} & \bar{\Phi}_{\mathrm{Imp}}(q(T)) \end{bmatrix}, \tag{2.39}$$

where $\bar{\Phi}_{\mathrm{Imp}}(q(T))$ represents appropriate part of the solution of (2.36). Nevertheless, for the purpose of the multi-step walking reference trajectory design in Section 4.2, the impact matrix including only angular velocities is defined as follows

$$\Phi_{\mathrm{Imp}}(q(T)) = \begin{bmatrix} -1 & -1 \\ 0 & -1 \end{bmatrix} \times \bar{\Phi}_{\mathrm{Imp}}(q(T)), \tag{2.40}$$

where $\bar{\Phi}_{\mathrm{Imp}}(q(T))$ represents again the appropriate part of the solution of (2.36). This matrix is used in the multi-step walking reference trajectory design where only angular velocities are taken into the account.

In [10] an integration of the continuous-time and the discrete-time dynamics into a general model of hybrid systems is provided.

In the case of 4-link the idea of legs switching is the same. The relations between angular positions at the end of the previous step and at the beginning of the new step are as follows

$$\widetilde{q}_1 = \pi - q_1 - q_2 - q_3 - q_4, \qquad \widetilde{q}_2 = 2\pi - q_2, \qquad \widetilde{q}_3 = -q_4, \qquad \widetilde{q}_4 = -q_3. \tag{2.41}$$

Furthermore, their time derivatives representing the relations between angular velocities at the end of the previous step after the impact and at the beginning of the new step of 4-link are given as follows

$$\dot{\widetilde{q}}_1 = -\dot{q}_1 - \dot{q}_2 - \dot{q}_3 - \dot{q}_4, \qquad \dot{\widetilde{q}}_2 = -\dot{q}_2, \qquad \dot{\widetilde{q}}_3 = -\dot{q}_4, \qquad \dot{\widetilde{q}}_4 = -\dot{q}_3. \tag{2.42}$$

The definition of the impact matrix of 4-link corresponds to the definition of equation (2.39) in Acrobot case. Summarizing, the relations given by Acrobot equations (2.37), (2.38) or by 4-link equations (2.41), (2.42) form the matrix $G(x, u)$ in (2.2).

2.3 Chapter conclusion

This chapter presented mathematical models of two underactuated walking robots, namely Acrobot and 4-link using classical Euler-Lagrange approach. Both models are supplemented by the impact map of angular velocities in order to unambiguously define the angular velocities of the robot after the swing leg hits the ground at the end of the step.

The developed mathematical models are used to design the pseudo-passive reference trajectory or to design feedback controllers whereas the impact map is used in the multi-step walking reference trajectory design or in a verification of a stability tracking during more steps later on.

Chapter 3

Exact feedback linearization

The purpose of this chapter is to present the partial exact feedback linearization of the Acrobot model. Later on, the partially linear form of the 4-link model will be derived using the one of the Acrobot model and the so-called embedding of the generalized Acrobot into 4-link. In other words, the majority of this chapter will be devoted to Acrobot.

It is not possible to apply a classical linear control approach directly to the Acrobot model due to its nonlinearities. Therefore, in order to control Acrobot in a way resembling the human walk, a nonlinear control method is used. In the literature, one can find various control approaches applied to a general underactuated mechanical system including Acrobot. In particular, a passive based control was used in order to control a biped robot in [122], the underactuated biped is controlled via a sliding mode control method in [92], a fuzzy control approach is used to control an underactuated robot in [17], whereas a partial feedback linearization method is used in [117, 119] in order to control Acrobot in a desired way. The partial exact feedback linearization presented in this section can be viewed as a generalization of the well-known and widely used in robotics computed-torque method which corresponds to the full exact feedback linearization of the fully actuated mechanical system.

3.1 Partial feedback linearization of Acrobot

The exact feedback linearization approach is based on the idea that the new nonlinear control law is obtained as a controller for an inner-loop which exactly linearizes the nonlinear system using a state space change of coordinates. The outer-loop control in the new coordinates can be designed using a suitable classical linear method so that the required control tasks are fulfilled. More specifically, consider the following nonlinear

system in the standard form

$$\begin{aligned} \dot{x} &= f(x) + g(x)u, \quad && x \in \mathbb{R}^n,\ u \in \mathbb{R}, \\ y &= h(x), && y \in \mathbb{R}, \end{aligned} \tag{3.1}$$

where $f(x)$, $g(x)$ are smooth vector fields defined on $\mathbb{R}^n$ and $h(x)$ is smooth function defined on $\mathbb{R}^n$. The following state feedback transformation introducing new input $v \in \mathbb{R}$

$$u = \alpha(x) + \beta(x)\, v \tag{3.2}$$

together with a change of variables

$$z = T(x) \tag{3.3}$$

transforms the original nonlinear system (3.1) into its new equivalent form, provided (3.2) and (3.3) define (locally or globally) smoothly invertible transformation between (x, u) and (z, v). System (3.1) is then called as (locally or globally) exact feedback linearizable if the corresponding equivalent system is the linear one.

The exact feedback linearization method is efficient method to handle nonlinear systems control, however, the field of applicability of these methods is, indeed, very limited, especially in real applications. Nevertheless, the partial feedback linearization method can be applied to a wider class of nonlinear systems on the assumption that the corresponding zero dynamics is stable. The zero dynamics is in certain sense analogue of the maximal unobservable part of a linear system. Stability of the zero dynamics has to be verified so that the partial feedback linearized form of a nonlinear system can be used.

In general, to achieve either the full state feedback linearization or the partial feedback linearization one can seek a suitable auxiliary output function h having the convenient relative degree r [59]. In the case of the state feedback linearization technique, the relative degree of the output function h is equal to the dimension of the nonlinear system, i.e. to n. On the other hand, in the case of the partial feedback linearization technique, the relative degree of the output function h is strictly lower than the degree of the nonlinear system n. It is well-known [59] that the single-input single-output system has generically always at least one-dimensional input-output exact linearizable part. Nevertheless, getting an output function h with maximal relative degree r in order to have the smallest possible zero dynamics is, in general, very difficult task [59, 68].

3.1.1 The maximal order of exact linearization of Acrobot

To find the maximal degree of Acrobot linearization let us rewrite the original equation of motion of Acrobot (2.7) into the following form

$$\begin{bmatrix} \ddot{q}_1 \\ \ddot{q}_2 \end{bmatrix} = -D^{-1}(q)C(q,\dot{q})\dot{q} - D^{-1}(q)G(q) + D^{-1}(q)\begin{bmatrix} 0 \\ u \end{bmatrix}. \tag{3.4}$$

Introducing $x_1 = q_1$, $x_2 = \dot{q}_1$, $x_3 = q_2$, $x_4 = \dot{q}_2$, the original equation of motion of Acrobot is expressed in the standard form (3.1), where vector fields $f(x)$, $g(x)$ are defined as follows

$$f(x) = \Big[f_1(x),\, f_2(x),\, f_3(x),\, f_4(x)\Big]^{\mathrm{T}}, \quad g(x) = \Big[g_1(x),\, g_2(x),\, g_3(x),\, g_4(x)\Big]^{\mathrm{T}}, \tag{3.5}$$

and where $f_1(x) = x_2$, $f_2(x) = \frac{-(d_{22}c_{11}-d_{12}c_{21})x_2-(d_{22}c_{12}-d_{12}c_{22})x_4-(d_{22}G_1-d_{12}G_2)}{d_{11}d_{22}-d_{12}^2}$, $f_3(x) = x_4$, $f_4(x) = \frac{-(d_{11}c_{21}-d_{12}c_{11})x_2-(d_{11}c_{22}-d_{12}c_{12})x_4-(d_{11}G_2-d_{12}G_1)}{d_{11}d_{22}-d_{12}^2}$, $g_1 = 0$, $g_2 = \frac{-d_{12}}{d_{11}d_{22}-d_{12}^2}$, $g_3 = 0$, $g_4 = \frac{d_{11}}{d_{11}d_{22}-d_{12}^2}$.

To determine maximal order of the partial exact feedback linearization of Acrobot, the following definitions are given here in order to keep basic concepts from nonlinear control theory.

Definition 3.1.1 *Lie bracket of two vector fields $f(x)$, $g(x)$ is another vector field denoted $[f,g](x)$ and defined as*

$$[f,g](x) = \frac{\partial g(x)}{\partial x}f(x) - \frac{\partial f(x)}{\partial x}g(x).$$

Repeated bracketing of a vector field $g(x)$ with the same vector field $f(x)$ is possible. In order to avoid a confusing notation in the form $[f,[f,\ldots,[f,g]\ldots]]$, a recursive operation is defined as follows

$$ad_f^k g(x) = [f, ad_f^{k-1} g](x), \quad k \geq 1, \quad ad_f^0 g(x) = g(x).$$

Definition 3.1.2 *A distribution is any collection of vector fields closed with respect to linear operations. Moreover a distribution $\triangle(x)$ is called involutive if the Lie bracket $[f_1,f_2](x)$ of any pair of vector fields $f_1(x)$ and $f_2(x)$ which belongs to $\triangle(x)$ is a vector field which belongs to $\triangle(x)$, i.e.*

$$f_1(x) \in \triangle(x),\, f_2(x) \in \triangle(x) \quad \Rightarrow \quad [f_1,f_2](x) \in \triangle(x).$$

Further, define a sequence of distributions, $\triangle_0, \triangle_1, \triangle_2$ related to a given system (3.1). Namely the distribution $\triangle_0(x)$ is defined as follows

$$\triangle_0(x) = \text{span}\{g\}. \tag{3.6}$$

Recall that, any 1-dimensional regular distribution is involutive [59], so it is $\triangle_0(x)$ provided $g(0) \neq 0$. Next, the distribution $\triangle_{i+1}(x)$, $i \geq 0$ is defined as follows

$$\triangle_{i+1}(x) = \text{span}\{g, \text{ad}_f g, \ldots, ad_f^{i+1} g\}. \tag{3.7}$$

To find the maximal linearizable part, Theorem 2.4.2 from [83], can be used and it is repeated here for the reader's convenience as the following

Theorem 3.1.3 *Nonlinear system 3.1 is locally partially state feedback linearizable with index r if the distribution $\triangle_{r-2}(x)$ has constant rank less than or equal to $n-1$ in neighborhood of the origin U_0, and*

$$ad_f^{r-1} g(x) \notin \triangle_{r-2}(x) = \text{span}\{g, ad_f g, \ldots, ad_f^{r-2} g\}, \qquad \forall x \in U_0.$$

To check conditions of Theorem 3.1.3 for Acrobot model (3.4), realize first that it is system of the form (3.1) with (3.5). As $g(x)$ is nonzero around working configuration, the distribution $\triangle_0$ is one-dimensional, regular and therefore involutive. Next, Lie bracket $[f, g](x)$ is computed as follows

$$[f,g](x) = \begin{bmatrix} \frac{\theta_2+\theta_3\cos x_3}{\theta_1\theta_2-\theta_3^2\cos^2 x_3} \\ -\frac{\theta_3\sin x_3(2x_2+x_4)}{\theta_1\theta_2-\theta_3^2\cos^2 x_3} \\ -\frac{\theta_1+\theta_2+2\theta_3\cos x_3}{\theta_1\theta_2-\theta_3^2\cos^2 x_3} \\ \frac{(\theta_1 x_2+\theta_2 x_2+\theta_2 x_4+2\theta_3 x_2\cos x_3+\theta_3 x_4\cos x_3)}{(2\theta_3\sin x_3(\theta_2+\theta_3\cos x_3))^{-1}(\theta_1\theta_2-\theta_3^2\cos^2 x_3)^2} \end{bmatrix}.$$

To show that the distribution $\triangle_1(x)$ is involutive one has to check that the vector field $\big[g,[f,g]\big](x)$ belongs to the distribution $\triangle_1(x)$ for all x. The vector field $\big[g,[f,g]\big](x)$ is computed as follows

$$\big[g,[f,g]\big](x) = \begin{bmatrix} 0 \\ -\frac{2\theta_3\sin x_3(\theta_1+\theta_3\cos x_3)(\theta_2+\theta_3\cos x_3)(\theta_2+\theta_3\cos x_3)}{(\theta_1\theta_2-\theta_3^2\cos^2 x_3)^3} \\ 0 \\ \frac{2\theta_3\sin x_3(\theta_1+\theta_3\cos x_3)(\theta_2+\theta_3\cos x_3)(\theta_1+\theta_2+2\theta_3\cos x_3)}{(\theta_1\theta_2-\theta_3^2\cos^2 x_3)^3} \end{bmatrix},$$

and therefore it holds

$$\big[g,[f,g]\big](x) = \frac{2\theta_3\sin x_3(\theta_1+\theta_3\cos x_3)(\theta_2+\theta_3\cos x_3)}{(\theta_1\theta_2-\theta_3^2\cos^2 x_3)^2}\, g(x). \tag{3.8}$$

So that the distribution $\triangle_1(x)$ is, indeed, involutive.

Using Theorem 3.1.3 one can see that the involutivity of $\triangle_1(x)$ actually guarantees the partial exact linearization of Acrobot of order 3. Moreover, one can see that $\triangle_2(x)$ is not involutive. Again, it is the well-known result [83], Theorem 2.4.2 that involutivity of $\triangle_2(x)$ is necessary and sufficient condition for the full exact feedback linearization.

Summarizing, Acrobot has three dimensional exact feedback linearizable part and one dimensional part that can never be linearized. Acrobot is a nice example of a nonlinear system with partial feedback linearization property. Therefore, in following subsections two different partial feedback linearization method for the Acrobot model are shown.

Before doing that, let us repeat that Euler-Lagrange equations of motions (2.6) lead in the case of Acrobot to dynamical equation of motion of mechanical system (2.7) in the form

$$D(q)\ddot{q} + C(q,\dot{q})\dot{q} + G(q) = \begin{bmatrix} 0 \\ \tau_2 \end{bmatrix},$$

which gives 2-DOF underactuated mechanical system

$$\begin{aligned} d_{11}\ddot{q}_{11} + d_{12}\ddot{q}_2 + c_{11}\dot{q}_1 + c_{12}\dot{q}_2 + g_1 &= 0, \\ d_{21}\ddot{q}_{11} + d_{22}\ddot{q}_2 + c_{21}\dot{q}_1 + c_{22}\dot{q}_2 + g_2 &= \tau_2. \end{aligned} \tag{3.9}$$

The easiest way to find the exact feedback linearization is to define a suitable auxiliary output with appropriate relative degree.

3.1.2 Spong exact feedback linearization of Acrobot of order 2

Due to the second order structure of (3.9) it is rather straightforward to find exact feedback linearization of order 2, i.e. to define auxiliary output having relative degree equal to 2. Namely, it was shown in [115, 120] that the invertible change of control input

$$\tau = \alpha(q)\, u + \beta(q,\dot{q}) \tag{3.10}$$

transforms dynamics (3.9) into the partial linearized system of order 2. Namely, to do so rewrite the first line of (3.9) as follows

$$\ddot{q}_1 = d_{11}^{-1}\left(-d_{12}\,\ddot{q}_2 - c_{11}\dot{q}_1 - c_{12}\dot{q}_2 - g_1\right) \tag{3.11}$$

and substitute into the second line of (3.9). After some rearrangement one has the following form of the second line of (3.9)

$$\left(d_{22} - d_{21}d_{11}^{-1}d_{12}\right)\ddot{q}_2 + \left(c_{21} - d_{21}d_{11}^{-1}c_{11}\right)\dot{q}_1 + \left(c_{22} - d_{21}d_{11}^{-1}c_{12}\right)\dot{q}_2 + g_2 - d_{21}d_{11}^{-1}q_1 = \tau_2. \tag{3.12}$$

Now, a feedback linearizing controller for (3.9) could be defined as follows

$$\tau_2 = \left(d_{22} - d_{21}d_{11}^{-1}d_{12}\right)u + \left(c_{21} - d_{21}d_{11}^{-1}c_{11}\right)\dot{q}_1 + \left(c_{22} - d_{21}d_{11}^{-1}c_{12}\right)\dot{q}_2 + g_2 - d_{21}d_{11}^{-1}q_1. \tag{3.13}$$

The original system is feedback equivalent to the following partial or input/output linear system of order 2. The system is input/output linear from u to the output $y_2 = q_2$, namely

$$\begin{aligned} d_{11}\ddot{q}_1 + c_{11}\dot{q}_1 + c_{12}\dot{q}_2 + g_1 &= -d_{12}\,u \\ \ddot{q}_2 &= u \\ y_2 &= q_2. \end{aligned} \tag{3.14}$$

Equation (3.14) can be rewritten into the following form

$$\begin{aligned} \dot{q}_1 &= p_1 \\ \dot{p}_1 &= -d_{11}^{-1}d_{12}\,u - d_{11}^{-1}c_{11}\,p_1 - d_{11}^{-1}c_{12}\,p_2 - d_{11}^{-1}g_1 \\ \dot{q}_2 &= p_2 \\ \dot{p}_2 &= u. \end{aligned} \tag{3.15}$$

The output equation $y_2 = q_2$ is related with the location of Acrobot input τ_2 which directly actuates angle q_2. Therefore, such partial linearization is called as the collocated linearization of Acrobot, see [117]. In the same publication the so-called non-collocated linearization is introduced, i.e. the input-output exact feedback linearization having the underactuated angle q_1 as the auxiliary output.

To sum up, it was shown in [117] that 2-DOF underactuated systems with input τ_2 collocated with an output $y = q_2$ can be partially linearized by the feedback

$$\tau_2 = \left(d_{22} - \frac{d_{21}d_{12}}{d_{11}}\right)v + \left(f_2 - \frac{d_{21}f_1}{d_{11}}\right), \tag{3.16}$$

to obtain the original system (3.9) in the following partially linearized form

$$\begin{aligned} \ddot{q}_1 &= J(q)v + R(q,\dot{q}), \\ \ddot{q}_2 &= v, \end{aligned} \tag{3.17}$$

where $J(q) = -d_{12}/d_{11}$ and $R(q,\dot{q}) = -f_1/d_{11}$ are expressed via entries of the matrices $D(q)$ and $F(q,\dot{q}) = C(q,\dot{q})\dot{q} + G(q)$ in (2.7).

3.1.3 Partial exact feedback linearization of Acrobot of order 3

It was shown in [51, 96] that if a generalized momentum conjugated to a cyclic variable is not conserved (as it is the case of Acrobot) then there exists a set of outputs that defines

one-dimensional exponentially stable zero dynamics. In Acrobot case that means that it is possible to find a function $\overline{y}(q,\dot{q})$ with relative degree 3 that transforms the original system (2.7) by a local coordinate transformation $z = T(q,\dot{q})$, namely

$$z_1 = \overline{y}, \quad z_2 = \dot{\overline{y}}, \quad z_3 = \ddot{\overline{y}}, \quad z_4 = f(q,\dot{q}), \tag{3.18}$$

into a new input/output linear system with one-dimensional nonlinear zero dynamics:

$$\dot{z}_1 = z_2, \quad \dot{z}_2 = z_3, \quad \dot{z}_3 = \alpha(q,\dot{q})\tau_2 + \beta(q,\dot{q}) = w, \quad \dot{z}_4 = \psi_1(q,\dot{q}) + \psi_2(q,\dot{q})\tau_2. \tag{3.19}$$

The following theorem, introduced in [96] deals with the transformation of Acrobot nonlinear dynamics equations (2.7) into a normal form (3.19).

Theorem 3.1.4 *Consider underactuated system with two degrees of freedom (3.9) q_1, q_2 and symmetry property $D(q) = D(q_2)$. Assume the shape variable q_2 is actuated. Then, the following global change of coordinates:*

$$\begin{aligned} z_1 &= q_1 + \gamma(q_2), \\ z_2 &= d_{11}(q_2)\dot{q}_1 + d_{12}(q_2)\dot{q}_2 := \partial\mathcal{L}/\partial\dot{q}_1, \\ \xi_1 &= q_2, \\ \xi_2 &= \dot{q}_2 \end{aligned} \tag{3.20}$$

transforms dynamics of (3.9) into a cascade nonlinear system in normal form

$$\begin{aligned} \dot{z}_1 &= m_{11}^{-1}(\xi_1)z_2, \\ \dot{z}_2 &= g(z_1,\xi_1), \\ \dot{\xi}_1 &= \xi_2, \\ \dot{\xi}_2 &= u, \end{aligned} \tag{3.21}$$

where

$$\gamma(q_2) = \int_0^{q_2} \frac{d_{12}(s)}{d_{11}(s)} ds, \qquad g(z_1,\xi_1) = -\frac{\partial\mathcal{P}(q)}{\partial q_1} \mid_{q_1 = z_1 - \gamma(\xi_1),\, q_2 = \xi_1}.$$

By virtue of Theorem 3.1.4, in the case of Acrobot, there are two independent functions with relative degree 3 transforming the original system into the desired normal form (3.19), namely

$$\sigma = \frac{\partial\mathcal{L}}{\partial\dot{q}_1} = (\theta_1 + \theta_2 + 2\theta_3\cos q_2)\dot{q}_1 + (\theta_2 + \theta_3\cos q_2)\dot{q}_2, \tag{3.22}$$

$$p = q_1 + \gamma(q_2) = q_1 + \int_0^{q_2} \frac{d_{12}(s)}{d_{11}(s)} ds. \tag{3.23}$$

After analytical computation of the integral in the equation above, the function p is defined as follows

$$p = q_1 + \frac{q_2}{2} + \frac{2\theta_2 - \theta_1 - \theta_2}{\sqrt{(\theta_1 + \theta_2)^2 - 4\theta_3^2}} \arctan\left(\sqrt{\frac{\theta_1 + \theta_2 - 2\theta_3}{\theta_1 + \theta_2 + 2\theta_3}} \tan\frac{q_2}{2}\right). \tag{3.24}$$

Actually, time derivative of σ in (3.22) can be expressed as follows

$$\dot{\sigma} = \frac{d}{dt}\frac{\partial \mathcal{L}}{\partial \dot{q}_1}, \tag{3.25}$$

moreover, after substitution (3.22) in the first line of Euler-Lagrange equation (2.6), which corresponds to the underactuated angle q_1, following relation holds

$$\dot{\sigma} = \frac{d}{dt}\frac{\partial \mathcal{L}}{\partial \dot{q}_1} = \frac{\partial \mathcal{L}}{\partial q_1} = -\theta_4\, g \sin(q_1) - \theta_5\, g \sin(q_1 + q_2) = -\frac{\partial \mathcal{P}(q)}{\partial q_1}. \tag{3.26}$$

After substitution from material parameter equation (2.19) into (3.26) one can see that the following expression holds

$$\dot{\sigma} = \frac{x_{cm}}{g(m_1 + m_2)}, \tag{3.27}$$

where x_{cm} is x-position of the center of mass of Acrobot. In other words, $\dot{\sigma}$ is proportional to the x-position of Acrobot center of mass.

Moreover, $\dot{\sigma}$ has relative degree 2, i.e. σ has relative degree 3. Furthermore, by some straightforward but laborious computations the following relation holds

$$\dot{p} = d_{11}(q_2)^{-1}\sigma, \tag{3.28}$$

where $d_{11}(q_2) = (\theta_1 + \theta_2 + 2\theta_3 \cos q_2)$ is the corresponding element of the inertia matrix $D(q)$ in (2.7), i.e. $\dot{p}$ has relative degree 2 and therefore p should have relative degree 3 as well.

The zero dynamics is used to investigate internal stability when the corresponding output is constrained to zero. For the simplest cases, i.e. the auxiliary output is $\overline{y} = Cp(q)$ or $\overline{y} = C\sigma(q, \dot{q})$ the resulting zero dynamics is only critically stable. However, considering the output function $\overline{y} = C_1 p(q) + C_2\sigma(q, \dot{q})$ one gets the following zero dynamics $\dot{p} + C_1[C_2 d_{11}(q_2)]^{-1}p = 0$ which is asymptotically stable whenever C_1/C_2 is positive, $d_{11}(q_2)$ being the corresponding part of the inertia matrix $D(q)$ in (2.7). Unfortunately, the corresponding transformations have a complex set of singularities, unless C_1 is very small, which is not suitable for practical purposes.

Finally, note that detailed classification of the underactuated mechanical systems using variety of normal forms can be found in [95].

It was shown in [30] that functions p, σ mentioned above having maximal relative degree 3 can be used to a transformation of the original nonlinear equation of Acrobot into the normal form using another transformation than the change of coordinates given in Theorem 3.1.4. Namely, the following transformation can be defined:

$$\xi_1 = p, \quad \xi_2 = \sigma, \quad \xi_3 = \dot{\sigma}, \quad \xi_4 = \ddot{\sigma}, \tag{3.29}$$

where p and σ are given in (3.22), (3.24). Applying (3.28), (3.29) to (2.7) Acrobot dynamics in partial exact linearized form is obtained

$$\dot{\xi}_1 = d_{11}(q_2)^{-1}\xi_2, \quad \dot{\xi}_2 = \xi_3, \quad \dot{\xi}_3 = \xi_4, \quad \dot{\xi}_4 = \alpha(q)\tau_2 + \beta(q, \dot{q}) = w, \tag{3.30}$$

with new coordinates ξ and input w being well defined whenever $\alpha(q)^{-1} \neq 0$. An important feature here is that the set of possible singularities where $\alpha(q)^{-1} = 0$ depends only on positions, not on velocities. In [30] the region where such a transformation can be applied is expressed explicitly. Namely, straightforward computations show that

$$\xi = \begin{bmatrix} \xi_1 \\ \xi_2 \\ \xi_3 \\ \xi_4 \end{bmatrix} = T(q_1, q_2, \dot{q}_1, \dot{q}_2) := \begin{bmatrix} T_1 \\ T_2 \\ T_3 \\ T_4 \end{bmatrix}, \tag{3.31}$$

where the transformation $T(q_1, q_2, \dot{q}_1, \dot{q}_2)$ after reordering the second and the third line is given as follows

$$\begin{bmatrix} T_1 \\ T_3 \\ T_2 \\ T_4 \end{bmatrix} = \begin{bmatrix} p(q_1, q_2) \\ \theta_4 g \sin q_1 + \theta_5 g \sin(q_1 + q_2) \\ \Phi_2(q_1, q_2) \begin{bmatrix} \dot{q}_1 \\ \dot{q}_2 \end{bmatrix} \end{bmatrix}, \tag{3.32}$$

where σ and p are given by (3.22), (3.24) and Φ_2 by (3.35) later on. It is obvious that transformations T_1 and T_3 depend on angular positions q_1 and q_2 only. It holds by (3.31), (3.32) that

$$\frac{\partial[\xi_1, \xi_3, \xi_2, \xi_4]^\top}{\partial[q^\top, \dot{q}^\top]^\top} = \begin{bmatrix} \Phi_1(q_1, q_2) & 0 \\ \Phi_3(q, \dot{q}) & \Phi_2(q_1, q_2) \end{bmatrix}, \tag{3.33}$$

where $q := [q_1, q_2]^\top$, $\Phi_3(q, \dot{q})$ is a certain (2×2) matrix of smooth functions while

$$\Phi_1(q_1, q_2) = \begin{bmatrix} 1 & \frac{\theta_2 + \theta_3 \cos q_2}{\theta_1 + \theta_2 + 2\theta_3 \cos q_2} \\ \theta_4 g \cos q_1 + \theta_5 g \cos(q_1 + q_2) & \theta_5 g \cos(q_1 + q_2) \end{bmatrix}, \tag{3.34}$$

$$\Phi_2(q_1, q_2) = \begin{bmatrix} \theta_1 + \theta_2 + 2\theta_3 \cos q_2 & \theta_2 + \theta_3 \cos q_2 \\ \theta_4 g \cos q_1 + \theta_5 g \cos(q_1 + q_2) & \theta_5 g \cos(q_1 + q_2) \end{bmatrix}. \tag{3.35}$$

3.2 Acrobot embedding into 4-link

The idea of Acrobot embedding into 4-link was presented in [28]. Acrobot embedding method consists in selection of constraining functions for knees control $\phi_3(q_2)$, $\phi_4(q_2)$ with dependence on the angle in the hip q_2 whereas the angle in the hip is controlled in the same way as it would be the Acrobot angle.

By virtue of the embedding method, it is not necessary to develop a new control strategy for 4-link, instead, 4-link can be controlled using the already developed control strategies for Acrobot together with constraining functions for bending of the swing leg and straighten of the stance leg during one step.

Dependencies of angles q_3 and q_4 on angle q_2 are represented by constraining functions $\phi_3(q_2), \phi_4(q_2)$ for knees control. New coordinates as $\bar{q}_1, \ldots, \bar{q}_4, \dot{\bar{q}}_1, \ldots \dot{\bar{q}}_4, \bar{\tau}_2, \ldots, \bar{\tau}_4$ are crucial for the embedding method.

The coordinates change taking the "old" coordinates in (2.7) into new coordinates is defined as follows:

$$\begin{aligned}
\bar{q}_1 &= q_1, \ \bar{q}_2 = q_2, \\
\dot{\bar{q}}_1 &= \dot{q}_1, \ \dot{\bar{q}}_2 = \dot{q}_2, \\
\bar{\tau}_2 &= \tau_2, \\
\bar{q}_3 &= q_3 - \phi_3(q_2), \\
\dot{\bar{q}}_3 &= \dot{q}_3 - \tfrac{\partial \phi_3(q_2)}{\partial q_2} \dot{q}_2, \\
\bar{\tau}_3 &= \ddot{q}_3 - \tfrac{\partial \phi_3(q_2)}{\partial q_2} \ddot{q}_2 - \tfrac{\partial^2 \phi_3(q_2)}{\partial q_2^2} \dot{q}_2^2, \\
\bar{q}_4 &= q_4 - \phi_4(q_2), \\
\dot{\bar{q}}_4 &= \dot{q}_4 - \tfrac{\partial \phi_4(q_2)}{\partial q_2} \dot{q}_2, \\
\bar{\tau}_4 &= \ddot{q}_4 - \tfrac{\partial \phi_4(q_2)}{\partial q_2} \ddot{q}_2 - \tfrac{\partial^2 \phi_4(q_2)}{\partial q_2^2} \dot{q}_2^2,
\end{aligned} \tag{3.36}$$

where $\ddot{q}_2, \ddot{q}_3, \ddot{q}_4$ are substituted from original dynamical equation for 4-link, represented by general equation (2.7). The definition of constraining functions $\phi_3(q_2)$, $\phi_4(q_2)$ for knees control will be discussed later. It is shown in [28] that the transformation of coordinates (3.36) is invertible. For more details see [28].

By virtue of embedding method, results developed for Acrobot can be simply adapted here. The following transformation is defined

$$\xi = \mathcal{T}(\bar{q}, \dot{\bar{q}}): \quad \xi_1 = p, \quad \xi_2 = \sigma, \quad \xi_3 = \dot{\sigma}, \quad \xi_4 = \ddot{\sigma}, \tag{3.37}$$

where p and σ are well known linearizing functions (3.22), (3.24) in new coordinates (3.36), namely

$$\sigma = \frac{\partial \mathcal{L}}{\partial \dot{\bar{q}}_1}, \tag{3.38}$$

$$p = \bar{q}_1 + \int_0^{\bar{q}_2} \bar{d}_{11}(s)^{-1} \bar{d}_{12}(s) \mathrm{d}s. \tag{3.39}$$

The bar above q, $\dot{q}$ represents new coordinates (3.36) and the same bar above dynamic equation's matrices (2.7) represents the dynamics of the embedded Acrobot in new coordinates (3.36). After substitution (3.38), (3.39) into (3.37) particular form of transformation (3.37) in new coordinates (3.36) is as follows

$$\begin{aligned}
\xi_1 &= \bar{q}_1 + \textstyle\int_0^{\bar{q}_2} \bar{d}_{11}(s)^{-1} \bar{d}_{12}(s) \mathrm{d}s, \\
\xi_2 &= \bar{d}_{11}(\bar{q}_2)\dot{\bar{q}}_1 + \bar{d}_{12}(\bar{q}_2)\dot{\bar{q}}_2, \\
\xi_3 &= -\overline{G}_1(\bar{q}), \\
\xi_4 &= -\tfrac{\partial \overline{G}_1}{\partial \bar{q}_1}(\bar{q})\dot{\bar{q}}_1 - \tfrac{\partial \overline{G}_1}{\partial \bar{q}_2}(\bar{q})\dot{\bar{q}}_2, \\
w &= -\dot{\bar{q}}^\top \tfrac{\partial^2 \overline{G}_1}{\partial \bar{q}^2}(\bar{q})\dot{\bar{q}} - \left[\tfrac{\partial \overline{G}_1}{\partial \bar{q}_1}(\bar{q}), \tfrac{\partial \overline{G}_1}{\partial \bar{q}_2}(\bar{q})\right] \times \overline{D}(\bar{q})^{-1} \left[\begin{bmatrix} 0 \\ \bar{\tau} \end{bmatrix} - \overline{C}(\bar{q}, \dot{\bar{q}})\dot{\bar{q}} - \overline{G}(\bar{q}) \right].
\end{aligned} \tag{3.40}$$

New matrices $\overline{D}(q_2)$, $\overline{C}(q_{1,2}, \dot{q}_{1,2})$ and $\overline{G}(q_1, q_2)$ are defined as follows

$$\overline{D}(\bar{q}) = \overline{\phi}^\top D(q)\, \overline{\phi}, \tag{3.41}$$

$$\overline{C}(\bar{q}, \dot{\bar{q}}) = \overline{\phi}^\top C(q, \dot{q})\, \overline{\phi} + \overline{\phi}^\top D(q) \begin{bmatrix} 0 & 0 & 0 & 0 \\ 0 & 0 & 0 & 0 \\ 0 & \frac{\partial^2 \phi_3(q_2)}{\partial q_2^2}\dot{q}_2 & 0 & 0 \\ 0 & \frac{\partial^2 \phi_4(q_2)}{\partial q_2^2}\dot{q}_2 & 0 & 0 \end{bmatrix}, \tag{3.42}$$

$$\overline{G}(\bar{q}) = \overline{\phi}^\top G(q)\, \overline{\phi}, \tag{3.43}$$

where matrices $D(q)$, $C(q,\dot{q})$ and $G(q)$ are matrices of 4-link dynamical model equation. Function $\overline{\phi}$ is defined as follows

$$\overline{\phi} = \begin{bmatrix} 1 & 0 & 0 & 0 \\ 0 & 1 & 0 & 0 \\ 0 & \frac{\partial \phi_3(q_2)}{\partial q_2}\dot{q}_2 & 1 & 0 \\ 0 & \frac{\partial \phi_4(q_2)}{\partial q_2}\dot{q}_2 & 0 & 1 \end{bmatrix}. \tag{3.44}$$

Moreover, the first derivatives of $\overline{G}_1$ with respect to $\bar{q}$, i.e. $\frac{\partial \overline{G}_1}{\partial \bar{q}_1}(\bar{q})$ and $\frac{\partial \overline{G}_1}{\partial \bar{q}_2}(\bar{q})$ are defined as follows

$$\frac{\partial \overline{G}_1(\bar{q})}{\partial \bar{q}_1} = \frac{\partial G_1(q)}{\partial q_1}, \quad \frac{\partial \overline{G}_1(\bar{q})}{\partial \bar{q}_2} = \frac{\partial G_1(q)}{\partial q_2} + \frac{\partial G_1(q)}{\partial q_3}\frac{\partial \phi_3(q_2)}{\partial q_2}\dot{q}_2 + \frac{\partial G_1(q)}{\partial q_4}\frac{\partial \phi_4(q_2)}{\partial q_2}\dot{q}_2. \tag{3.45}$$

The second derivative of $\overline{G}_1(\bar{q})$ with respect to $\bar{q}$, i.e. $\frac{\partial^2 \overline{G}_1(\bar{q})}{\partial \bar{q}^2}$ is defined as follows

$$\frac{\partial^2 \overline{G}_1(\bar{q})}{\partial \bar{q}^2} = \begin{bmatrix} 1 & 0 & 0 & 0 \\ 0 & 1 & \frac{\partial \phi_3(q_2)}{\partial q_2}\dot{q}_2 & \frac{\partial \phi_4(q_2)}{\partial q_2}\dot{q}_2 \end{bmatrix} \frac{\partial^2 G_1(q)}{\partial q^2} \begin{bmatrix} 1 & 0 \\ 0 & 1 \\ 0 & \frac{\partial \phi_3(q_2)}{\partial q_2}\dot{q}_2 \\ 0 & \frac{\partial \phi_4(q_2)}{\partial q_2}\dot{q}_2 \end{bmatrix} + \begin{bmatrix} 0 & 0 \\ 0 & \frac{\partial G_1(q)}{\partial q_3}\phi_3'' + \frac{\partial G_1(q)}{\partial q_4}\phi_4'' \end{bmatrix}. \tag{3.46}$$

To complete the definition of $\overline{G}_1(\bar{q})$ above, the second time derivatives of constraining functions ϕ_3'' and ϕ_4'' are defined as follows

$$\phi_3'' = \frac{\partial \phi_3(q_2)}{\partial q_2}\ddot{q}_2 + \frac{\partial^2 \phi_3(q_2)}{\partial q_2^2}\dot{q}_2^2, \quad \phi_4'' = \frac{\partial \phi_4(q_2)}{\partial q_2}\ddot{q}_2 + \frac{\partial^2 \phi_4(q_2)}{\partial q_2^2}\dot{q}_2^2. \tag{3.47}$$

The dynamics of the embedded Acrobot expressed in partial exact linearized form, i.e. linearizing coordinates (3.40) with dependence (3.28) in new coordinates (3.36) are as follows

$$\begin{aligned} \dot{\xi}_1 &= \bar{d}_{11}(\bar{q}_2)^{-1}\xi_2, \quad \dot{\xi}_2 = \xi_3, \quad \dot{\xi}_3 = \xi_4, \\ \dot{\xi}_4 &= \alpha(\bar{q})\tau_2 + \beta(\bar{q},\dot{\bar{q}}) = w \end{aligned} \tag{3.48}$$

with the new coordinates ξ and the input w being well defined wherever $\alpha(\bar{q})^{-1} \neq 0$.

3.3 Chapter conclusion

In this chapter the exact feedback linearization was applied to a general nonlinear model of Acrobot such that the original nonlinear dynamics of Acrobot (2.7) was transformed using

change of coordinates (3.29) and property (3.28) into partially linearized form (3.30). The partially linearized form of Acrobot (3.30) can be used for a reference trajectory design or an exponentially stable state feedback design to track a given reference trajectory. Furthermore, the so-called generalized Acrobot was defined and embedded into the 4-link system to facilitate the walking design for the 4-link case later on.

Chapter 4

Walking trajectory design

The aim of this chapter is to present methods to design walking trajectories for two underactuated walking robots, namely for Acrobot and for 4-link. With slight abuse of notations we will refer to them in the sequel as to pseudo-passive trajectory and multi-step walking trajectory.

4.1 Pseudo-passive trajectory design

The pseudo-passive trajectory was firstly introduced for Acrobot in [30]. The trajectory design is done in ξ coordinates in such a way a reference model fulfills one step according to desired time of the step and desired length of the step. From the partially linearized form and from the meaning of the variables it can be seen that the pseudo-passive trajectory ensures a movement of the center of mass of the walking robot horizontally forward with constant horizontal velocity. Initial conditions on the pseudo-passive trajectory result in no input action in the exact feedback linearized coordinates (3.29), i.e. $w^{ref} \equiv 0$. The word "pseudo" expresses the fact that real torque is not zero, but $\tau_2^{ref} = (\beta(q, \dot{q}) - w^{ref})/\alpha(q, \dot{q})$, due to the linearizing relation between real torque τ_2 and the virtual input w in the partial exact linearized form (3.30).

In [30], the algorithm was presented enabling computing the initial positions $q(0)$ and velocities $\dot{q}(0)$ ensuring the step starts and ends with both "legs" on the ground with required length of the step together with required time duration of the step. The trajectory was successfully used in Acrobot walking control in [3, 4, 14]. The trajectory design was extended in [28] by virtue of the embedding method and the pseudo-passive trajectory for 4-link was successfully used in the application of 4-link walking control. A design of the algorithm for Acrobot and its extension to 4-link will be briefly repeated here.

4.1.1 Pseudo-passive trajectory for Acrobot

To generate the pseudo-passive reference trajectory of the swing phase, a reference model of Acrobot is considered. Therefore, consider the reference model of Acrobot in the following partial exact linearized coordinates related to coordinates of original Acrobot (3.29)

$$\xi_1^{ref} = p^{ref}, \quad \xi_2^{ref} = \sigma^{ref}, \quad \xi_3^{ref} = \dot{\sigma}^{ref}, \quad \xi_4^{ref} = \ddot{\sigma}^{ref}. \tag{4.1}$$

Reference coordinates lead to the reference model of Acrobot with reference dynamics related to dynamics of original Acrobot (3.30) as follows

$$\dot{\xi}_1^{ref} = d_{11}(q_2)^{-1}\xi_2^{ref}, \quad \dot{\xi}_2^{ref} = \xi_3^{ref}, \quad \dot{\xi}_3^{ref} = \xi_4^{ref}, \quad \dot{\xi}_4^{ref} = w^{ref}. \tag{4.2}$$

The Acrobot step is designed in order to fulfill three assumptions

1. step symmetry, i.e. the initial and the final angular positions are the same,
2. the step is done in desired time T,
3. the Acrobot center of mass is horizontally shifted in desired length D.

The reference step design is performed using linearizing coordinates ξ. Reference system (4.2) performs the step according to given initial conditions $\xi_1(0)$, $\xi_2(0)$, $\xi_3(0)$ and $\xi_4(0)$ and input control w^{ref}.

From meaning of linearizing coordinates (3.29) it follows that coordinates ξ_1 and ξ_3 are related to the angular positions whereas coordinates ξ_2 and ξ_4 are related to the angular velocities. First assumption for the step design comes from the step symmetry. It means that the initial and the final angular positions are exactly the same and together with the last assumption, i.e. from required length of the step D, initial conditions for coordinates $\xi_1(0)$ and $\xi_3(0)$ are directly given by transformation (3.32). Coordinate ξ_4 is related to horizontal velocity of the Acrobot center of mass. Clearly, in (3.27) the dependence between $\dot{\sigma}$ and x-position of the center of mass of Acrobot is defined. According to reference Acrobot coordinates (4.1) and reference Acrobot dynamics (4.2) it is necessary to define input control $w^{ref} = 0$, otherwise the Acrobot center of mass would accelerate or decelerate. Therefore, the initial condition for coordinate $\xi_4(0)$ is given from desired length of the step D and from the desired time T of the step. The last initial condition for remaining coordinate $\xi_2(0)$ is tuned up numerically in a way the swing step finishes the step exactly on the ground.

The reference pseudo-passive trajectory has been successfully tested in simulations, especially in applications of its tracking by "real" Acrobot, see Chapter 5. In Figures 4.1a and b one can see courses of reference angular positions and velocities of the reference pseudo-passive trajectory, respectively. In Figure 4.2 one can see the animation of the reference pseudo-passive step.

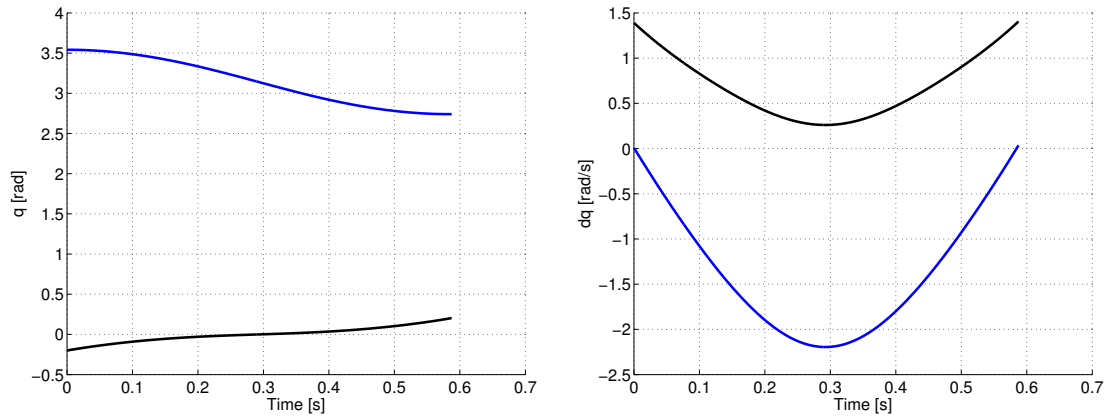

(a) (b)

Figure 4.1. Course of the reference angular positions (a) and velocities (b) of the reference pseudo-passive step. Black lines represent q_1, $\dot{q}_1$ and blue lines represent q_2, $\dot{q}_2$.

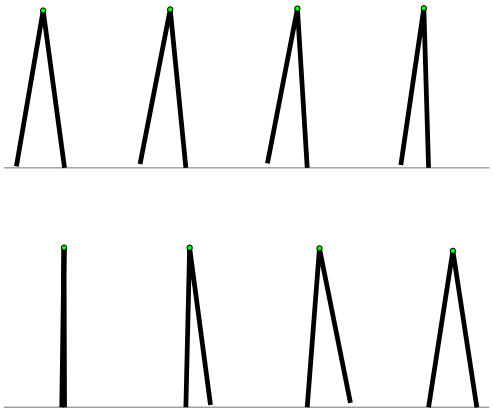

Figure 4.2. The animation of the reference pseudo-passive step.

4.1.2 Pseudo-passive trajectory for 4-link

The design of the pseudo-passive trajectory for 4-link is based on Acrobot design, especially on the design of initial conditions for linearized coordinates $\xi_1(0)$, $\xi_2(0)$, $\xi_3(0)$ and $\xi_4(0)$. Moreover, in addition to Acrobot design, it is necessary to design constraining functions for knees of both legs in 4-link case. Therefore, the design of constraining functions $\phi_3(q_2)$ and $\phi_4(q_2)$ will be done at first.

In the case of 4-link depicted in Figure 2.1b, the virtual constraint functions $\phi_3(q_2)$ and $\phi_4(q_2)$ are defined as follows

$$\begin{aligned} \phi_3 &= 16 b_{stance} \frac{(q_2-q_{2_0})^2 (q_2-q_{2_T})^2}{(-q_{2_0}+q_{2_T})^4} + q_{3_0}, \\ \phi_4 &= 16 b_{swing} \frac{(q_2-q_{2_0})^2 (q_2-q_{2_T})^2}{(-q_{2_0}+q_{2_T})^4} + q_{4_0}, \end{aligned} \tag{4.3}$$

where q_{2_0} and q_{2_T} are the values of the angle q_2 at the beginning and the end of the step, respectively, while q_{3_0} and q_{4_0} are the initial values of the angle q_3 and q_4, respectively. Finally, b_{stance} and b_{swing} are the maximal values of the stretching of the stance and the bending of the swing leg, respectively. Note also, that in Figure 2.1b the angle q_3 is defined to be negative at the beginning of the step, so its growing indeed corresponds to stretching the "knee" of the stance leg, while q_4 is defined to be positive at the beginning of the step, so its growing indeed corresponds to the bending of the swing leg. In Figure 4.4 one can see that the stance leg is stretching until the middle of the step then it is bending back to its initial value. The swing leg is doing other way around. Parameters b_{stance}, b_{swing} can be used to adjust those bending and stretching, so that hitting the ground during the step is avoided.

The rest of the pseudo-passive reference trajectory design for 4-link is the same as in the case of Acrobot thanks to the embedding method, i.e. it is necessary to define initial conditions of linearized coordinates $\xi_1(0)$, $\xi_3(0)$ and $\xi_4(0)$ for the embedded Acrobot (3.40) according to the desired configuration of the step. The initial value of $\xi_2(0)$ is found numerically in a way that the swing leg finishes on the ground at the end of the step. Performing the step during numerical tuning or during a simulation is done with predefined input control $w^{ref} = 0$.

In Figures 4.3a and b one can see courses of the reference angular positions and velocities of the pseudo-passive reference trajectory, respectively. In Figure 4.4 one can see the duration of the reference pseudo-passive step.

4.2 Multi-step trajectory design

The aim of this section is to present an algorithm to design a cyclic walking-like trajectory which is crucial to have a hybrid exponentially stable multi-step tracking of this trajectory

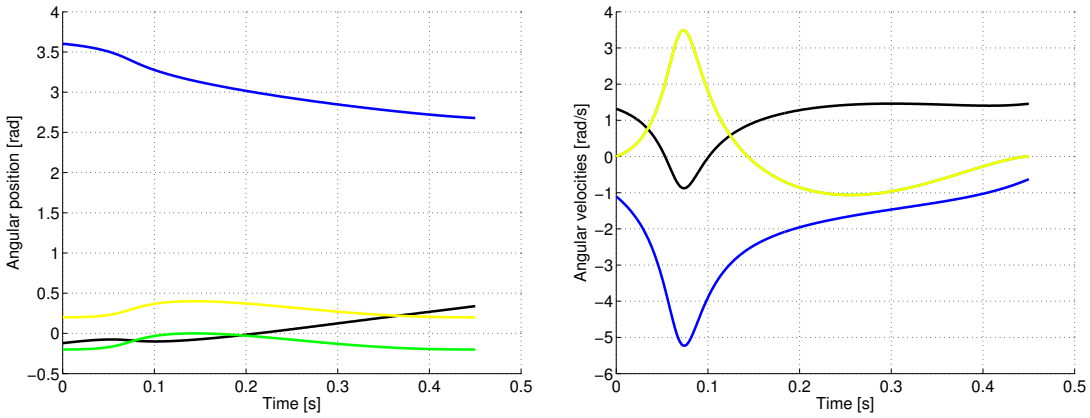

(a) (b)

Figure 4.3. Course of the reference angular positions (a) and velocities (b) of the reference pseudo-passive step. Black lines represent q_1, $\dot{q}_1$, blue lines represent q_2, $\dot{q}_2$, green lines represent q_3, $\dot{q}_3$, and yellow lines represent q_4, $\dot{q}_4$. In the figure (b), the curve of angular velocities $\dot{q}_3$ is covered by the curve of angular velocities $\dot{q}_4$.

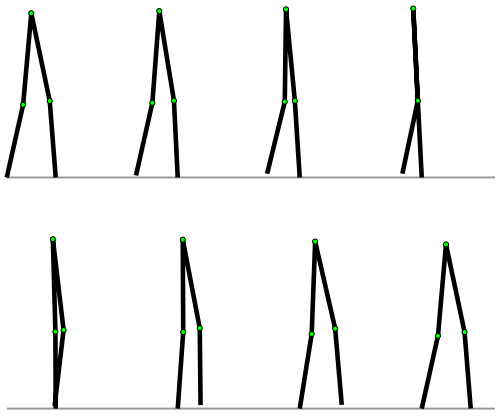

Figure 4.4. The animation of the reference pseudo-passive step.

later on. This design is not an easy task because initial conditions of the multi-step walking trajectory are changed during the single step into different end conditions and these should be subsequently mapped by the impact map into the same initial conditions of the next step as they were at the beginning of the previous step. Partial linearized coordinates are used to design of the multi-step walking trajectory. Such a trajectory is then used to demonstrate the sustainable walking based on the swing phase exponentially stable tracking.

The idea of the multi-step walking trajectory for Acrobot was firstly introduced in [6] and its extension to 4-link was done in [11]. The main advantage of the cyclic walking like trajectory consists in almost no initial error at the beginning of the new step. In contrast, the pseudo-passive trajectory in [28, 30] would have a "renewed" fixed initial error at the beginning of each next step. The multi-step walking trajectory can be simply described as follows

$$\dot{q}(0) = \Phi_{\mathrm{Imp}}(q(T))\,\dot{q}(T^{-}), \tag{4.4}$$

where $\Phi_{\mathrm{Imp}}(q(T))$ is the impact matrix including legs relabeling influence, $q(T)$ is a configuration of Acrobot or 4-link at the end of the step, $\dot{q}(T^{-})$ are angular velocities "just before" the impact, while $\dot{q}(0)$ are angular velocities at the beginning of the next step and by (4.4) they are requested to be equal to those "just after" the impact and re-labeling. For the Acrobot case, the impact matrix is defined by (2.40). Its extension for 4-link is straightforward.

Summarizing, the crucial element in the multi-step walking trajectory design is the impact matrix $\Phi_{\mathrm{Imp}}(q(T))$ that determines the relation between angular velocities at the beginning of the new step and angular velocities at the end of the previous step and it is given by (2.40). Recall that the way how the impact matrix is obtained including legs relabeling effect was shown in detail in Section 2.2.

4.2.1 Acrobot multi-step walking trajectory design

In this section, the design of the multi-step walking trajectory for Acrobot will be presented. The key issue here is to design proper initial angular velocities of Acrobot as its angular positions are naturally continuous even after the impact and due to the symmetry of the postures (the both "legs" of Acrobot are supposed to have the same length).

Based on the impact map, the cyclic multi-step walking trajectory may be derived in the following way. First, denote as $\Phi_{\mathrm{Imp}}(q)$ the impact matrix realizing the influence of the impact on angular velocities including their relabeling due to switching of the legs.

More precisely, it holds that

$$\begin{bmatrix} \dot{q}_1(T^+) \\ \dot{q}_2(T^+) \end{bmatrix} = \Phi_{\mathrm{Imp}}(q(T)) \begin{bmatrix} \dot{q}_1(T^-) \\ \dot{q}_2(T^-) \end{bmatrix}, \tag{4.5}$$

where $\dot{q}_1(T^-), \dot{q}_2(T^-)$ are the angular velocities "just before" the impact, while $\dot{q}_1(T^+)$, $\dot{q}_2(T^+)$ are the angular velocities "just after" the impact and the relabeling, $q(T)$ is the angular configuration of Acrobot at the end of the step. The cyclic multi-step walking trajectory is defined to be such a trajectory that

$$\begin{bmatrix} \dot{q}_1(T^+) \\ \dot{q}_2(T^+) \end{bmatrix} = \begin{bmatrix} \dot{q}_1(0) \\ \dot{q}_2(0) \end{bmatrix}, \tag{4.6}$$

i.e. after the impact at the end of the step the configuration and the angular velocities after relabeling are the same as at the beginning of that step and thereby the next step can repeat exactly the previous one. Notice, that the impact does not affect the angular configuration of Acrobot being affected just by the relabeling only, i.e. $q_1(T)$, $q_2(T)$ are relabeled into $q_1(T^+)$, $q_2(T^+)$ by (2.37) and by symmetry of postures $q_1(T^+) = q_1(0)$ and $q_2(T^+) = q_2(0)$. Course of the step is given by velocities $\dot{q}_1(0)$, $\dot{q}_2(0)$ and input torque τ_2^{ref}, or w^{ref} in partial exact feedback linearized coordinates. The input w^{ref} will be searched in the form $w^{ref} = a + b\,t,\ a, b \in \mathbb{R}$. Therefore, the target trajectory design consists in finding 4 scalar real parameters $a, b, \dot{q}_1(0)$, $\dot{q}_2(0)$ to fulfill 4 independent requirements: average velocity of the center of mass should be D/T, the swing leg should end exactly on the ground for $t = T$ and two conditions (4.6).

In new coordinates (3.31), (3.32), the angular configuration of the step uniquely determines $\xi_{1,3}(0)$ as follows:

$$\begin{aligned} \xi_1(0) &= p(q_1(0), q_2(0)), \\ \xi_3(0) &= G_1(q_1(0), q_2(0)), \end{aligned}$$

where G_1 is gravitational term component given by (2.22). Moreover, the length of the step $D > 0$ is clearly related to $\xi_3(T) - \xi_3(0)$, as it will be shown later on (actually, ξ_3 is proportional to the value of the distance between the stance leg pivot point and the projection of the center of mass onto the walking surface). The course speed of the step is given by the initial angular velocities $\dot{q}_1(0), \dot{q}_2(0)$ being uniquely related (thanks to the partial exact feedback linearizing change of coordinates (3.31), (3.32)), to $\xi_2(0)$ and $\xi_4(0)$ as follows

$$\begin{bmatrix} \xi_2(0) \\ \xi_4(0) \end{bmatrix} = \Phi_2(q(0)) \begin{bmatrix} \dot{q}_1(0) \\ \dot{q}_2(0) \end{bmatrix}, \tag{4.7}$$

where the matrix Φ_2 is given by (3.35) which in turns stems from exact feedback linearization, see [30] or Section 3.1.3 for details.

As a matter of fact, substituting ξ_3 from change of coordinates (3.32) into (3.27), the variable ξ_3 provides the following nice interpretation

$$\frac{\xi_3}{g}(m_1+m_2)^{-1} = x_c, \tag{4.8}$$

where x_c is the horizontal Cartesian coordinate of the center of mass with respect to the origin placed into the pivot point of the stance leg. Both legs have the same mass, therefore, the previous equation can be also interpreted as follows

$$\xi_3(T) - \xi_3(0) = D\, g\, 2\, m. \tag{4.9}$$

As a consequence, the desired step can be designed choosing

$$w^{ref} = a + b\, t, \quad a, b \in \mathbb{R} \tag{4.10}$$

in such a way that

a) $\xi_3(T) = \xi_3(0) + D\, g\, 2\, m$,

b) $q_1(T)$ is such that both legs are on the ground,

c) $\left[\dot{q}_1(T^+), \dot{q}_2(T^(+))\right]' = \left[\dot{q}_1(0), \dot{q}_2(0)\right]'$.

Substituting the above w^{ref} (4.10) into the Acrobot model in ξ coordinates gives

$$\begin{aligned}
\dot{\xi}_1(t) &= d_{11}^{-1}(q_2)\xi_2(t),\\
\xi_2(t) &= \xi_2(0) + \xi_3(0)t + \xi_4(0)\frac{t^2}{2} + a\frac{t^3}{6} + b\frac{t^4}{24},\\
\xi_3(t) &= \xi_3(0) + \xi_4(0)t + a\frac{t^2}{2} + b\frac{t^3}{6},\\
\xi_4(t) &= \xi_4(0) + at + b\frac{t^2}{2},
\end{aligned}$$

while by condition b) and by (4.9) one has

$$D\, g\, 2\, m = \xi_3(T) - \xi_3(0) = \xi_4(0)T + a\frac{T^2}{2} + b\frac{T^3}{6},$$

and therefore

$$\xi_4(0) = \left(D\, g\, 2\, m - a\frac{T^2}{2} - b\frac{T^3}{6}\right) T^{-1}. \tag{4.11}$$

Moreover, by condition c) it holds

$$
\begin{aligned}
(4.12)\qquad & \begin{bmatrix} \dot{q}_1(0) \\ \dot{q}_2(0) \end{bmatrix} = \Phi_{\mathrm{Imp}}(q(T)) \begin{bmatrix} \dot{q}_1(T^-) \\ \dot{q}_2(T^-) \end{bmatrix} = \Phi_{\mathrm{Imp}}(q(T))\Phi_2^{-1}(q(T)) \begin{bmatrix} \xi_2(T) \\ \xi_4(T) \end{bmatrix} = \\
& \Phi_{\mathrm{Imp}}(q(T))\Phi_2^{-1}(q(T)) \times \begin{bmatrix} \xi_2(0) + \xi_3(0)T + \xi_4(0)\frac{T^2}{2} + a\frac{T^3}{6} + b\frac{T^4}{24} \\ \xi_4(0) + aT + b\frac{T^2}{2} \end{bmatrix} = \\
& \Phi_{\mathrm{Imp}}(q(T))\Phi_2^{-1}(q(T)) \times \\
& \qquad \left(\begin{bmatrix} \xi_2(0) \\ 0 \end{bmatrix} + \begin{bmatrix} \xi_3(0)(T) + D\,g\,m\,T \\ \frac{D\,g\,2\,m}{T} \end{bmatrix} + \begin{bmatrix} a\left(\frac{T^3}{6} - \frac{T^3}{4}\right) & b\left(\frac{T^4}{24} - \frac{T^4}{12}\right) \\ a\left(T - \frac{T}{2}\right) & b\left(\frac{T^2}{2} - \frac{T^2}{6}\right) \end{bmatrix} \right).
\end{aligned}
$$

Summarizing

$$
\begin{aligned}
(4.13)\qquad & \begin{bmatrix} \xi_2(0) \\ \frac{D\,g\,2\,m}{T} - a\frac{T}{2} - b\frac{T^2}{6} \end{bmatrix} = \Phi_2(q(0))\Phi_{\mathrm{Imp}}(q(T)) \times \\
& \qquad \Phi_2^{-1}(q(T)) \left(\begin{bmatrix} \xi_2(0) \\ 0 \end{bmatrix} + \begin{bmatrix} \xi_3(0)(T) + D\,g\,m\,T \\ \frac{D\,g\,2\,m}{T} \end{bmatrix} + \begin{bmatrix} -\frac{T^3}{12} & -\frac{T^4}{24} \\ \frac{T}{2} & \frac{T^2}{3} \end{bmatrix} \begin{bmatrix} a \\ b \end{bmatrix} \right).
\end{aligned}
$$

This means that

$$
\begin{aligned}
(4.14)\qquad & \begin{bmatrix} a \\ b \end{bmatrix} = \left(\Phi_2(q(0))\Phi_{\mathrm{Imp}}(q(T))\Phi_2^{-1}(q(T)) \times \begin{bmatrix} -\frac{T^3}{12} & -\frac{T^4}{24} \\ \frac{T}{6} & \frac{T^2}{3} \end{bmatrix} + \begin{bmatrix} 0 & 0 \\ \frac{T}{2} & \frac{T^2}{6} \end{bmatrix} \right)^{-1} \times \\
& \left(\begin{bmatrix} 0 \\ \frac{D\,g\,2\,m}{T} \end{bmatrix} - \Phi_2(q(0))\Phi_{\mathrm{Imp}}(q(T))\Phi_2^{-1}(q(T)) \times \begin{bmatrix} \xi_3(0)T + D\,g\,m\,T \\ \frac{D\,g\,2\,m}{T} \end{bmatrix} + \right. \\
& \qquad \left. \left[I - \Phi_2(q(0))\Phi_{\mathrm{Imp}}(q(T))\Phi_2^{-1}(q(T)) \right] \begin{bmatrix} \xi_2(0) \\ 0 \end{bmatrix} \right).
\end{aligned}
$$

The last relation suggests the following algorithm for cyclic multi-step walking trajectory tuning. For any given initial condition $\xi_2(0)$ one computes by (4.14) a, b and consequently also by (4.11) $\xi_4(0)$ such that "if impact occurs", then angular velocities after the impact and relabeling are exactly the same as at the beginning of the step. Therefore, the only issue to be solved and tuned is that, indeed, exactly at $t = T$ impact occurs, i.e. the swing leg hits the ground exactly at $t = T$. This is done by numerical tuning of $\xi_2(0)$ being the only remaining free parameter. Simple dichotomy algorithm is able to repeat the above procedure adjusting $\xi_2(0)$ until the swing leg ends exactly on the ground at $t = T$.

In Figures 4.5a and b, one can see the course of reference angular positions and velocities of the multi-step walking reference trajectory, respectively. In Figure 4.6 one can see the animation of the multi-step walking reference trajectory.

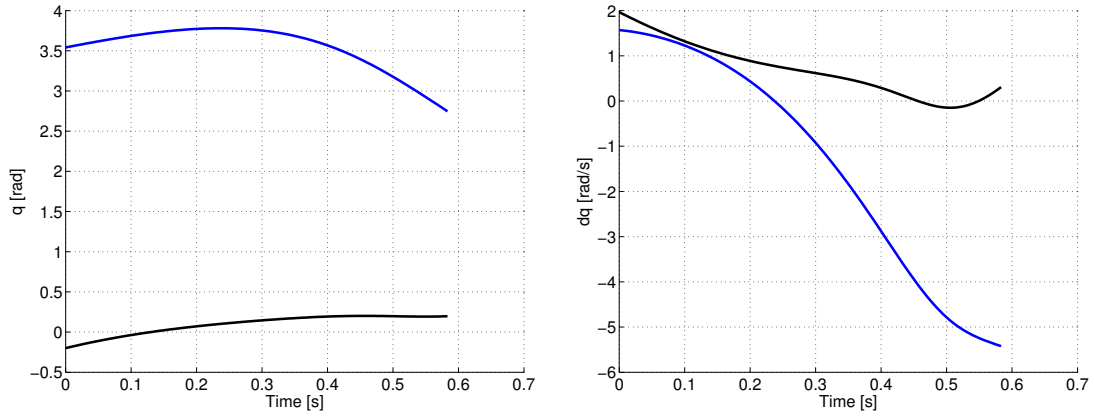

(a) (b)

Figure 4.5. Course of the reference angular positions (a) and velocities (b) of the multi-step walking reference trajectory. Black lines represent q_1, $\dot{q}_1$ and blue lines represent q_2, $\dot{q}_2$.

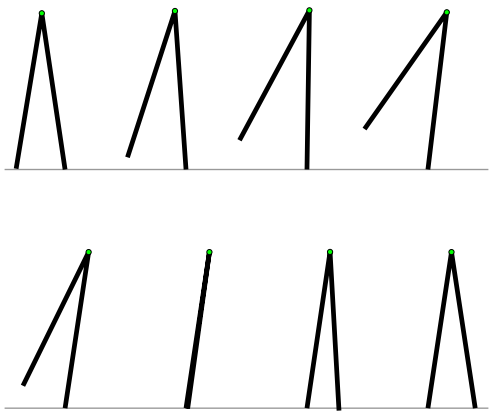

Figure 4.6. The animation of the multi-step walking reference trajectory.

To demonstrate the multi-step walking trajectory, this trajectory has been tuned and then tracked during 3 steps. The feedback control strategy described in [3] and in Chapter 5 later on was used. The corresponding simulations are shown in Figures 4.7a, b.

For the sake of comparison, the feedback tracking of the pseudo-passive trajectory was simulated during 2 steps with the same control approach. The corresponding simulations are shown in Figures 4.8a, b. At the end of the first step the "real" trajectory is close to the pseudo-passive reference trajectory, however, after the impact the beginning of the

"real" trajectory is mapped far away from the beginning of the reference one and the tracking algorithm is not able to minimize the initial error caused by the impact. As a consequence, the simulation crashes in the middle of the second step. In the contrast to the cyclic trajectory, there is an additional initial error, caused by the impact, which has to be minimized during the step for the pseudo-passive trajectory.

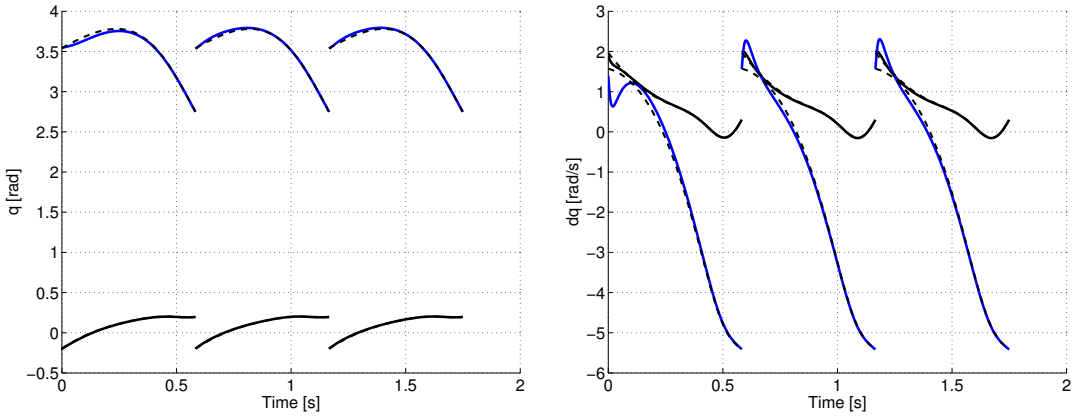

(a) (b)

Figure 4.7. Tracking of the multi-step walking reference trajectory. Angular positions (a) and angular velocities (b).

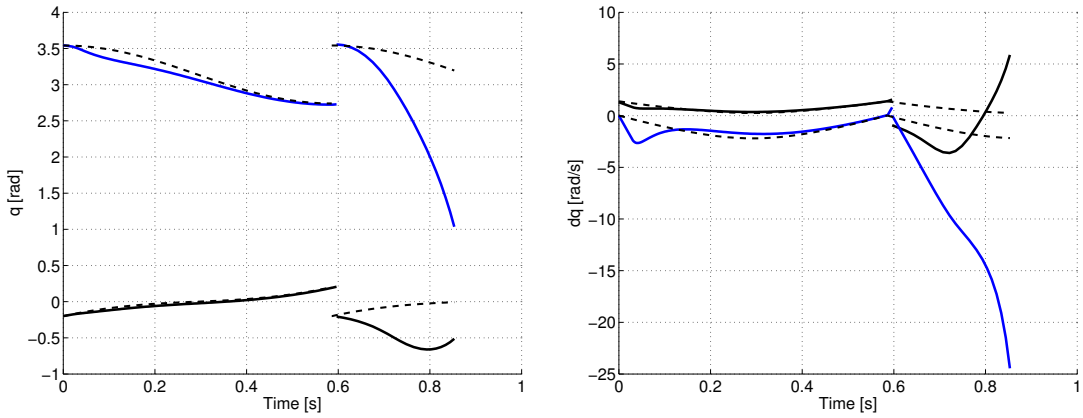

(a) (b)

Figure 4.8. Tracking the pseudo-passive reference trajectory during two steps. Angular positions (a) and angular velocities (b).

4.2.2 4-link multi-step walking trajectory design

In this section, the design of the multi-step walking trajectory for 4-link will be suggested. The trajectory design is based on the Acrobot multi-step walking trajectory

design by virtue of the so-called embedding method and it is extended by yet another algorithm helping to define the proper values of the initial and the final derivatives of the constraining functions.

Proper initial angular velocities of 4-link are crucial for the multi-step walking trajectory design as it was in Acrobot case. Conditions for angular positions are automatically satisfied due to matching of 4-link postures at the beginning and at the end of the step. The walking like cyclic trajectory is again such a trajectory where the angular velocities just after the impact at the end of the step are equal to velocities at the beginning of the next step, i.e.

$$\begin{bmatrix} \dot{q}_1(T^+) \\ \dot{q}_2(T^+) \\ \dot{q}_3(T^+) \\ \dot{q}_4(T^+) \end{bmatrix} = \begin{bmatrix} \dot{q}_1(0) \\ \dot{q}_2(0) \\ \dot{q}_3(0) \\ \dot{q}_4(0) \end{bmatrix}, \tag{4.15}$$

where $\dot{q}_{\mathrm{x}}(T^+)$ represents the angular velocity at the end of the step after the impact and the relabeling whereas $\dot{q}_{\mathrm{x}}(0)$ represents the angular velocity at the beginning of the step. In such a way, the next step starts in the same way as the previous one.

The relation between angular velocities at the end of the step before and after the impact is given by the impact matrix $\Phi_{\mathrm{Imp}}(q)$ as follows

$$\begin{bmatrix} \dot{q}_1(T^+) \\ \dot{q}_2(T^+) \\ \dot{q}_3(T^+) \\ \dot{q}_4(T^+) \end{bmatrix} = \Phi_{\mathrm{Imp}}(q(T)) \begin{bmatrix} \dot{q}_1(T^-) \\ \dot{q}_2(T^-) \\ \dot{q}_3(T^-) \\ \dot{q}_4(T^-) \end{bmatrix}, \tag{4.16}$$

where $\dot{q}_{\mathrm{x}}(T^-)$ are angular velocities "just before" the impact, while $\dot{q}_{\mathrm{x}}(T^+)$ are angular velocities "just after" the impact and the relabeling. For details about obtaining (4.16) see Section 2.2. In the case of 4-link, the impact matrix has the following form

$$\Phi_{\mathrm{Imp}}(q(T)) = \begin{bmatrix} \phi_{11} & \phi_{12} & \phi_{13} & \phi_{14} \\ \phi_{21} & \phi_{22} & \phi_{23} & \phi_{24} \\ \phi_{31} & \phi_{32} & \phi_{33} & \phi_{34} \\ \phi_{41} & \phi_{42} & \phi_{43} & \phi_{44} \end{bmatrix}, \tag{4.17}$$

where ϕ_{xx} are scalar entries of the impact matrix.

By virtue of the method of embedding the generalized Acrobot into 4-link, the angles in knees q_3 and q_4 depend on the angle in the hip q_2 via constraining functions $\phi_3(q_2)$ and

$\phi_4(q_2)$. Moreover, angular velocities in knees $\dot{q}_3$ and $\dot{q}_4$ depend on the angular velocity in the hip $\dot{q}_2$ as follows

$$\dot{q}_3 = \frac{\partial \phi_3(q_2)}{\partial q_2}\dot{q}_2, \quad \dot{q}_4 = \frac{\partial \phi_4(q_2)}{\partial q_2}\dot{q}_2. \tag{4.18}$$

One can see from equation (4.18) that the angular velocities in knees and in the hip are connected through virtual constraints derivatives. The idea of presented multi-step walking trajectory design consists in a design of values $\dot{q}_3$ and $\dot{q}_4$ at the beginning and at the end of the step in such a way that (4.18) is preserved by the impact whatever $\dot{q}_1$, $\dot{q}_2$, $\dot{q}_3$, $\dot{q}_4$ are. Afterward, the design of initial and final values of $\dot{q}_1$ and $\dot{q}_2$ will be done separately for embedded generalized Acrobot (3.40).

The initial and the final value design of derivatives of constraining functions

To simplify the forthcoming derivation of suitable values $\frac{\partial \phi_3(q_2)}{\partial q_2}$ and $\frac{\partial \phi_4(q_2)}{\partial q_2}$ the following notation is introduced

$$b_3 = \frac{\partial \phi_3(q_2(0))}{\partial q_2}, \quad f_3 = \frac{\partial \phi_3(q_2(T))}{\partial q_2}, \tag{4.19}$$

$$b_4 = \frac{\partial \phi_4(q_2(0))}{\partial q_2}, \quad f_4 = \frac{\partial \phi_4(q_2(T))}{\partial q_2}. \tag{4.20}$$

For the same reason, in the forthcoming derivation, the angular velocities at the end of the step "just before" the impact are denoted as $\dot{q}_{1234}(T)$ instead of $\dot{q}_{1234}(T^-)$. Therefore equation (4.16) has the following form

$$\begin{bmatrix} \dot{q}_1(0) \\ \dot{q}_2(0) \\ \dot{q}_3(0) \\ \dot{q}_4(0) \end{bmatrix} = \Phi_{\mathrm{Imp}}(q(T)) \begin{bmatrix} \dot{q}_1(T) \\ \dot{q}_2(T) \\ f_3\,\dot{q}_2(T) \\ f_4\,\dot{q}_2(T) \end{bmatrix}. \tag{4.21}$$

From (4.21) one has as follows

$$\begin{bmatrix} \dot{q}_1(0) \\ \dot{q}_2(0) \end{bmatrix} = \left[\begin{array}{c|c} \phi_{11} & \phi_{12} + \phi_{13}f_3 + \phi_{14}f_4 \\ \hline \phi_{21} & \phi_{22} + \phi_{23}f_3 + \phi_{24}f_4 \end{array}\right] \begin{bmatrix} \dot{q}_1(T) \\ \dot{q}_2(T) \end{bmatrix} \tag{4.22}$$

$$\begin{bmatrix} \dot{q}_3(0) \\ \dot{q}_4(0) \end{bmatrix} = \left[\begin{array}{c|c} \phi_{31} & \phi_{32} + \phi_{33}f_3 + \phi_{34}f_4 \\ \hline \phi_{41} & \phi_{42} + \phi_{43}f_3 + \phi_{44}f_4 \end{array}\right] \begin{bmatrix} \dot{q}_1(T) \\ \dot{q}_2(T) \end{bmatrix}. \tag{4.23}$$

Indeed, substituting $\dot{q}_2(0)$ from (4.22) into (4.18) gives

$$\begin{bmatrix} \dot{q}_3(0) \\ \dot{q}_4(0) \end{bmatrix} = \begin{bmatrix} b_3\,\dot{q}_2(0) \\ b_4\,\dot{q}_2(0) \end{bmatrix} = \begin{bmatrix} b_3\left(\phi_{21}\dot{q}_1(T) + (\phi_{22} + \phi_{23}f_3 + \phi_{24}f_4)\,\dot{q}_2(T)\right) \\ b_4\left(\phi_{21}\dot{q}_1(T) + (\phi_{22} + \phi_{23}f_3 + \phi_{24}f_4)\,\dot{q}_2(T)\right) \end{bmatrix} \tag{4.24}$$

and substituting equation (4.24) into (4.23) gives the final equation as follows

$$\begin{bmatrix} b_3\left(\phi_{21}\dot{q}_1(T) + (\phi_{22} + \phi_{23}f_3 + \phi_{24}f_4)\,\dot{q}_2(T)\right) \\ b_4\left(\phi_{21}\dot{q}_1(T) + (\phi_{22} + \phi_{23}f_3 + \phi_{24}f_4)\,\dot{q}_2(T)\right) \end{bmatrix} = \begin{bmatrix} \phi_{31} & \phi_{32} + \phi_{33}f_3 + \phi_{34}f_4 \\ \phi_{41} & \phi_{42} + \phi_{43}f_3 + \phi_{44}f_4 \end{bmatrix} \begin{bmatrix} \dot{q}_1(T) \\ \dot{q}_2(T) \end{bmatrix}. \tag{4.25}$$

After rearrangement, the form of equation (4.25) is as follows

$$\begin{bmatrix} b_3\phi_{21} - \phi_{31} & b_3\left(\phi_{22} + \phi_{23}f_3 + \phi_{24}f_4\right) - \phi_{32} - \phi_{33}f_3 - \phi_{34}f_4 \\ b_4\phi_{21} - \phi_{41} & b_4\left(\phi_{22} + \phi_{23}f_3 + \phi_{24}f_4\right) - \phi_{42} - \phi_{43}f_3 - \phi_{44}f_4 \end{bmatrix} \begin{bmatrix} \dot{q}_1(T) \\ \dot{q}_2(T) \end{bmatrix} = 0. \tag{4.26}$$

Values of coefficients b_3, b_4, f_3 and f_4 are computed realizing that (4.26) should hold for every $\dot{q}_1(T)$, $\dot{q}_2(T)$. Therefore, the matrix on the left hand side of (4.26) should be zero. This gives b_3, b_4, f_3 and f_4 as follows

$$b_3 = \frac{\phi_{31}}{\phi_{21}}, \quad b_4 = \frac{\phi_{41}}{\phi_{21}}, \tag{4.27}$$

$$\begin{bmatrix} f_3 \\ f_4 \end{bmatrix} = \begin{bmatrix} \phi_{23}\frac{\phi_{31}}{\phi_{21}} - \phi_{33} & \phi_{24}\frac{\phi_{31}}{\phi_{21}} - \phi_{34} \\ \phi_{23}\frac{\phi_{41}}{\phi_{21}} - \phi_{43} & \phi_{24}\frac{\phi_{41}}{\phi_{21}} - \phi_{44} \end{bmatrix}^{-1} \begin{bmatrix} \phi_{32} - \phi_{22}\frac{\phi_{31}}{\phi_{21}} \\ \phi_{42} - \phi_{22}\frac{\phi_{41}}{\phi_{21}} \end{bmatrix}. \tag{4.28}$$

Multi-step walking trajectory design for embedded Acrobot

In the previous part, the initial and the final derivatives of constraining functions $\phi_3(q_2)$, $\phi_4(q_2)$ were defined in order to separate the design of initial and final values of angular velocities $\dot{q}_1$, $\dot{q}_2$ from $\dot{q}_3$, $\dot{q}_4$. The initial and the final values of angular velocities $\dot{q}_3$ and $\dot{q}_4$ are given by equations (4.27), (4.28) whereas the initial and the final values of $\dot{q}_1$, $\dot{q}_2$ will be determined here.

Remaining values of angular velocities $\dot{q}_1$, $\dot{q}_2$ at the beginning and at the end of the step will be determined by adaptation of already developed method for Acrobot in [6] by

virtue of the embedding method of generalized Acrobot into 4-link. For this reason, only main points of the multi-step walking trajectory design will be mentioned here.

The angular configuration of the step is given by $q_1(0)$, $q_2(0)$, time of the step T and length of the step D are given as well. Moreover, the impact does not affect the angular configuration being affected by the relabeling only. Course of the step is given by velocities $\dot{q}_1(0)$, $\dot{q}_2(0)$ and input torque τ_2^{ref}, or w^{ref} in partial exact feedback linearized coordinates. We aim to look for the input w^{ref} in the form $w^{ref} = a + b\,t,\ a, b \in \mathbb{R}$. Therefore, the target trajectory design consists in finding 4 scalar real parameters a, b, $\dot{q}_1(0)$, $\dot{q}_2(0)$ to fulfill 4 independent requirements: the average velocity of the center of mass should be D/T, the swing leg should end exactly on the ground for $t = T$ and the first two conditions from (4.15).

The design will be done in ξ coordinates (3.40). According to the coordinates definition, the coordinates $\xi_1(0)$ and $\xi_3(0)$ are given by angular configuration of the step, moreover, $\xi_3(T) - \xi_3(0) = 2\,D\,g\,m$, where m is total mass of 4-link and D is length of the step. The coordinate $\xi_4(0)$ is defined according to (4.11) as follows

$$\xi_4(0) = \frac{\xi_3(T) - \xi_3(0)}{T} - a\frac{T}{2} - b\frac{T^2}{6}. \tag{4.29}$$

Parameters a, b are defined as follows

$$\begin{bmatrix} a \\ b \end{bmatrix} = (\mathcal{A} - \mathcal{B})^{-1}\,\mathcal{C}, \tag{4.30}$$

where

$$\mathcal{A} = \begin{bmatrix} -\frac{T^3}{12} & -\frac{T^4}{24} \\ \frac{T}{2} & \frac{T^2}{3} \end{bmatrix}, \quad \mathcal{B} = \Phi^{\xi}_{\mathrm{Imp}} \begin{bmatrix} 0 & 0 \\ -\frac{T}{2} & -\frac{T^2}{6} \end{bmatrix}, \tag{4.31}$$

$$\mathcal{C} = \begin{bmatrix} \xi_2(0) + \frac{\xi_3(T)-\xi_3(0)}{T}\frac{T^2}{2} + \xi_3(0)T \\ \frac{\xi_3(T)-\xi_3(0)}{T} \end{bmatrix} - \Phi^{\xi}_{\mathrm{Imp}} \begin{bmatrix} \xi_2(0) \\ \frac{\xi_3(T)-\xi_3(0)}{T} \end{bmatrix}. \tag{4.32}$$

$\Phi^{\xi}_{\mathrm{Imp}}$ is the impact matrix expressed in ξ coordinates. The only remaining parameter to be defined is $\xi_2(0)$. This parameter is determined by a simple numerical dichotomy algorithm ensuring that the swing leg finishes exactly on the ground at the desired time T.

In Figures 4.9a and b, one can see the course of the reference angular positions and velocities of the multi-step walking reference trajectory, respectively. In Figure 4.10 one can see the animation of the reference multi-step walking trajectory.

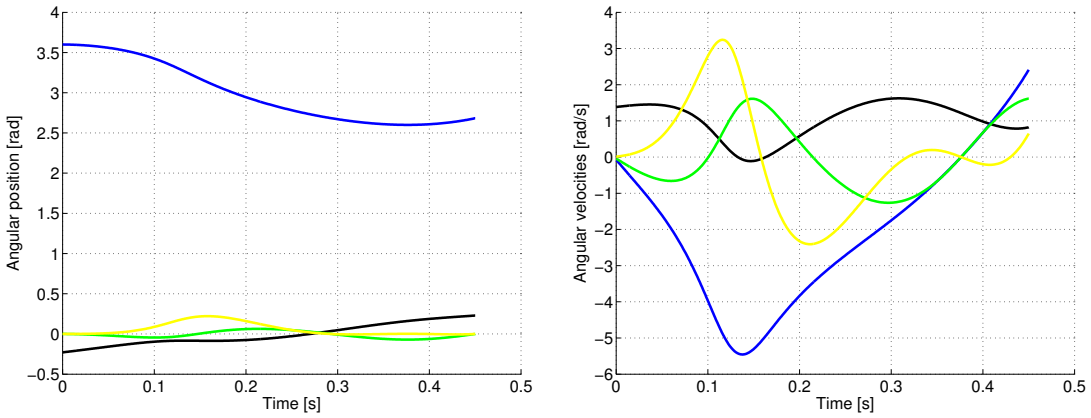

(a) (b)

Figure 4.9. Course of the reference angular positions (a) and velocities (b) of the reference multi-step walking trajectory. Black lines represent q_1, $\dot{q}_1$, blue lines represent q_2, $\dot{q}_2$, green lines represent q_3, $\dot{q}_3$, and yellow lines represent q_4, $\dot{q}_4$.

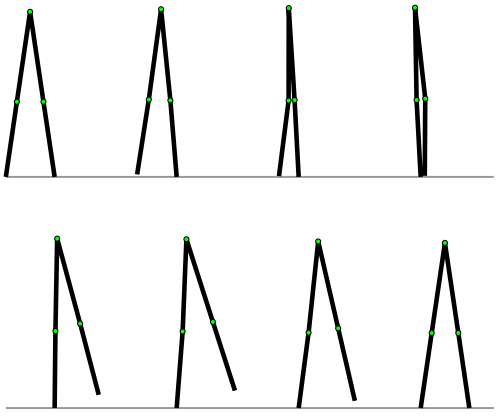

Figure 4.10. The animation of the reference multi-step walking trajectory.

The advantage of the multi-step walking trajectory for the generalized Acrobot can be demonstrated similarly as in the case of the multi-step walking trajectory for Acrobot. Both trajectories, the pseudo-passive trajectory and the multi-step walking trajectory have been tracked during several steps with a feedback control strategy from [28]. The corresponding simulations of the multi-step walking reference trajectory tracking during 3 steps with an initial error in angular positions and velocities are shown in Figures 4.11a, b and 4.12a, b. One can easily see that the convergence during three steps to reference angular positions and velocities depicted in figures with dotted line is not significantly influenced by the impact. However, in simulations of pseudo-passive reference trajectory tracking in two steps, depicted in Figures 4.13a, b and 4.14a, b, one can see that after the impact the beginning of the 4-link trajectory is mapped far away from the beginning of the reference one and the tracking algorithm is not able to minimize the initial error caused by the impact and therefore the simulation crashes at the beginning of the second step.

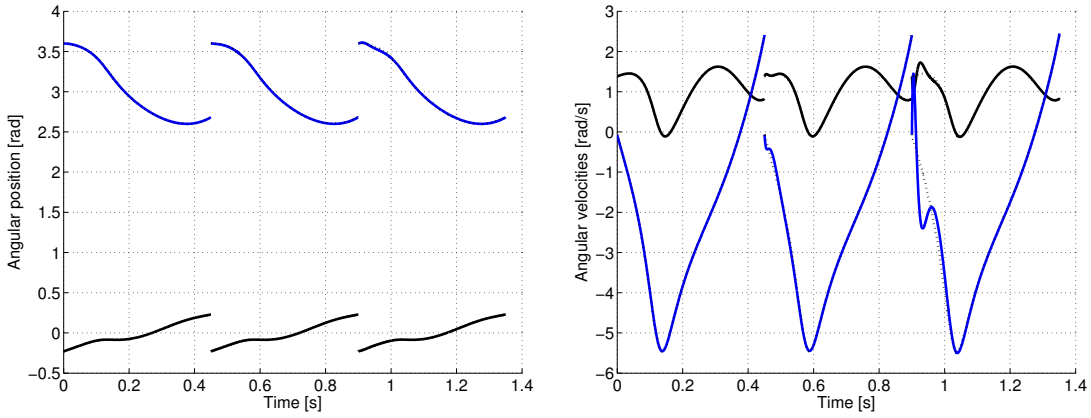

(a) (b)

Figure 4.11. Tracking of the multi-step walking reference trajectory for 3 steps walking. Angular positions q_1 (black line), q_2 (blue line) and references (dotted line) (a) and angular velocities $\dot{q}_1$ (black line), $\dot{q}_2$ (blue line) and references (dotted line) (b).

4.3 Chapter conclusions

Algorithms for the design of two reference trajectories for Acrobot and for 4-link have been presented in this chapter and used to tune either the so-called pseudo-passive reference trajectory or the so-called multi-step walking reference trajectory. The pseudo-passive trajectory ensures a movement of the center of mass of the walking robot horizontally forward with constant horizontal velocity whereas the multi-step walking trajectory have

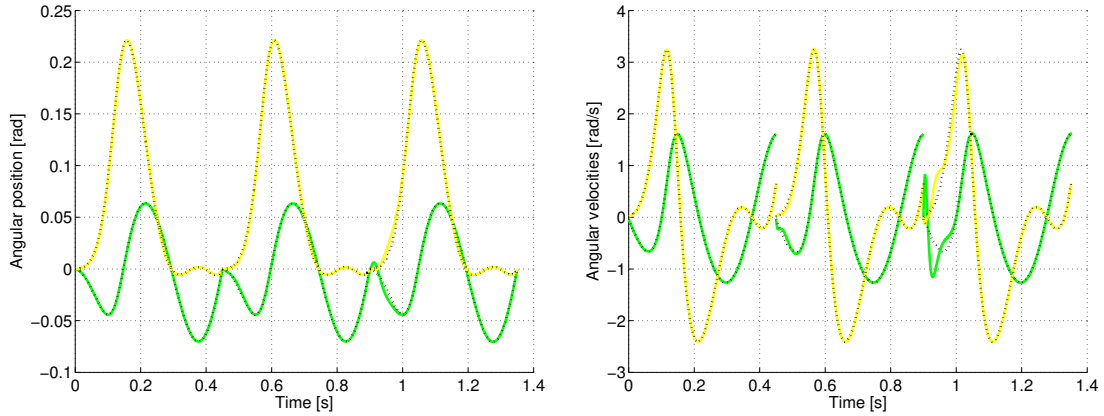

(a) (b)

Figure 4.12. Tracking of the multi-step walking reference trajectory for 3 steps walking. Angular positions q_3 (green line), q_4 (yellow line) and references (dotted line) (a) and angular velocities $\dot{q}_3$ (green line), $\dot{q}_4$ (yellow line) and references (dotted line) (b).

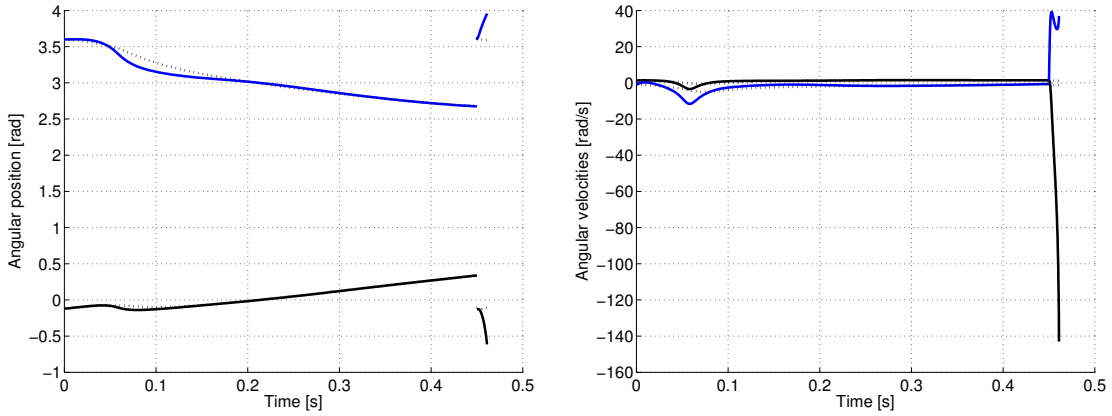

(a) (b)

Figure 4.13. Tracking of the pseudo-passive reference trajectory in 2 steps. Angular positions q_1 (black line), q_2 (blue line) and references (dotted line) (a) and angular velocities $\dot{q}_1$ (black line), $\dot{q}_2$ (blue line) and references (dotted line) (b).

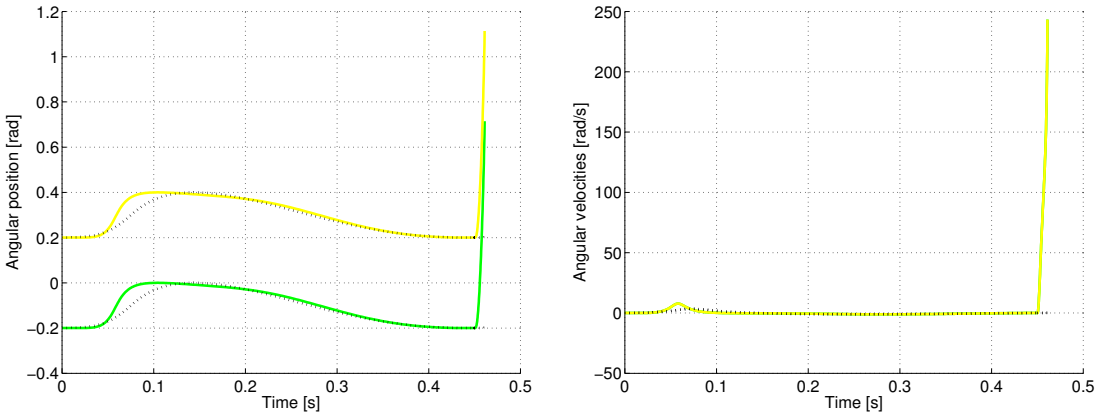

(a) (b)

Figure 4.14. Tracking of the pseudo-passive reference trajectory in 2 steps. Angular positions q_3 (green line), q_4 (yellow line) and references (dotted line) (a) and angular velocities $\dot{q}_3$ (green line), $\dot{q}_4$ (yellow line) and references (dotted line) (b).

after the impact and re-labeling the same initial angular velocities as at the beginning of the step. The clear advantages of the multi-step reference trajectory have been demonstrated.

Chapter 5

Reference trajectory tracking

A control application usually consists of two independent parts. The first part involves generation of a reference trajectory to be tracked whereas the second part involves a controller design according to a robust, optimal or another criterion. The reference trajectory was already developed in the previous chapter and in the current chapter it is to be tracked in order to achieve walking like movement resemblant to a human walk. As it might have been expected, asymptotic or even exponential tracking constitutes a principally more complicated problem than the stabilization since the corresponding error dynamics has a more complex time dependent structure than Acrobot or 4-link itself.

Ideas of the feedback tracking derived and firstly presented in [30, 136], or in [134], are given here as well as their extensions presented in [3, 7, 9, 14, 28]. Roughly speaking, to achieve state feedback tracking of the desired trajectory generated by the reference input w^{ref} one has to set $w = w^{ref} + feedb(e_1, e_2, e_3, e_4, t)$, where $feedb(\cdot)$ is a suitable state error feedback, possibly depending on time. The method in [14] is based on the robust approach whereas methods in [3, 7, 9, 28] are based on a deeper knowledge of the reference system to be tracked.

The current chapter is related to Acrobot control, nevertheless by virtue of the embedding method, the proposed control algorithms can be straightforwardly extended to the 4-link control as well. Moreover, tracking of the pseudo-passive trajectory only is considered in this chapter.

5.1 Tracking task in linearized coordinates

In the application of the reference trajectory tracking, the reference trajectory is generated by an open loop control of "reference" Acrobot. In more detail, the reference system in

the partial exact linearized coordinates (4.2)

$$\dot{\xi}_1^{ref} = d_{11}(q_2)^{-1}\xi_2^{ref}, \quad \dot{\xi}_2^{ref} = \xi_3^{ref}, \quad \dot{\xi}_3^{ref} = \xi_4^{ref}, \quad \dot{\xi}_4^{ref} = w^{ref} \tag{5.1}$$

generates the desired reference trajectory using a suitable open loop control w^{ref} in order to generate either the pseudo-passive or the multi-step walking reference trajectory to be tracked by Acrobot. To do so, "real" Acrobot dynamics in partial exact linearized form (3.30)

$$\dot{\xi}_1 = d_{11}(q_2)^{-1}\xi_2, \quad \dot{\xi}_2 = \xi_3, \quad \dot{\xi}_3 = \xi_4, \quad \dot{\xi}_4 = \alpha(q)\tau_2 + \beta(q,\dot{q}) = w \tag{5.2}$$

is used too.

To obtain the exponentially stable state feedback, subtract the "reference" system (5.1) from the "real" one (5.2), i.e. introduce error $e =: \xi - \xi^{ref}$ for which it holds

$$\begin{aligned} \dot{e}_1 &= d_{11}^{-1}(\phi_2(\xi_1,\xi_3))\xi_2 - d_{11}^{-1}(\phi_2(\xi_1^{ref},\xi_3^{ref}))\xi_2^{ref}, \\ \dot{e}_2 &= e_3, \quad \dot{e}_3 = e_4, \quad \dot{e}_4 = w - w^{ref}. \end{aligned} \tag{5.3}$$

Moreover, straightforward computations based on Taylor expansions adjust the first line of the error dynamics into the following form

$$\begin{aligned} \dot{e}_1 &= \mu_1(t)e_1 + \mu_2(t)e_2 + \mu_3(t)e_3 + o(e), \\ \dot{e}_2 &= e_3, \quad \dot{e}_3 = e_4, \quad \dot{e}_4 = w - w^{ref}, \end{aligned} \tag{5.4}$$

which depicts dependency of $\dot{e}_1$ on errors e_1, e_2, e_3 using known functions $\mu_1(t)$, $\mu_2(t)$ and $\mu_3(t)$ defined as follows

$$\mu_1(t) = \xi_2^{ref}(t)\frac{\partial[d_{11}^{-1}]}{\partial q_2}\frac{\partial\phi_2}{\partial\xi_1}(q_2^{ref}(t)), \tag{5.5}$$

$$\mu_2(t) = d_{11}^{-1}(q_2^{ref}(t)), \tag{5.6}$$

$$\mu_3(t) = \xi_2^{ref}(t)\frac{\partial[d_{11}^{-1}]}{\partial q_2}\frac{\partial\phi_2}{\partial\xi_3}(q_2^{ref}(t)). \tag{5.7}$$

Functions $\mu_{1,2,3}(t)$ can be simply expressed by virtue of the error dynamics definition for both reference trajectory for Acrobot or for 4-link. In Figures 5.16, 5.17 one can see their real waveforms. Their detailed analytical expression for the Acrobot pseudo-passive reference trajectory could be found in [3]. In those figures one can easily see that functions $\mu_{1,2,3}(t)$ are bounded, continuous and differentiable. All the properties are exploited in feedback control algorithms in [3, 7, 9, 14, 28] presented later on.

It is straightforward to express error dynamics (5.4) as the open-loop continuous time-varying linear system

$$\dot{e} = A(t)e + Bu, \tag{5.8}$$

where

$$A(t) = \begin{pmatrix} \mu_1(t) & \mu_2(t) & \mu_3(t) & 0 \\ 0 & 0 & 1 & 0 \\ 0 & 0 & 0 & 1 \\ 0 & 0 & 0 & 0 \end{pmatrix}, \qquad B = \begin{pmatrix} 0 \\ 0 \\ 0 \\ 1 \end{pmatrix}.$$

Then the tracking problem consists in finding a state-feedback controller in its typical form

$$u = Ke, \quad K = \begin{pmatrix} K_1 & K_2 & K_3 & K_4 \end{pmatrix}, \tag{5.9}$$

producing the following closed-loop system

$$\dot{e} = (A + BK)\, e = \begin{pmatrix} \mu_1(t) & \mu_2(t) & \mu_3(t) & 0 \\ 0 & 0 & 1 & 0 \\ 0 & 0 & 0 & 1 \\ K_1 & K_2 & K_3 & K_4 \end{pmatrix} e, \tag{5.10}$$

where bounds for $\mu(t) = (\mu_1(t), \mu_2(t), \mu_3(t))$ are given by (5.5)-(5.7).

In [30], the exponential tracking of the suitable target trajectory generated by an open-loop reference control was obtained. In particular, designed tracking feedback could handle limited initial tracking error only and its performance was limited to the case when the Acrobot walking-like movement was very slow. This was caused by the specific and analytic method to stabilize tracking error dynamics there. Following chapters demonstrate an extension of the control approach initiated in [30] in order to find either a robust or a more precise controller for Acrobot or for 4-link.

5.2 LMI based stabilization of the error dynamics

In this section, the error dynamics stabilization via a numerical tuning using an LMI approach is used to improve the limited results from [30]. The basic idea from [15, 14] is interpreted here.

Despite the fact that entries of $\mu(t)$ are known functions the basic idea here is to treat them as unknown disturbances satisfying some constraints. If constraints are tight enough, one can think about solving quadratic stability conditions and design a unique feedback stabilization of such an "uncertain" system. Obviously, such a feedback would be at the same time solving tracking problem (5.9), (5.10).

To pursue this idea, LMI conditions for a quadratic stability were obtained in [15, 14]. Consider the well-known Lyapunov inequality to be solved for all boundary values of $\mu(t)$ by finding a suitable symmetric positive definite matrix S and a vector K

$$(A(\mu) + BK)^{\mathrm{T}} S + S\,(A(\mu) + BK) \preceq 0, \tag{5.11}$$

$$S = S^{\mathrm{T}} \succ 0. \tag{5.12}$$

Such a problem is in fact bilinear with respect to unknowns. Denoting

$$Q = S^{-1}, \quad Y = KS^{-1} \tag{5.13}$$

the following LMI condition for the quadratically stabilizing feedback design is derived:

$$QA^{\mathrm{T}}(\mu) + A(\mu)Q + Y^{\mathrm{T}}B^{\mathrm{T}} + BY \preceq 0. \tag{5.14}$$

Notice that the pair $(A(\mu), B)$ is controllable if and only if

$$\mu_1\mu_3 + \mu_2 \neq 0. \tag{5.15}$$

If the set of possible values of $\mu(t)$ contains, or stays close to the singular set given by (5.15), LMI (5.14) becomes infeasible or almost infeasible.

As already indicated, bounds on $\mu(t)$ during a single step of Acrobot can be obtained numerically, see Figures 5.1a, b where the trajectory $\mu(t)$ for the pseudo-passive reference trajectory is depicted. Two cases of LMI solving are considered here. Firstly, when the trajectory $\mu(t)$ is estimated by a box-like (rectangular) set and secondly by a prism-like (non-rectangular) set.

Consider the first case when the convex set is defined as a rectangular box, see Figure 5.1a. Each vertex of the box is defined by a combination of upper and lower bounds on entries of $\mu(t)$. Summarizing, we have 8 constraints

$$\begin{aligned} &QA_i^{\mathrm{T}} + A_iQ + Y^{\mathrm{T}}B^{\mathrm{T}} + BY \preceq 0, i = 1, \ldots, 8, \\ &A_1 = A\left(\overline{\mu_1}, \overline{\mu_2}, \overline{\mu_3}\right),\ A_2 = A\left(\underline{\mu_1}, \overline{\mu_2}, \overline{\mu_3}\right),\ \ldots, \\ &A_7 = A\left(\underline{\mu_1}, \underline{\mu_2}, \overline{\mu_3}\right),\ A_8 = A\left(\underline{\mu_1}, \underline{\mu_2}, \underline{\mu_3}\right). \end{aligned} \tag{5.16}$$

In the second case the parameter set is reduced to a convex set much closer to the actual trajectory $\mu(t)$. The number of LMI constraints is thereby reduced to 6. Two constraints are the same as previously, remaining 4 constraints are defined via vertices relatively close to each other and centered around parameters value at the middle of the step. It is nicely seen from Figure 5.1b that this set is reasonably small. In both cases, LMIs are solved using the YALMIP parser and the SeDuMi solver with Matlab.

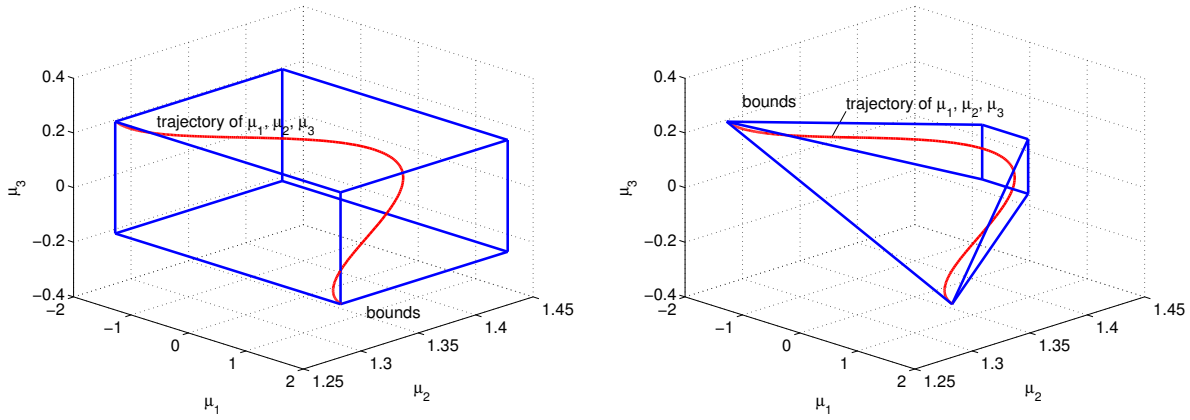

(a) (b)

Figure 5.1. The trajectory $\mu(t)$ for the pseudo-passive reference trajectory encapsulated by a rectangular box (a) and the trajectory $\mu(t)$ for the pseudo-passive reference trajectory encapsulated by a prismatic box (b).

Simulations - Convex rectangular parameter set

Solving the resulting LMI with 8 constraints according to Figure 5.1a gives the state-feedback gain $K = 10^5 \cdot (-3.5810, -1.8147, -0.1854, -0.0037)$. In simulations of the reference trajectory tracking, the errors in initial angular positions are zero but the errors in initial angular velocities are about 5% of reference initial angular velocities. The initial torque as a result of quite large gain is unrealistic for the "real" model of Acrobot, so, a saturation limit in the range $\pm 25\,\mathrm{Nm}$ is used, see Figure 5.3a.

The effect of the saturation limit during the trajectory tracking is clearly visible in Figures 5.2a, b. Experimentally, the saturation limit could not be further lowered without loosing the stable tracking. Yet it is still quite unrealistic. Acrobot walking with that saturation limit is shown in Figure 5.3b.

Summarizing, using the rectangular box to estimate the values of $\mu(t)$ produces highly conservative and practically unacceptable design. Fortunately, tighter bounding sets can be used to estimate the values of $\mu(t)$, as shown below.

Simulations - Convex prismatic parameter set

Solving the resulting LMI with 6 constraints according to Figure 5.1b yields the state-feedback gain $K = 10^4 \cdot (-1.9087 - 1.2097 - 0.1781 - 0.0090)$. The gains are significantly smaller than in the case of the rectangular box. One can see the quality of the tracking in Figures 5.4a, b and can compare the effect of the saturation limit. Convergence is very good now and the saturation limit in the range $\pm 10\mathrm{Nm}$ now ensures a realistic imple-

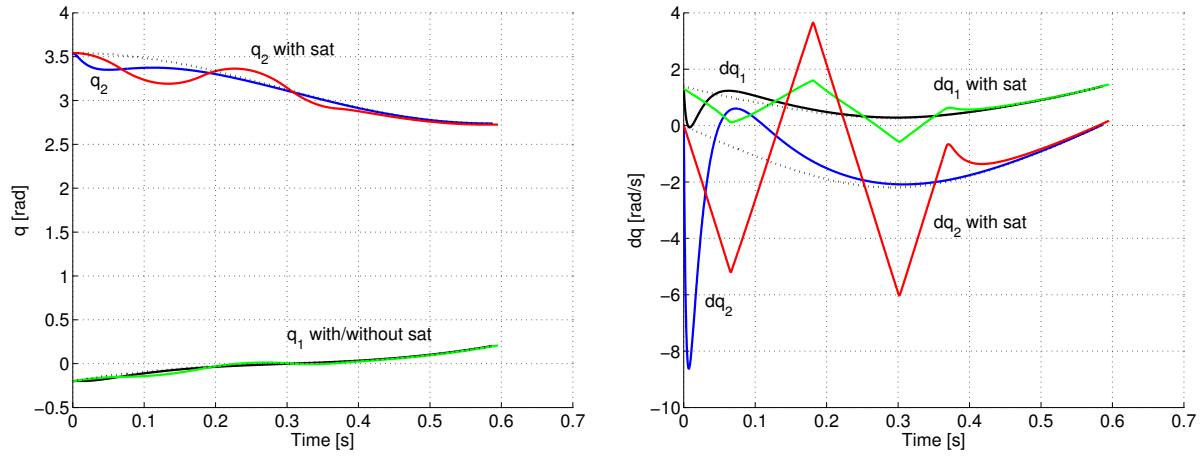

(a) (b)

Figure 5.2. Angular positions q_1, q_2 (a) and angular velocities $\dot{q}_1$, $\dot{q}_2$ (b) with and without saturation $\pm 25\,\mathrm{Nm}$ and references (dotted line) for the rectangular bounds on $\mu(t)$.

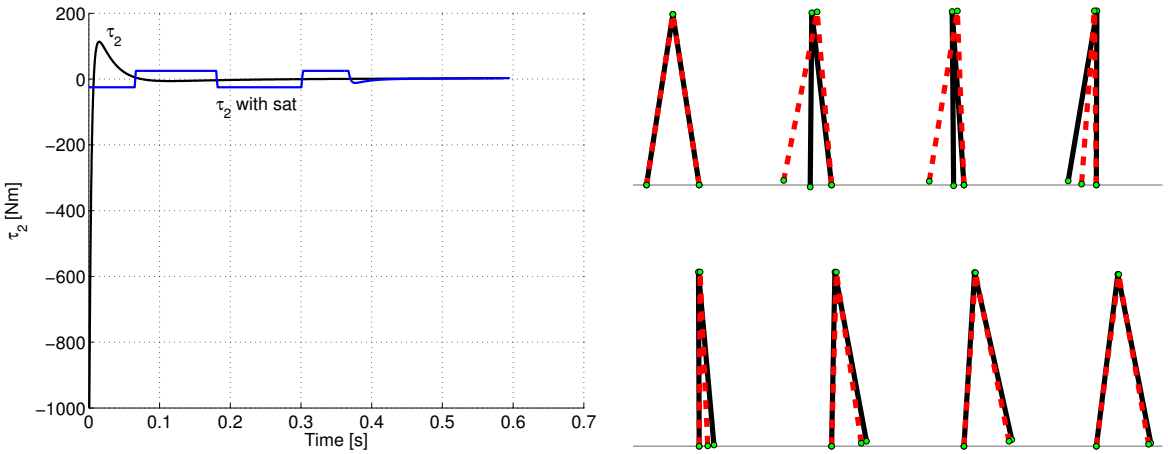

(a) (b)

Figure 5.3. (a) Torque τ_2 with and without saturation $\pm 25\,\mathrm{Nm}$ for rectangular bounds on $\mu(t)$. (b) The animation of the single step with sampling time $0.08\,\mathrm{s}$. The dashed line is the reference, the full line represents "real" Acrobot.

mentation. In simulations of the reference trajectory tracking, errors in initial angular velocities are about 5% of the reference initial angular velocities.

Finally, Figure 5.5b shows the animation of Acrobot walking with the prismatic parameter set based controller and torque saturation in the range ±10Nm. The course of the required torque with and without saturation limit is depicted in Figure 5.5a.

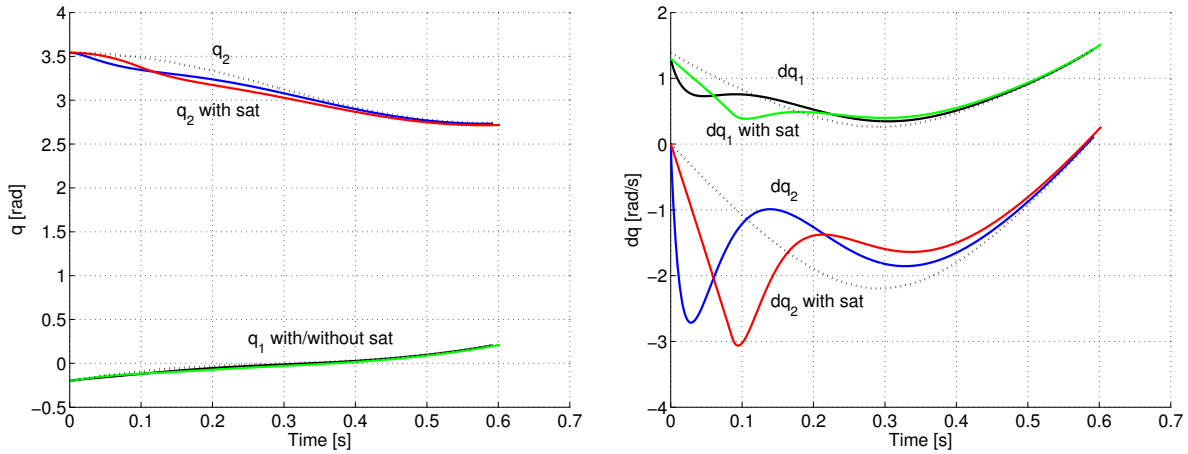

(a) (b)

Figure 5.4. Angular positions q_1, q_2 (a) and angular velocities $\dot{q}_1$, $\dot{q}_2$ (b) with and without saturation ±10 Nm and references (dotted line) for prismatic bounds on $\mu(t)$.

5.3 Analytical design of the exponential tracking

This section aims to describe results presented in [3] where the exponential tracking of the pseudo-passive reference trajectory based on the precise knowledge of the function $\mu_3(t)$ was obtained. Moreover, it also uses its differentiability and the knowledge of ranges of functions $\mu_{1,2,3}(t)$ and $\dot{\mu}_3(t)$. In fact, this time functions are well-known from the reference model and therefore required information is available. Namely, in [3] the following theorem was obtained.

Theorem 5.3.1 *Consider the following notation*

$$\bar{e}_1 = e_1 - \mu_3(t)e_2, \quad \bar{\mu}_2(t) = \mu_2(t) + \mu_1(t)\mu_3(t) - \dot{\mu}_3(t). \tag{5.17}$$

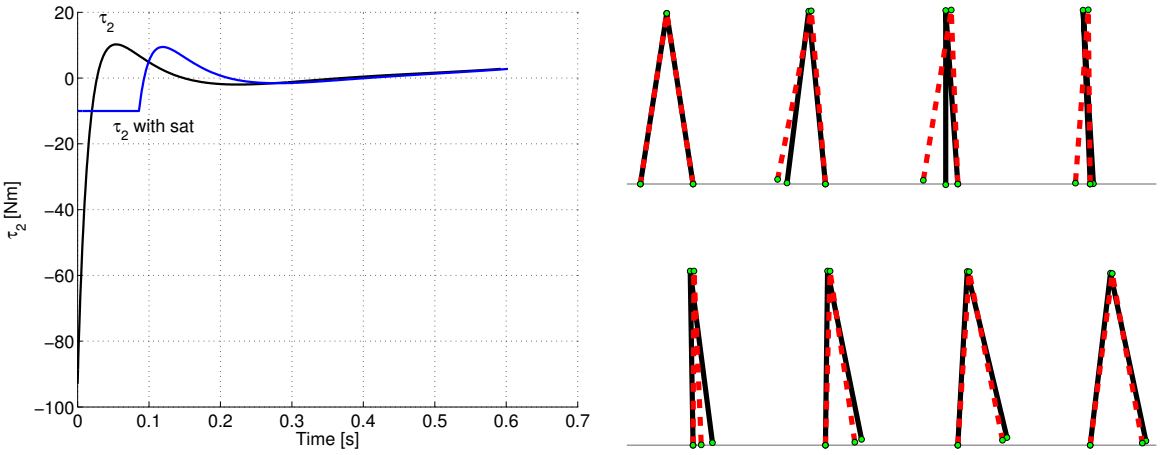

(a) (b)

Figure 5.5. (a) Torque τ_2 with and without saturation $\pm 10\,\mathrm{Nm}$ for the prismatic bounds on $\mu(t)$. (b) The animation of the single step with sampling time $0.08\,\mathrm{s}$. The dashed line is the reference, the full line represents the "real" Acrobot.

Then the system (5.4) takes the following form

$$
\begin{aligned}
\dot{\overline{e}}_1 &= \mu_1(t)\overline{e}_1 + \overline{\mu}_2(t)e_2,\\
\dot{e}_2 &= e_3,\\
\dot{e}_3 &= e_4,\\
\dot{e}_4 &= \Theta^3\widetilde{K}_1\overline{e}_1 + \Theta^3\widetilde{K}_2 e_2 + \Theta^2\widetilde{K}_3 e_3 + \Theta\widetilde{K}_4 e_4.
\end{aligned}
\tag{5.18}
$$

Furthermore, assume that there exist suitable real constants $M^1, M_2, M^2 \in \mathbb{R}^+$ *such that* $\forall t \geq 0$ *it holds:*

$$
\begin{aligned}
|\mu_1| &\leq M^1,\\
0 < M_2 \leq \overline{\mu}_2(t) &\leq M^2.
\end{aligned}
\tag{5.19}
$$

Assume that $\widetilde{K}_{2,3,4}$ *are such that the polynomial* $\lambda^3 + \widetilde{K}_4\lambda^2 + \widetilde{K}_3\lambda + \widetilde{K}_2$ *is Hurwitz and, moreover,*

$$
M^1 - M_2\frac{\widetilde{K}_1}{\widetilde{K}_2} < 0. \tag{5.20}
$$

Then there exists a sufficiently large $\Theta > 0$ *such that the feedback*

$$
w = \Theta^3\widetilde{K}_1 e_1 + \Theta^3[\widetilde{K}_2 - \widetilde{K}_1\mu_3(t)]e_2 + \Theta^2\widetilde{K}_3 e_3 + \Theta\widetilde{K}_4 e_4
$$

globally exponentially stabilizes original system (5.4).

The proof of Theorem 5.3.1 is given in [3]. The computation and analytical analysis of the expression $\mu_2(t) + \mu_1(t)\mu_3(t) - \dot{\mu}_3(t)$ is laborious, nevertheless, numerical computation, depicted in Figure 5.6 shows that the assumption of Theorem 5.3.1 regarding limits of that expression is nicely satisfied.

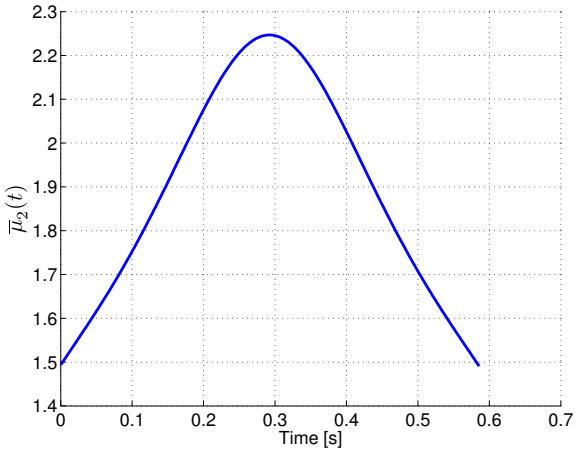

Figure 5.6. Graph of the dependence of $\mu_2(t) + \mu_1(t)\mu_3(t) - \dot{\mu}_3(t)$ on time.

Simulations

To track the above pseudo-passive reference trajectory, Theorem 5.3.1 is used with gains $\widetilde{K} = -(9,\ 6,\ 12,\ 8)$ and with the "amplifying" parameter $\Theta = 20$. One can clearly see the quality of tracking with and without saturation limit in Figures 5.7a, b. In simulations of the reference trajectory tracking, errors in initial angular velocities are about 5% of reference initial angular velocities.

Finally, an animation of corresponding Acrobot walking with torque saturation in the range ± 10Nm is shown in Figure 5.8b. The course of the required torque with and without saturation limit is depicted in Figure 5.8a.

5.4 Extended analytical design of the exponential tracking

This section aims to describe results presented in [7] where the exponential tracking of the multi-step walking reference trajectory based on the precise knowledge of functions $\mu_{1,2,3}(t)$ was obtained. This approach uses the knowledge of ranges of functions $\mu_{1,2,3}(t)$ and differentiability of functions $\mu_{1,2,3}(t)$ up to the order three or four in the case of function $\mu_2(t)$. A time-varying linear feedback in the form $w - w^r = \hat{K}_1(t)e_1 + \ldots + \hat{K}_4(t)e_4$

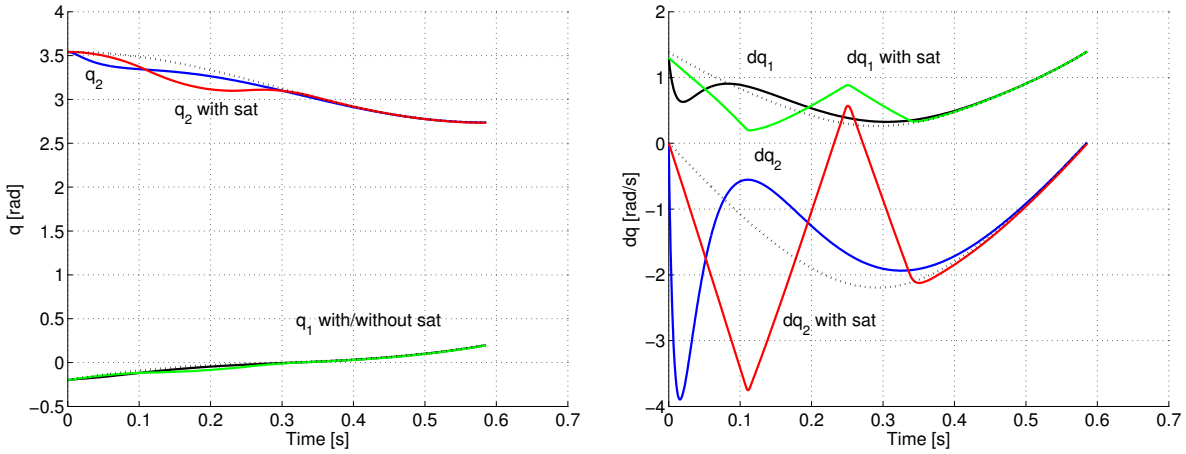

(a) (b)

Figure 5.7. Angular positions q_1, q_2 (a) and angular velocities $\dot{q}_1$, $\dot{q}_2$ (b) with and without saturation $\pm 10\,\mathrm{Nm}$ and references (dotted line).

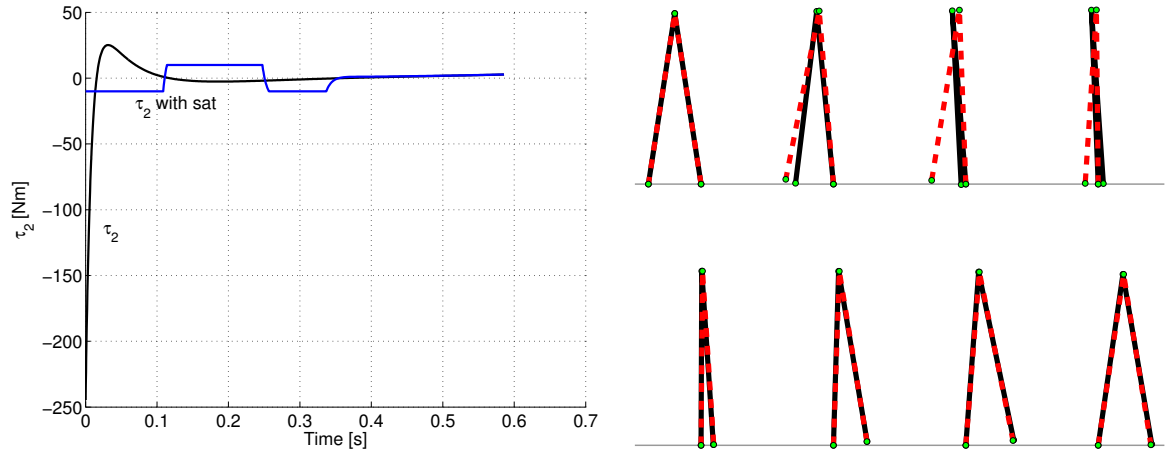

(a) (b)

Figure 5.8. (a) Torque τ_2, with and without saturation $\pm 10\,\mathrm{Nm}$. (b) The animation of the single step is shown with sampling time $\Delta t = 0.08\,\mathrm{s}$. The dashed line is the reference, the full line represents the "real" Acrobot.

is used here. To derive such a feedback, a time varying system was transformed using a time varying transformation and a feedback into a simple linear system with constant coefficients. This transformed system was stabilized using a linear constant feedback later on and recomputed into original coordinates thereby resulting in a time varying feedback. In this sense it is direct extension of the approach from [3] presented in Section 5.3 where ranges of functions $\mu_{1,2,3}(t)$ and the precise knowledge of function $\mu_3(t)$ and its derivative were taken into the account.

To present this approach in detail, continue in transformation started in Section 5.3, i.e. equation (5.17) and its time derivatives are used here in order to transform the original system (5.4) into a simple linear system with constant coefficients. By virtue of this, a design of a fundamental matrix of the error dynamics (5.4) in an explicit form is enabled.

Theorem 5.4.1 *Let $\bar{e} = (\bar{e}_1, \ldots, \bar{e}_4)^\top$ be a new error variable related to $e = (e_1, \ldots, e_4)^\top$ defined in (5.4) as follows*

$$\bar{e}_1 = e_1 - \mu_3 e_2, \tag{5.21}$$

$$\bar{e}_2 = \mu_1 \bar{e}_1 + \bar{\mu}_2 e_2 = \mu_1 e_1 + (\mu_2 - \dot{\mu}_3) e_2, \tag{5.22}$$

$$\bar{e}_3 = (\dot{\mu}_1 + \mu_1^2) e_1 + (\dot{\mu}_2 - \ddot{\mu}_3 + \mu_1\mu_2) e_2 + \bar{\mu}_2 e_3, \tag{5.23}$$

$$\begin{aligned}\bar{e}_4 = {} & (\mu_1(\dot{\mu}_1 + \mu_1^2) + \ddot{\mu}_1 + 2\mu_1\dot{\mu}_1) e_1 + (\mu_2(\dot{\mu}_1 + \mu_1^2) + \ddot{\mu}_2 - \mu_2^{(3)} + \mu_1\dot{\mu}_2 + \dot{\mu}_1\mu_2) e_2 + \\ & (\mu_3(\dot{\mu}_1 + \mu_1^2) + \dot{\mu}_2 - \ddot{\mu}_2 + \mu_1\mu_2 + \dot{\bar{\mu}}_2) e_3 + \bar{\mu}_2 e_4,\end{aligned} \tag{5.24}$$

$$\begin{aligned}\bar{w} = {} & (\mu_1\alpha + \dot{\mu}_1\beta + \mu_1\gamma + \mu_1^{(3)} + 2\dot{\mu}_1\dot{\mu}_1 + 2\mu_1\ddot{\mu}_1) e_1 + (\mu_2\alpha + \dot{\mu}_2\beta + \mu_2\gamma + \\ & \mu_2^{(3)} - \mu_2^{(4)} + 2\dot{\mu}_1\dot{\mu}_2 + \mu_1\ddot{\mu}_2 + \ddot{\mu}_1\mu_2) e_2 + \dot{\bar{\mu}}_2 e_4 + \bar{\mu}_2(w - w^r) + \\ & (\mu_3\alpha + \dot{\mu}_3\beta + \mu_3\gamma + \ddot{\mu}_2 - \mu_2^{(3)} + \dot{\mu}_1\mu_2 + \mu_1\dot{\mu}_2 + \ddot{\bar{\mu}}_2) e_3,\end{aligned} \tag{5.25}$$

where $\bar{\mu}_2 = \mu_2 + \mu_1\mu_3 - \dot{\mu}_3$, $\alpha = \mu_1(\dot{\mu}_1 + \mu_1^2) + \ddot{\mu}_1 + 2\mu_1\dot{\mu}_1$, $\beta = \dot{\mu}_1 + \mu_1^2$, $\gamma = \ddot{\mu}_1 + 2\mu_1\dot{\mu}_1$. Then the original system (5.4) takes the following linear form

$$\dot{\bar{e}}_1 = \bar{e}_2, \quad \dot{\bar{e}}_2 = \bar{e}_3, \quad \dot{\bar{e}}_3 = \bar{e}_4, \quad \dot{\bar{e}}_4 = \bar{w}. \tag{5.26}$$

The proof of Theorem 5.4.1 is given in [7].

The above transformation between e, $w - w^r$ and $\bar{e}$, $\bar{w}$ can be written in a compact form as follows

$$\bar{e} = X(t)e, \quad \bar{w} = \widetilde{K}(t)e + L(t)(w - w^r), \tag{5.27}$$

$$e = X^{-1}\bar{e}, \quad w - w^r = L^{-1}(t)(\bar{w} - \widetilde{K}(t)e), \tag{5.28}$$

where the matrix $X(t)$ has the following form

$$X(t) = \begin{bmatrix} 1 & -\mu_3 & 0 & 0 \\ \mu_1 & \mu_2 - \dot{\mu}_3 & 0 & 0 \\ \dot{\mu}_1 + \mu_1^2 & \mu_1\mu_2 + \dot{\mu}_2 - \ddot{\mu}_2 & \bar{\mu}_2 & 0 \\ \mu_1(3\dot{\mu}_1 + \mu_1^2) + \ddot{\mu}_1 & \mu_2(2\dot{\mu}_1 + \mu_1^2) + \ddot{\mu}_2 - \mu_2^{(3)} + \mu_1\dot{\mu}_2 & \mu_3(\dot{\mu}_1 + \mu_1^2) + \dot{\mu}_2 - \ddot{\mu}_2 + \mu_1\mu_2 + \dot{\bar{\mu}}_2 & \bar{\mu}_2 \end{bmatrix}, \tag{5.29}$$

and the vector $\widetilde{K}(t)$ and the scalar $L(t)$ are as follows

$$\widetilde{K}(t) = \begin{bmatrix} \mu_1\alpha + \dot{\mu}_1\beta + \mu_1\gamma + \mu_1^{(3)} + 2\dot{\mu}_1\dot{\mu}_1 + 2\mu_1\ddot{\mu}_1 \\ \mu_2\alpha + \dot{\mu}_2\beta + \mu_2\gamma + \mu_2^{(3)} - \mu_2^{(4)} + 2\dot{\mu}_1\dot{\mu}_2 + \mu_1\ddot{\mu}_2 + \ddot{\mu}_1\mu_2 \\ \mu_3\alpha + \dot{\mu}_3\beta + \mu_3\gamma + \ddot{\mu}_2 - \mu_2^{(3)} + \dot{\mu}_1\mu_2 + \mu_1\dot{\mu}_2 + \ddot{\bar{\mu}}_2 \\ \dot{\bar{\mu}}_2 \end{bmatrix}^{\mathrm{T}}, \quad L(t) = \bar{\mu}_2\,. \tag{5.30}$$

Using transformations (5.21)-(5.24) the open-loop system (5.8) is transformed into the following form

$$\dot{\bar{e}} = \widetilde{A}\bar{e} + \widetilde{B}\bar{w},\ \widetilde{A} = \begin{bmatrix} 0\ 1\ 0\ 0 \\ 0\ 0\ 1\ 0 \\ 0\ 0\ 0\ 1 \\ 0\ 0\ 0\ 0 \end{bmatrix},\ \widetilde{B} = \begin{bmatrix} 0 \\ 0 \\ 0 \\ 1 \end{bmatrix}, \tag{5.31}$$

where by (5.27), (5.8) $\widetilde{A}$ and $\widetilde{B}$ are given as follows

$$\widetilde{A} = X(t)\left(A(t) - BL^{-1}(t)\widetilde{K}(t)\right)X^{-1}(t) + \frac{dX(t)}{dt}X^{-1}(t), \tag{5.32}$$

$$\widetilde{B} = X(t)BL^{-1}(t). \tag{5.33}$$

Choosing a linear constant feedback $\bar{w} = K_1\bar{e}_1 + \ldots + K_4\bar{e}_4$, the closed-loop system (5.31) has the following form

$$\dot{\bar{e}} = \left(\widetilde{A} + \widetilde{B}K\right)\bar{e} = \begin{pmatrix} 0 & 1 & 0 & 0 \\ 0 & 0 & 1 & 0 \\ 0 & 0 & 0 & 1 \\ K_1 & K_2 & K_3 & K_4 \end{pmatrix}\bar{e}. \tag{5.34}$$

The resulting time-varying feedback for original system (5.8) is therefore by (5.27)-(5.34) as follows

$$w - w^r = L^{-1}(t)(KX(t)e - \widetilde{K}(t)e) := \hat{K}(t)e. \tag{5.35}$$

The solution of differential equations (5.34) is easy to find by standard linear methods. Then, using transformations (5.27)-(5.28) one can compute the explicit solution of the closed loop system in original e coordinates. This fact will be used in the sequel to analyze a hybrid stability later on.

Simulations

Higher derivations of functions $\mu_{1,2,3}(t)$ are complicated and their computations during a simulation are time-consuming. Therefore, their derivations along the reference trajectory were computed off-line in approximately 300 points for one step. Values of reference functions $\mu_{1,2,3}(t)$ and their derivations were interpolated among these points during the simulation. Consequently, this approach is possible to use in the on-line control of Acrobot.

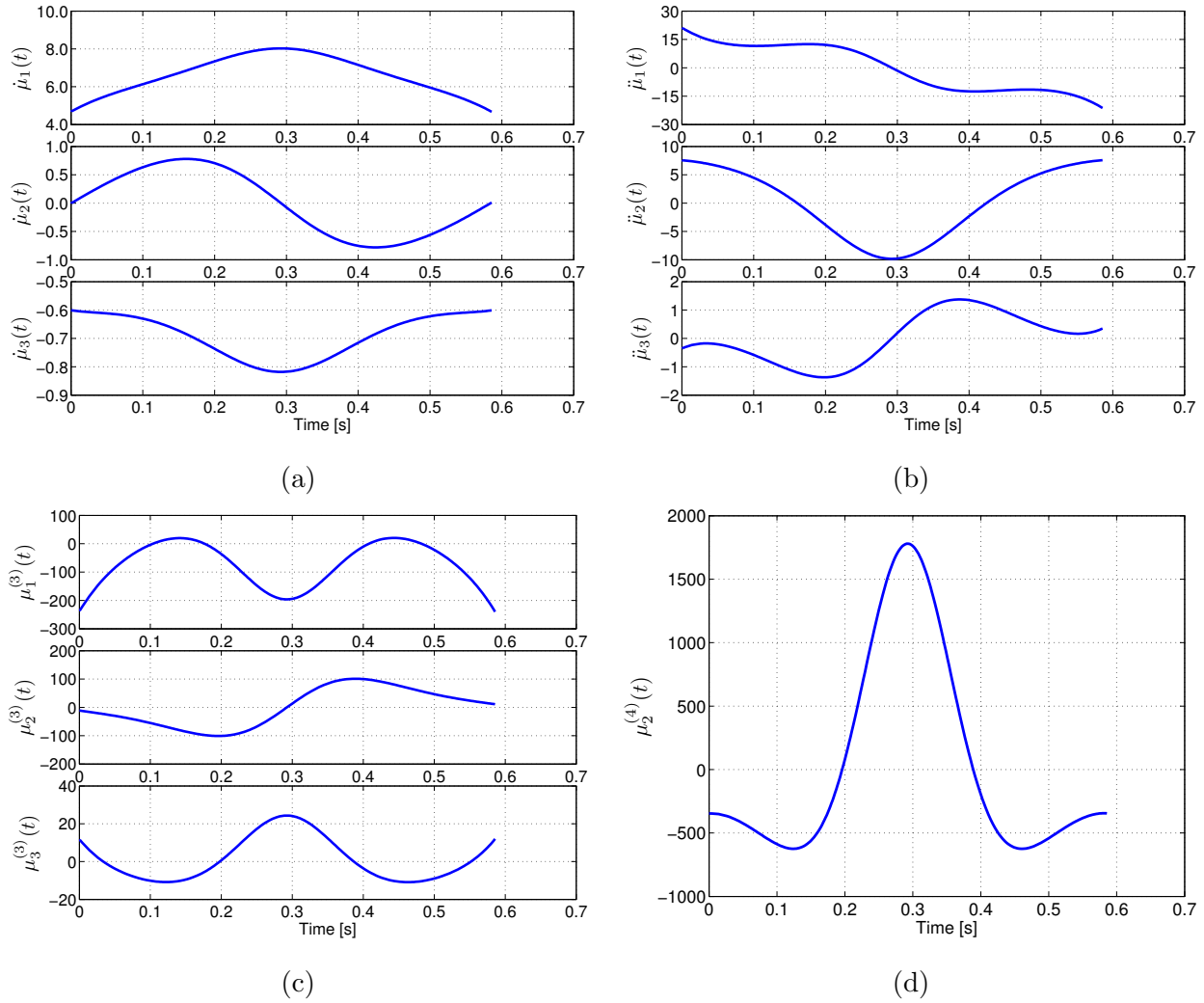

Figure 5.9. Higher derivations of functions $\mu_{1,2,3}(t)$ (a) the first derivation (b) the second derivation (c) the third derivation (d) the fourth derivation of $\mu_2(t)$.

In Figure (5.9) one can see the higher derivations of functions $\mu_{1,2,3}(t)$ up to the order three, moreover, up to the order four in the case of $\mu_2(t)$ function.

In [7], Theorem 5.4.1 was demonstrated in simulations via feedback tracking of the multi-step walking reference trajectory. Nevertheless, to keep the consistency in presented simulations in this chapter, the simulation of Acrobot pseudo-passive reference trajectory tracking is shown here. Theorem 5.4.1 is used to track the pseudo-passive reference trajectory with gains $\widetilde{K} = 10^3 \cdot (-75.000, -19.250, -1.775, -0.070)$. One can clearly see the quality of the feedback tracking with and without torque saturation in Figures 5.10a, b. In reference trajectory tracking simulations, errors in initial angular velocities are about 5% of reference initial angular velocities.

Finally, the animation of corresponding Acrobot walking with torque saturation in the range ±15Nm is shown in Figure 5.11b. The course of the required torque with and without saturation limit is depicted in Figure 5.11a.

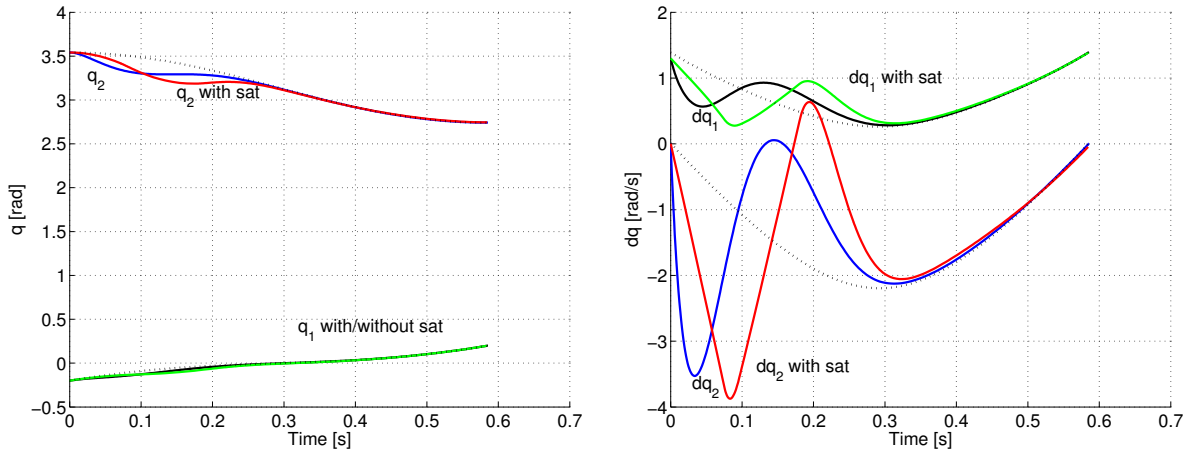

(a) (b)

Figure 5.10. Angular positions q_1, q_2 (a) and angular velocities $\dot{q}_1$, $\dot{q}_2$ (b) with and without saturation ±15 Nm and references (dotted line).

5.5 Approximate analytical design of the exponential tracking

This section aims to describe results presented in [9] where the theoretical framework enabling a design of an exponential feedback tracking for a general Acrobot trajectory allowing rigorous convergence proof was presented. It is based on the partial exact feedback linearization of Acrobot followed by further approximate feedback linearization [69]

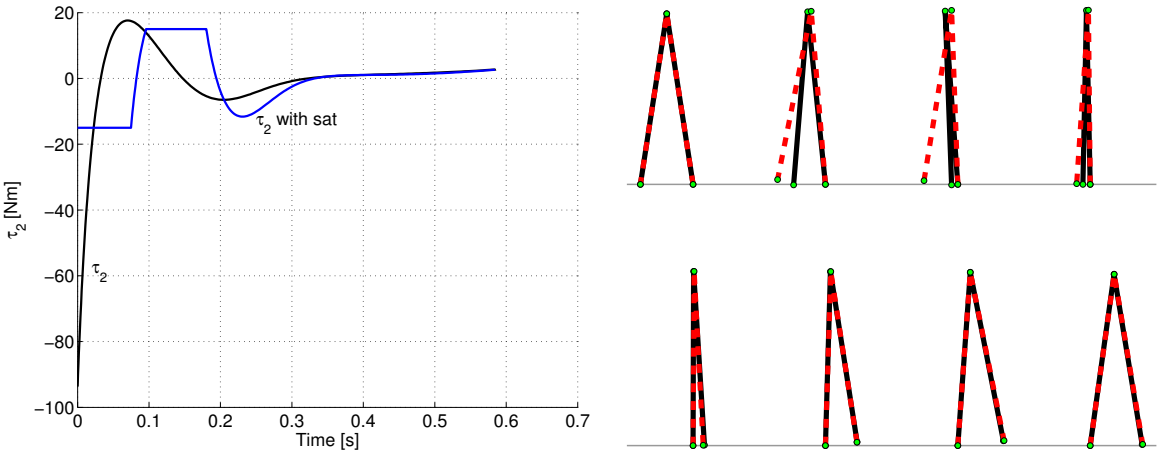

(a) (b)

Figure 5.11. (a) Torque τ_2, with and without saturation $\pm 15\,\mathrm{Nm}$. (b) The animation of the single step is shown with sampling time $\Delta t = 0.08\,\mathrm{s}$. The dashed line is the reference, the full line represents "real" Acrobot.

of tracking error dynamics for an arbitrary target trajectory. The novelty of the new approach lies in a neglecting made with respect to a tracking error along any general trajectory to be tracked, not just in some neighborhood of a fixed working point.

Previous techniques provide feedback to stabilize the above error dynamics. Their drawbacks are either high degree of conservatism or heuristic character. The basic difficulty here is a presence of a term depending linearly on e_3 in the first row of (5.4) with a time varying coefficient, which prevents an analytic design. As a matter of fact, this linear term can be removed by further exact state and a feedback transformation of the extended system (4.2), (5.3). This approach was successfully used in [9] and it is shown below.

Theorem 5.5.1 *Consider the extended system (4.2), (5.3) as the dynamical system having* 8 *dimensional state space, a controlled input* w *and a reference input* w^r*. Then there exists the following change of coordinates and a feedback transformation (locally regular in* e*)*

$$\eta = \Phi(\xi_1^r, \xi_2^r, \xi_3^r, \xi_4^r, e_1, e_2, e_3, e_4), \tag{5.36}$$

$$\mu = \gamma(w, w^r, \xi_1^r, \xi_2^r, \xi_3^r, \xi_4^r, e_1, e_2, e_3, e_4), \tag{5.37}$$

where $\Phi_{1,2,3,4}$ *are defined as follows*

$$\Phi_1 \equiv \xi_1^r,\ \ \Phi_2 \equiv \xi_2^r,\ \ \Phi_3 \equiv \xi_3^r,\ \ \Phi_4 \equiv \xi_4^r \tag{5.38}$$

and $\Phi_{5,6,7,8}$ *fulfill following conditions*

$$\Phi_k(\xi_1^r, \xi_2^r, \xi_3^r, \xi_4^r, 0, 0, 0, 0) \equiv 0, \quad \forall k = 5, 6, 7, 8. \tag{5.39}$$

The transformation transforms the extended system (4.2), (5.3) into the following form with state η*, a controlled input* μ *and a reference input* w^r

$$\dot{\eta}_1 = d_{11}^{-1}(q_2^r)\eta_2, \quad \dot{\eta}_2 = \eta_3, \quad \dot{\eta}_3 = \eta_4, \quad \dot{\eta}_4 = w^r, \tag{5.40}$$

$$\dot{\eta}_5 = \eta_6 + o(\eta), \quad \dot{\eta}_6 = \eta_7, \quad \dot{\eta}_7 = \eta_8, \quad \dot{\eta}_8 = \mu. \tag{5.41}$$

The proof of Theorem 5.5.1 is in [9].

The first part of transformed system (5.40) was relabeled only. Instead of ξ in (4.2) η is used in (5.40). However, the second part of transformed system (5.41) was significantly changed according to its original form (5.3). Using the transformation, defined below, a linear dependence on e_3 was removed from the first line of original system (5.3). The resulting system (5.41) contains only higher degree of the dependence on e_3 which could be neglected. Afterwards, the remaining system is composed of a chain of integrators and it could be stabilized using the standard linear approach, i.e. using the state feedback in the following form

$$\mu = k_1\,\eta_5 + k_2\,\eta_6 + k_3\,\eta_7 + k_4\,\eta_8, \tag{5.42}$$

where gains $k_{1,2,3,4}$ can be designed using the standard technique, such that the matrix

$$\begin{bmatrix} 0 & 1 & 0 & 0 \\ 0 & 0 & 1 & 0 \\ 0 & 0 & 0 & 1 \\ k_1 & k_2 & k_3 & k_4 \end{bmatrix} \tag{5.43}$$

is Hurwitz.

To demonstrate the proof of Theorem 5.5.1 and to obtain explicit expressions for μ given there consider the general error dynamics (5.3) and consider its first row in a more detail. Namely, one has

$$\begin{aligned} \dot{e}_1 = {} & \frac{\partial d_{11}^{-1}(\phi_2(\xi_{1,3}^r))}{\partial \xi_1}(\xi_2^r + e_2)e_1 + d_{11}^{-1}(\phi_2(\xi_{1,3}^r))e_2 + \frac{\partial d_{11}^{-1}(\phi_2(\xi_{1,3}^r))}{\partial \xi_3}(\xi_2^r + e_2)e_3 \\ & + d_{11}^{-1}(\phi_2(\xi_{1,3}))\xi_2 - d_{11}^{-1}(\phi_2(\xi_{1,3}^r))(\xi_2^r + e_2) - \frac{\partial d_{11}^{-1}(\phi_2(\xi_{1,3}^r))}{\partial \xi_1}(\xi_2^r + e_2)e_1 - \\ & \frac{\partial d_{11}^{-1}(\phi_2(\xi_{1,3}^r))}{\partial \xi_3}(\xi_2^r + e_2)e_3, \end{aligned}$$

which gives

$$\dot{e}_1 = \frac{\partial d_{11}^{-1}(\phi_2(\xi_1^r,\xi_3^r))}{\partial \xi_1}(\xi_2^r+e_2)e_1 + \frac{\partial d_{11}^{-1}(\phi_2(\xi_1^r,\xi_3^r))}{\partial \xi_3}(\xi_2^r+e_2)e_3 + d_{11}^{-1}(\phi_2(\xi_1^r,\xi_3^r))e_2 + (\xi_2^r+e_2)o(\|(e_1,e_3)^{\mathrm{T}}\|), \tag{5.44}$$

where

$$(\xi_2^r+e_2)o(\|(e_1,e_3)^{\mathrm{T}}\|) = (\xi_2^r+e_2)\Bigg(d_{11}^{-1}(\phi_2(\xi_1^r+e_1,\xi_3^r+e_2)) - d_{11}^{-1}(\phi_2(\xi_1^r,\xi_3^r)) - \frac{\partial d_{11}^{-1}(\phi_2(\xi_1^r,\xi_3^r))}{\partial \xi_1}e_1 - \frac{\partial d_{11}^{-1}(\phi_2(\xi_1^r,\xi_3^r))}{\partial \xi_3}e_3\Bigg). \tag{5.45}$$

Therefore it holds

$$\dot{e}_1 = \psi_1(q_1^r,q_2^r)(\xi_2^r+e_2)e_1 + \psi_2(q_2^r)e_2 + \psi_3(q_1^r,q_2^r)(\xi_2^r+e_2)e_3 + (\xi_2^r+e_2)o(\|(e_1,e_3)^{\mathrm{T}}\|), \tag{5.46}$$

where

$$\begin{aligned}
\psi_1(q_1^r,q_2^r) &:= \frac{\partial d_{11}^{-1}\left(q_2(\xi_1^r,\xi_3^r)\right)}{\partial \xi_1^r} = \frac{\partial d_{11}^{-1}}{\partial q_2}(q_2^r)\frac{\partial q_2}{\partial \xi_1^r},\\
\psi_2(q_2^r) &:= d_{11}^{-1}(\phi_2(\xi_1^r,\xi_3^r)),\\
\psi_3(q_1^r,q_2^r) &:= \frac{\partial d_{11}^{-1}\left(q_2(\xi_1^r,\xi_3^r)\right)}{\partial \xi_3^r} = \frac{\partial d_{11}^{-1}}{\partial q_2}(q_2^r)\frac{\partial q_2}{\partial \xi_3^r}.
\end{aligned}$$

Functions $\psi_{1,2,3}(q_1^r,q_2^r)$ are equivalent to functions $\mu_{1,2,3}(t)$ defined in (5.5), (5.6), (5.7). The only difference between functions $\psi_{1,2,3}(q_1^r,q_2^r)$ and $\mu_{1,2,3}(t)$ consists in dependency on a reference trajectory. Functions $\psi_{1,2,3}(q_1^r,q_2^r)$ depend on a general reference trajectory through angular positions q_1^r and q_2^r. Whereas functions $\mu_{1,2,3}(t)$ depend on a particular reference trajectory through time t. Summarizing

$$\begin{aligned}
&\dot{e}_1 = \psi_1(q_1^r,q_2^r)(\xi_2^r+e_2)e_1 + \psi_2(q_2^r)e_2 + \psi_3(q_1^r,q_2^r)(\xi_2^r+e_2)e_3 + (\xi_2^r+e_2)o(\|(e_1,e_3)^{\mathrm{T}}\|),\\
&\dot{e}_2 = e_3, \quad \dot{e}_3 = e_4, \quad \dot{e}_4 = w - w^r.
\end{aligned} \tag{5.47}$$

Consider the following transformation

$$\eta_5 := e_1 - \psi_3(q_1^r,q_2^r)\left[\frac{(\xi_2^r+e_2)^2 - (\xi_2^r)^2}{2}\right]. \tag{5.48}$$

The specific form of the transformation enables to make the full order linearization of (5.3) because the term connected with e_3 will be deleted from the first line of (5.48) and it will appear in the next line. From (5.48) we get

$$\dot{\eta}_5 = \dot{e}_1 - \psi_3(q_1^r,q_2^r)\left[\dot{e}_2(\xi_2^r+e_2) + e_2\dot{\xi}_2^r\right] - \psi_3^{(\mathrm{I})}(q_1^r,q_2^r)\left[\frac{(\xi_2^r+e_2)^2 - (\xi_2^r)^2}{2}\right]. \tag{5.49}$$

Substituting from (5.3) we obtain

$$\dot{\eta}_5 = \psi_1(q_1^r, q_2^r)(\xi_2^r+e_2)e_1 + \psi_2(q_2^r)e_2 - \psi_3(q_1^r, q_2^r)e_2\dot{\xi}_2^r - \psi_3^{(\mathrm{I})}(q_1^r, q_2^r)\left[\frac{(\xi_2^r+e_2)^2 - (\xi_2^r)^2}{2}\right] + (\xi_2^r + e_2)o(\|(e_1, e_3)^{\mathrm{T}}\|). \tag{5.50}$$

Now, we have the almost linearized the first equation by setting the new coordinate as follows

$$\eta_6 = \psi_1(q_1^r, q_2^r)(\xi_2^r+e_2)e_1+\psi_2(q_2^r)e_2-\psi_3(q_1^r, q_2^r)e_2\dot{\xi}_2^r-\psi_3^{(\mathrm{I})}(q_1^r, q_2^r)\left[\frac{(\xi_2^r+e_2)^2 - (\xi_2^r)^2}{2}\right], \tag{5.51}$$

which transforms the first equation

$$\dot{\eta}_5 = \eta_6 + (\xi_2^r + e_2)o(\|(e_1, e_3)^{\mathrm{T}}\|). \tag{5.52}$$

Differentiating η_6 along system trajectories by performing the usual algorithm of computing further time derivatives one obtains

$$\begin{aligned}\dot{\eta}_6 = {} & \psi_1^{(\mathrm{I})}(q_1^r, q_2^r)(\xi_2^r+e_2)e_1 + \psi_1(q_1^r, q_2^r)(\dot{\xi}_2^r+e_3)e_1 + \\ & \psi_1(q_1^r, q_2^r)(\xi_2^r+e_2)\left(d_{11}^{-1}(\phi_2(\xi_1^r+e_1, \xi_3^r+e_3))(\xi_2^r+e_2) - d_{11}^{-1}(\phi_2(\xi_1^r, \xi_3^r))\xi_2^r\right) + \\ & \frac{\partial\psi_2}{\partial q_2^r}(q_2^r)\dot{q}_2^r e_2 + \psi_2(q_2^r)e_3 - \psi_3(q_1^r, q_2^r)e_3\dot{\xi}_2^r - \psi_3(q_1^r, q_2^r)e_2\ddot{\xi}_2^r - \\ & \psi_3^{(\mathrm{II})}(q_1^r, q_2^r)\left[\frac{(\xi_2^r+e_2)^2-(\xi_2^r)^2}{2}\right] - \psi_3^{(\mathrm{I})}(q_1^r, q_2^r)\left[e_3(\xi_2^r+e_2) + 2e_2\dot{\xi}_2^r\right].\end{aligned} \tag{5.53}$$

Denoting the right hand side of (5.53) as $\eta_7 := \eta_7(\xi_1^r, \ldots, \xi_4^r, e_1, e_2, e_3)$ one has the transformed equation as follows

$$\dot{\eta}_6 = \eta_7(\xi_1^r, \ldots, \xi_4^r, e_1, e_2, e_3). \tag{5.54}$$

Now, differentiating further η_7 and η_8 with respect to time along system trajectories one has that

$$\dot{\eta}_7 = \eta_8(\xi_1^r, \ldots, \xi_4^r, e_1, \ldots, e_4), \tag{5.55}$$

$$\dot{\eta}_8 = \mu(w, w^r, \xi_1^r, \ldots, \xi_4^r, e_1, \ldots, e_4). \tag{5.56}$$

However, this has increasing complexity and, therefore, it is left for sake of shortness. Obviously, (5.55), (5.56) give the rest of transformations mentioned in theorem formulations. It can be also straightforwardly checked that the overall transformation is locally one-to-one.

Simulations

In [9], Theorem 5.5.1 was demonstrated in simulations via feedback tracking of the multi-step walking reference trajectory for Acrobot. Nevertheless, to be consistent with presented simulations in this chapter, the simulation of Acrobot pseudo-passive reference trajectory tracking is shown here in order that one can compare the corresponding simulations with simulations of remaining techniques to stabilize the error dynamics.

To track the pseudo-passive reference trajectory, Theorem 5.5.1 is used with gains $\widetilde{K} = -10^5 \cdot [5.2958,\ 2.9152,\ 0.4415,\ 0.0145]$. One can clearly see the quality of the feedback tracking with and without torque saturation in Figures 5.12a, b. In simulations of the reference trajectory tracking, errors in initial angular velocities are about 5% of reference initial angular velocities.

Finally, the animation of corresponding Acrobot walking with torque saturation in the range $\pm 10\,\mathrm{Nm}$ is shown in Figure 5.13b. The course of the required torque with and without saturation limit is depicted in Figure 5.13a.

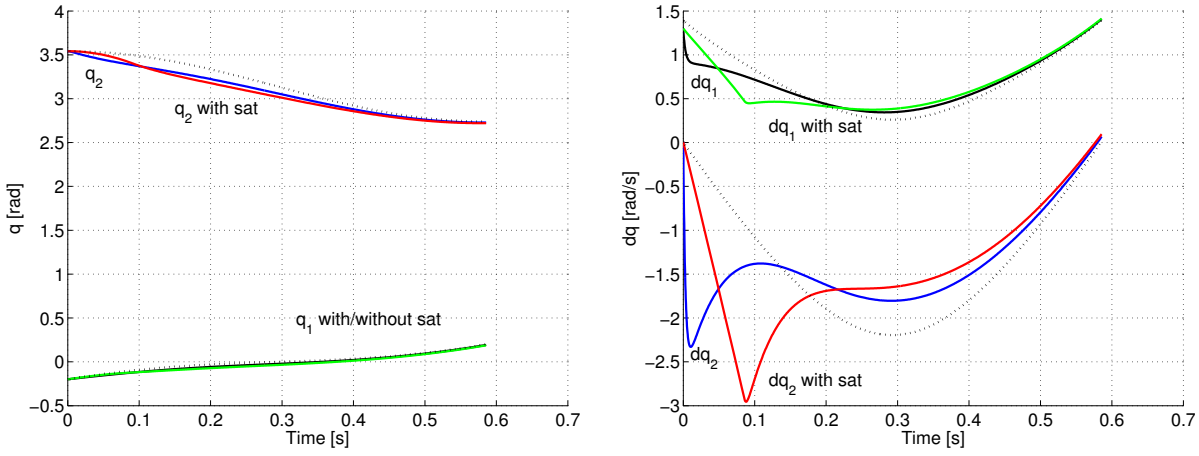

(a) (b)

Figure 5.12. Angular positions q_1, q_2 (a) and angular velocities $\dot{q}_1$, $\dot{q}_2$ (b) with and without saturation $\pm 10\,\mathrm{Nm}$ and references (dotted line).

5.6 Yet another analytical design of the exponential tracking

This section aims to describe results presented in [28] where the exponential tracking of the pseudo-passive reference trajectory based on the precise knowledge of functions $\mu_{1,2,3}(t)$ and time derivative of $\dot{\mu}_3(t)$ was obtained. In fact, this time functions are well

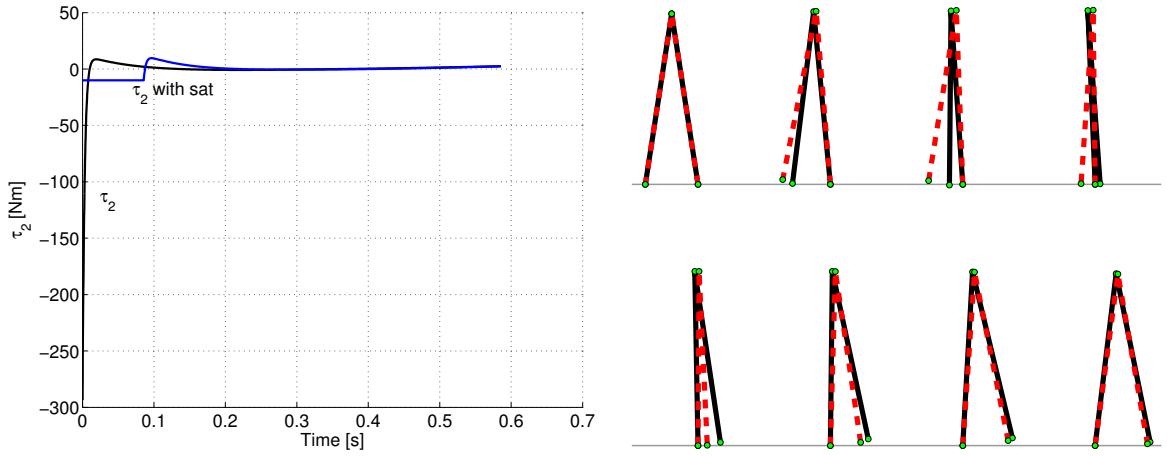

(a) (b)

Figure 5.13. (a) Torque τ_2, with and without saturation $\pm 10\,\mathrm{Nm}$. (b) The animation of the single step is shown with sampling time $\Delta t = 0.08\,\mathrm{s}$. The dashed line is the reference, the full line represents "real" Acrobot.

known from the reference model and therefore required information is available. In contrast to results described in Section 5.3, where only knowledge of function $\mu_3(t)$ was taken into account, the following technique seems to be even better.

Namely, in [28] the following theorem was obtained.

Theorem 5.6.1 *Let $\tilde{e} = (\tilde{e}_1, \ldots, \tilde{e}_4)^\top$ be a new error variable related to $e = (e_1, \ldots, e_4)^\top$ defined in (5.4) as follows*

$$\tilde{e}_1 = \frac{e_1 - \mu_3 e_2}{\mu_1\mu_3 - \dot{\mu}_3 + \mu_2}, \quad \tilde{e}_2 = e_2, \quad \tilde{e}_3 = e_3, \quad \tilde{e}_4 = e_4.$$

Then the error dynamics of $\tilde{e}$ is as follows

$$\begin{aligned} \dot{\tilde{e}}_1 &= \tilde{\mu}_1(t)\tilde{e}_1 + \tilde{e}_2 \\ \dot{\tilde{e}}_2 &= \tilde{e}_3 \\ \dot{\tilde{e}}_3 &= \tilde{e}_4 \\ \dot{\tilde{e}}_4 &= w, \end{aligned} \tag{5.57}$$

where

$$\tilde{\mu}_1(t) = \mu_1 - \frac{\dot{\mu}_1\mu_3 + \mu_1\dot{\mu}_3 - \ddot{\mu}_3 + \dot{\mu}_2}{\mu_1\mu_3 - \dot{\mu}_3 + \mu_2}. \tag{5.58}$$

Furthermore, assume that there exists $M_1 \in \mathbb{R}^+$ such that $|\tilde{\mu}_1(t)| \leq M_1$, $\forall t \geq 0$, then there exists a linear feedback law $w = K_1\tilde{e}_1 + K_2\tilde{e}_2 + K_3\tilde{e}_3 + K_4\tilde{e}_4$ that globally exponentially

stabilizes system (5.57). Moreover, if in addition there exist $M_2, M^2 \in \mathbb{R}^+$, *such that* $M^2 > \mu_1(t)\mu_3(t) - \dot{\mu}_3(t) + \mu_2(t) \geq M_2$, $\forall t \geq 0$, *then the feedback*

$$w = K_1 \frac{e_1 - \mu_3 e_2}{\mu_1 \mu_3 - \dot{\mu}_3 + \mu_2} + K_2 e_2 + K_3 e_3 + K_4 e_4$$

globally exponentially stabilizes original system (5.4).

Proof of Theorem 5.6.1 is given in [28].

Simulations

In [28], the presented theorem was demonstrated in simulations via feedback tracking of the pseudo-passive reference trajectory for 4-link. However, to be consistent with presented simulations in this chapter, the Acrobot pseudo-passive reference trajectory was tracked in order that one can compare simulations results of presented technique to stabilize the error dynamics.

To track the above pseudo-passive reference trajectory, Theorem 5.6.1 is used with gains $(K_1, K_2, K_3, K_4) = (-16, -32, -24, -8)$ and the "amplifying" parameter $\Theta = 10$. One can clearly see the quality of tracking with and without saturation in Figures 5.14a, b. In simulations of the reference trajectory tracking, errors in initial angular velocities are about 5% of reference initial angular velocities.

Finally, the animation of corresponding Acrobot walking with torque saturation in the range ± 15Nm is shown in Figure 5.15b. The course of the required torque with and without saturation limit is depicted in Figure 5.15a.

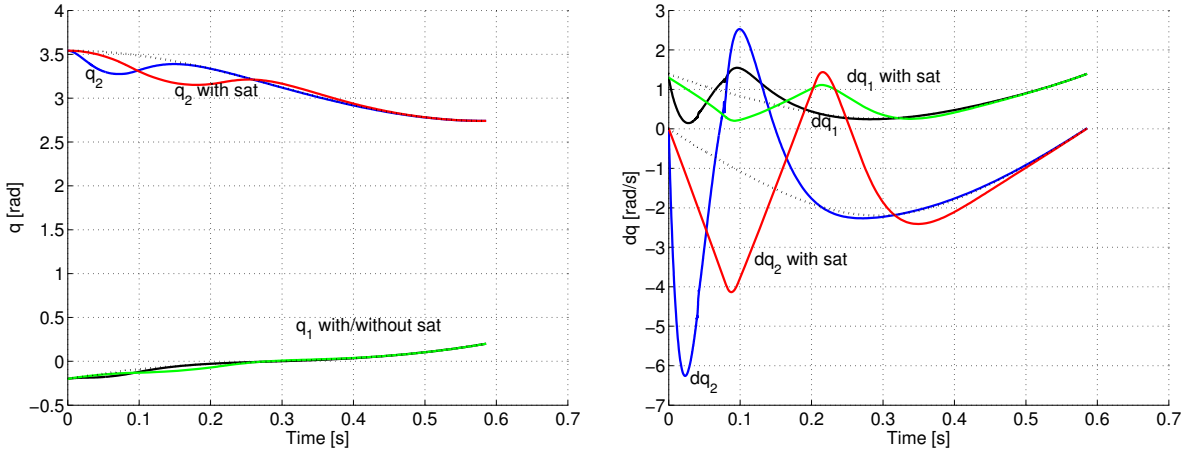

(a) (b)

Figure 5.14. Angular positions q_1, q_2 (a) and angular velocities $\dot{q}_1$, $\dot{q}_2$ (b) with and without saturation ± 10 Nm and references (dotted line).

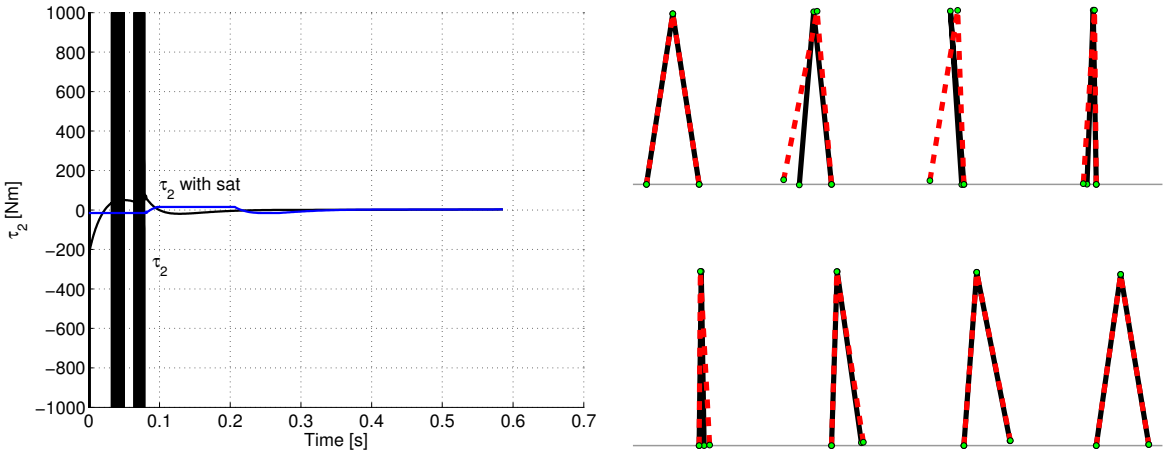

(a) (b)

Figure 5.15. (a) Torque τ_2, with and without saturation $\pm 15\,\mathrm{Nm}$. (b) The animation of the single step is shown with sampling time $\Delta t = 0.08\,\mathrm{s}$. The dashed line is the reference, the full line represents "real" Acrobot.

5.7 Ability of a general reference trajectory tracking

Tracking techniques presented in previous sections of this chapter were demonstrated in an application of a feedback tracking of the pseudo-passive reference trajectory for Acrobot only. Indeed, tracking techniques would be able to track either the multi-step walking reference trajectory for Acrobot or both reference trajectories for 4-link, i.e. the pseudo-passive and the multi-step walking reference trajectory. Nevertheless, simulations of feedback tracking of remaining reference trajectories are omitted for thesis space reasons. Obviously, there is no principal difference in the tracking various types of references during a single step.

The tracking ability of a reference trajectory depends on functions $\mu_{123}(t)$ which are given by the reference trajectory to be tracked. One can see the course of functions $\mu_{123}(t)$ depicted in Figures 5.16a, b for Acrobot reference trajectories and in Figures 5.17a, b for 4-link reference trajectories. Conditions and requirements given by theorems and tracking techniques presented in this chapter are fulfilled by functions $\mu_{123}(t)$ depicted in Figures 5.16a, b and 5.17a, b. Therefore, the presented tracking techniques could be used in the application of the feedback tracking of both reference trajectories either for Acrobot or for 4-link.

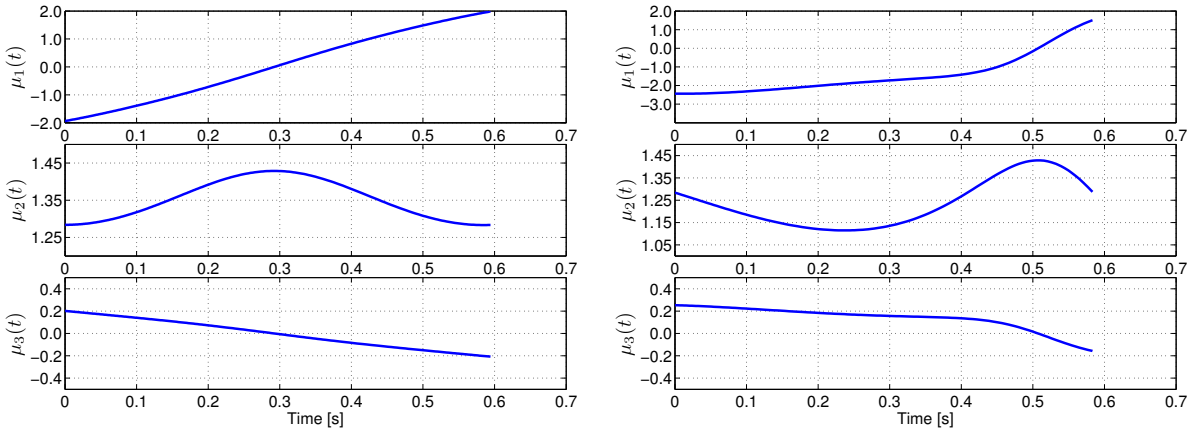

(a) (b)

Figure 5.16. Trajectory $\mu_{123}(t)$ for the pseudo-passive (a) and the multi-step walking (b) reference trajectory for Acrobot.

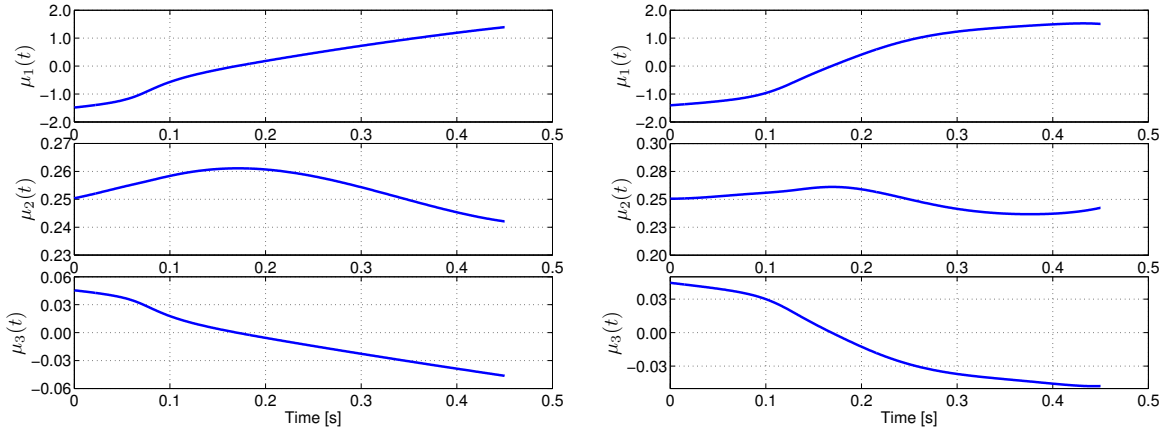

(a) (b)

Figure 5.17. Trajectory $\mu_{123}(t)$ for the pseudo-passive (a) and the multi-step walking (b) reference trajectory for 4-link.

5.8 Chapter conclusion

This chapter describes the results from [3, 7, 9, 14, 28] related to the tracking of the reference trajectory for the underactuated walking robot. Tracking techniques are based on the partially linear feedback form of Acrobot or by virtue of the embedding method of 4-link. The techniques are based either on a robust approach or on deeper knowledge of the reference system to be tracked to minimize the error between the reference and the "real" system. By virtue of the partial exact feedback linearization method, tracking techniques are able to track various type of reference trajectories, though they were demonstrated for the pseudo-passive one only.

Chapter 6

Observers

In the previous section, tracking methods based on the partial exact feedback linearization were developed under the assumption that all state variables are available for measurements. Nevertheless, this assumption is rarely fulfilled in real applications by virtue of either non-existent or too expensive appropriate sensor. In this case, it is possible either to manage the situation with measurable state variables only or to estimate remaining state variables. Both approaches are possible, nevertheless, neither exact linearization techniques nor state feedback techniques are generally usable with partially measurable state variables only. Therefore, the estimation of non-measurable state variables using available measurements is admissible alternative endorsed with a separation principle, i.e. an observer design can be done independently of a controller design. An observer is, roughly speaking, a dynamical system driven by the output of the original dynamical system, having the crucial property that observer states converge to those of the original dynamical system. Precise mathematical definition of the observer for a dynamical system will be given later on.

In the case of Acrobot or 4-link, it is difficult to measure the angle between its stance leg and the surface directly. Actually, this angle is underactuated and it is defined at a generally unknown point. Therefore, it is essential to design an observer for Acrobot or for 4-link such that the observer estimates unmeasurable states of the walking robot. This chapter summarizes results achieved in this respect. More specifically, two observers were designed for Acrobot. Both of them are based on the partial feedback linearized form of Acrobot.

First, the so-called reduced observer for Acrobot based on angular positions $q_{1,2}$ measurement was suggested in [4]. Angular velocities $\dot{q}_{1,2}$ were estimated by the reduced observer. Moreover, the underactuated angle q_1 can be measured indirectly using a laser-beam sensor and a triangulation method. From the definition of coordinates change (3.29), (3.31) coordinates ξ_1, ξ_3 depend on measured variables. They are determined

directly from measurements, however, remaining coordinates ξ_2, ξ_4 need to be estimated.

Secondly, another option of the observer design for Acrobot was presented in [5] where the design of the high gain observer based on angular position q_2 and angular velocity $\dot{q}_1$ measurement was obtained. In this case, the high-gain observer estimates angular position q_1 and angular velocity $\dot{q}_2$. Furthermore, the stability of a feedback tracking of a desired reference trajectory with estimated states by the high-gain observer was verified in [8] using the method of Poincaré sections, moreover, it was demonstrated in simulations as well. The high-gain observer was extended and applied to 4-link in [12] such that it estimates the underactuated angle of 4-link.

6.1 Observer design

Roughly speaking, an observer is a dynamical system driven by output of the original dynamical system with major property that observer states converge to states of the original dynamical system states. The well-known definition of the observer for a dynamical system is as follows.

Definition 6.1.1 *Consider the dynamical system*

$$\begin{aligned} \dot{x} &= f(x,u), \quad x \in \mathbb{R}^n, u \in \mathbb{R}, \\ y &= h(x), \quad y \in \mathbb{R}, \end{aligned} \tag{6.1}$$

than the observer of the dynamical system is the following system

$$\dot{z} = \tilde{f}(z, h(x), u), \quad \tilde{x} \in \mathbb{R}^n, u \in \mathbb{R}, \tag{6.2}$$

ensuring that for each bounded trajectory and input of system (6.1) for all $t \geq t_0$

$$\lim_{t\to\infty} e(t) = 0, \quad \text{where } e(t) := z(t) - x(t). \tag{6.3}$$

In the case of a linear system, the linear observer is constructed with the same structure as the original system and the output error term is added in order to ensure the convergence of the observation error to zero. Namely, the observer is defined as follows

$$\dot{\hat{x}} = A\hat{x}(t) + Bu(t) - L(C\hat{x} - y(t)). \tag{6.4}$$

In the case of linear time invariant systems (LTI), the observer is known as the Luenberger observer [79, 80]. The gain L is selected according to the condition that eigenvalues of $A - LC$ are placed in the left complex half-plane. Whereas in the case of linear time variant systems (LTV), the gain L has to be determined so that it is optimal in an appropriate sense. In virtue of this, the observer is called Kalman-Bucy filter [63, 64].

By virtue of a broad class of nonlinear systems several different types of observers for nonlinear systems were developed. One can find a survey of various observers for nonlinear systems in [88]. Particular observers different from each other in application field based on a particular form of the nonlinear system.

In the following subsections, the reduced observer from [4] and the high-gain observer from [5] for Acrobot are introduced and studied.

6.1.1 Reduced observer for Acrobot

Design of the reduced observer for angular velocities $\dot{q}_1, \dot{q}_2$ is based on the ability to measure the angular positions q_1 and q_2. It is not difficult to see that the knowledge of angles q_1 and q_2 is equivalent to the knowledge of variables $\xi_{1,3}$ in partial exact feedback linearization (3.30) due to transformations (3.32). The remaining variables $\xi_{2,4}$ will be estimated using the reduced observer. The angle q_2 is actuated, therefore, it is elementary to measure this angle directly using e.g. a rotary resolver. However, the underactuated angle q_1, which is defined at a previously unknown point during the step, is not easy to measure directly. Therefore, some indirect method should be used for the angle q_1 measurement.

In [4] a method based on a certain distance measurement using the laser beam sensor is suggested. On the support leg of Acrobot the device for the optical distance measurement is mounted. The angle between the direction of the laser beam and the stance leg is equal to a carefully selected angle α, see Figures 6.1, 6.2. Namely, $0 < \alpha < \tilde{q}_1$ and $\sin\alpha$ should not be too small, see (6.8) later on, so that some trade off is necessary. Nevertheless, $\tilde{q}_1$ is the angle between the stance leg and the ground surface which for a reasonable step varies in the range $(5\pi/12, 7\pi/12)$. Therefore, $\alpha = \pi/3$ is still reasonable with $\sin\alpha = \sqrt{3}/2$.

To compute the underactuated angle q_1, recall that it is defined in Figure 2.1a, realize first that $q_1 = \tilde{q}_1 - \pi/2$ where $\tilde{q}_1$ is defined in Figures 6.1, 6.2, i.e. in the sequel one need to compute the angle $\tilde{q}_1$ only. To do so, realize that the length of the stance leg l is known and it is same as the length of the swing leg. The distance l_1 between the optical laser beam distance sensor and the ground is measured and known.

It is not difficult to see that using the well-known trigonometric laws, the unknown angle $\tilde{q}_1$ is the following function $\tilde{q}_1(l_1)$ of the distance l_1:

$$\tilde{q}_1(l_1) = \begin{cases} \arcsin \frac{l_1 \sin\alpha}{\sqrt{l^2+l_1^2-2ll_1\cos\alpha}}, \ l_1 \geq \frac{l}{\cos\alpha}, \\ \pi - \arcsin \frac{l_1 \sin\alpha}{\sqrt{l^2+l_1^2-2ll_1\cos\alpha}}, \ l_1 \leq \frac{l}{\cos\alpha}. \end{cases} \tag{6.5}$$

One can easily see that

$$\widetilde{q}_1\left(\frac{l}{\cos\alpha}\right) = \arcsin\left(\frac{\frac{l}{\cos\alpha}\sin\alpha}{\sqrt{l^2+\frac{l^2}{\cos^2\alpha}-2l^2}}\right) = \tag{6.6}$$

$$\arcsin\left(\frac{\sin\alpha}{\sqrt{-\cos^2\alpha+1}}\right) = \arcsin(1) = \frac{\pi}{2},$$

and therefore the function $\tilde{q}_1(l_1)$ in (6.5) is a well defined continuous function. Moreover,

$$\frac{\partial\widetilde{q}_1}{\partial l_1} = \frac{\operatorname{sign}(l_1\cos\alpha - l)\sin\alpha}{\sqrt{1-\frac{l_1^2\sin^2\alpha}{l^2+l_1^2-2ll_1\cos\alpha}}}\frac{\sqrt{l^2+l_1^2-2ll_1\cos\alpha}-\frac{l_1(2l_1-2\cos\alpha)}{2\sqrt{l^2+l_1^2-2ll_1\cos\alpha}}}{l^2+l_1^2-2ll_1\cos\alpha} = \tag{6.7}$$

$$-\frac{l\sin\alpha}{l^2+l_1^2-2ll_1\cos\alpha}, \quad \forall l_1.$$

Relations (6.5), (6.6), (6.7) imply that $\widetilde{q}_1(l_1)$ is smooth function of l_1 for $\forall l_1 \Rightarrow 0$ if and only if $\widetilde{q}_1 < \pi$. Moreover, one can check directly that

$$|\frac{\partial\widetilde{q}_1}{\partial l_1}| \leq \frac{1}{l\sin\alpha}, \quad \forall l_1, \tag{6.8}$$

so that the sensitivity of $\widetilde{q}_1(l_1)$ with respect to the error in measurement of l_1 is very good.

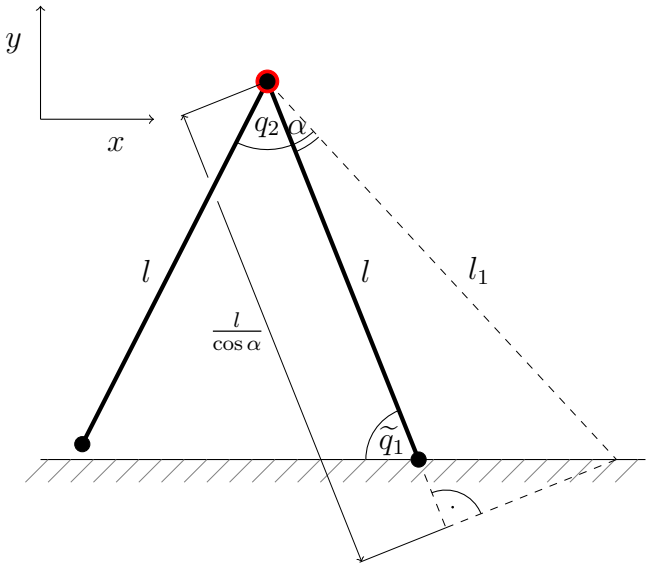

Figure 6.1. Measurement of the angle q_1 using a laser beam sensor at the beginning of the step.

Based on the previous considerations, consider the following problem to observe $\xi_{2,4}$ in (3.30) based on knowledge of $\xi_{1,3}$. To do so, consider following equations

$$\frac{\partial}{\partial t}\left(\widetilde{\xi}_2\right) = \xi_3 - k_2^2\xi_1 d_{11}^{-1}(q_2) - k_2\widetilde{\xi}_2 d_{11}^{-1}(q_2), \tag{6.9}$$

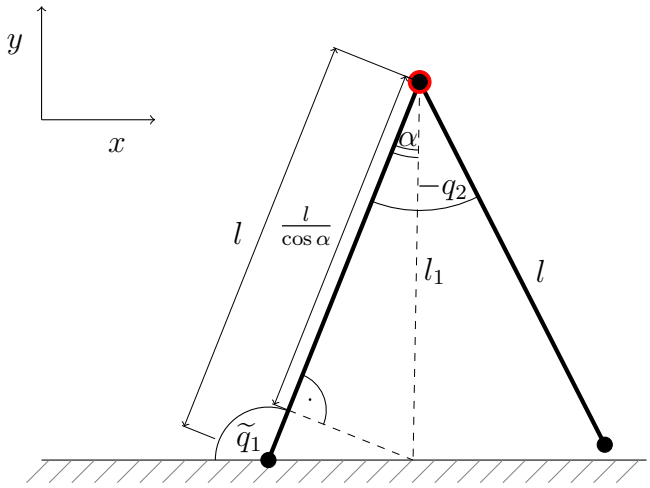

Figure 6.2. Measurement of the angle q_1 using a laser beam sensor at the end of the step.

$$\frac{\partial}{\partial t}\left(\xi_2 - k_2\xi_1\right) = \xi_3 - d_{11}^{-1}(q_2)\xi_2 k_2, \tag{6.10}$$

then the observer error e_2 can be expressed as follows

$$e_2 = \widetilde{\xi}_2 - \xi_2 + k_2\xi_1. \tag{6.11}$$

Dynamics of the error estimate e_2 is given by the following differential equation

$$\dot{e}_2 = -k_2 d_{11}^{-1}(q_2(t))\left(\widetilde{\xi}_2 + k_2\xi_1 - \xi_2\right) = -k_2 d_{11}^{-1}(q_2(t))e_2. \tag{6.12}$$

The solution of differential equation (6.12) is

$$e_2 = e_2(0)\exp^{-k_2\int_0^t d_{11}^{-1}(q_2(\tau))d\tau}. \tag{6.13}$$

And therefore for $k_2 > 0$ and $t \to \infty$, it holds that $e_2 \to 0$ exponentially and $\widetilde{\xi}_2 + k_2\xi_1 \to \xi_2$ exponentially as well.

Furthermore, consider the following equations

$$\frac{\partial}{\partial t}\left(\widetilde{\xi}_4\right) = \alpha(q)\tau_2 + \beta(q,\dot{\widehat{q}}) - k_4^2\xi_3 - k_4\widetilde{\xi}_4, \tag{6.14}$$

$$\frac{\partial}{\partial t}\left(\xi_4 - k_4\xi_3\right) = \alpha(q)\tau_2 + \beta(q,\dot{\widehat{q}}) - k_4\xi_4, \tag{6.15}$$

then the observer error e_4 can be expressed as follows

$$e_4 = \widetilde{\xi}_4 - \xi_4 + k_4\xi_3. \tag{6.16}$$

Dynamics of the error estimate e_4 is given by the following differential equation

$$\dot{e_4} = -k_4 \left(\widetilde{\xi}_4 - \xi_4 + k_4 \xi_3 \right) + \beta(q, \dot{\widehat{q}}) - \beta(q, \dot{q}). \tag{6.17}$$

Equation (6.17) can be rewritten in the following form

$$\dot{e_4} = -k_4 e_4 + \overline{\varphi}\left(\xi_1, \xi_2, \xi_3, \xi_4, e_2, e_4\right). \tag{6.18}$$

As a consequence, for $k_4 > 0$ and $t \to \infty$, it holds that $e_4 \to 0$ exponentially. And therefore $\widetilde{\xi}_4 + k_4 \xi_3 \to \xi_4$ exponentially as well.

Simulations

A feedback tracking of the pseudo-passive reference trajectory with observed angular velocities $\dot{q}_1, \dot{q}_2$ using the reduced observer is demonstrated here by simulations. In Figure 6.3a one can see a course of measured angular positions during the tracking. In Figure 6.3b one can see a time response of observed angular velocities and ability of the feedback tracking for observer gain $k_2 = 10$ and $k_4 = 10$. Initial errors of the observer, in $\widetilde{\xi}_2$, $\widetilde{\xi}_4$, are approximately 50% of real values ξ_2, ξ_4. In Figure 6.4a one can see convergence of the estimated coordinates $\widehat{\xi}_2$, $\widehat{\xi}_4$ to real coordinates ξ_2, ξ_4 and time responses of errors of estimates e_2, e_4.

It was shown in [4] that the lowest possible gains of the observer $k_2 = 1$ and $k_4 = 2$ could be used with initial observer errors approximately 2% of real values ξ_2, ξ_4. Moreover, in [4] an effect of higher gains for the observer is shown as well. The bigger gains for the observer are, the more quickly the estimates of coordinates converge to real coordinates. On the other hand, higher gains tend to amplify existing noise, thus reducing the accuracy of the estimates.

Finally, Figure 6.4b shows the animation of Acrobot walking during one step with observed angular velocities $\dot{q}_1, \dot{q}_2$ for observer gains $k_2 = 10$ and $k_4 = 10$.

6.1.2 High gain observer for Acrobot

By virtue of the form of Acrobot in partial linearized coordinates (3.30), a high gain observer [46, 68] is an appropriate observer for Acrobot. The design of the high gain observer for Acrobot is presented here. The design was firstly presented in [5] and extended in [8] and [12] later on. The high gain observer estimates states of Acrobot in linearizing coordinates (3.29), (3.31) as Acrobot controller (5.3) works in these coordinates as well. However, the high gain observer can not properly estimate Acrobot states in linearizing coordinates ξ without an output measurement to minimize the observer error. To do so, the original linearizing function p (3.24) is slightly changed such that the linearizing

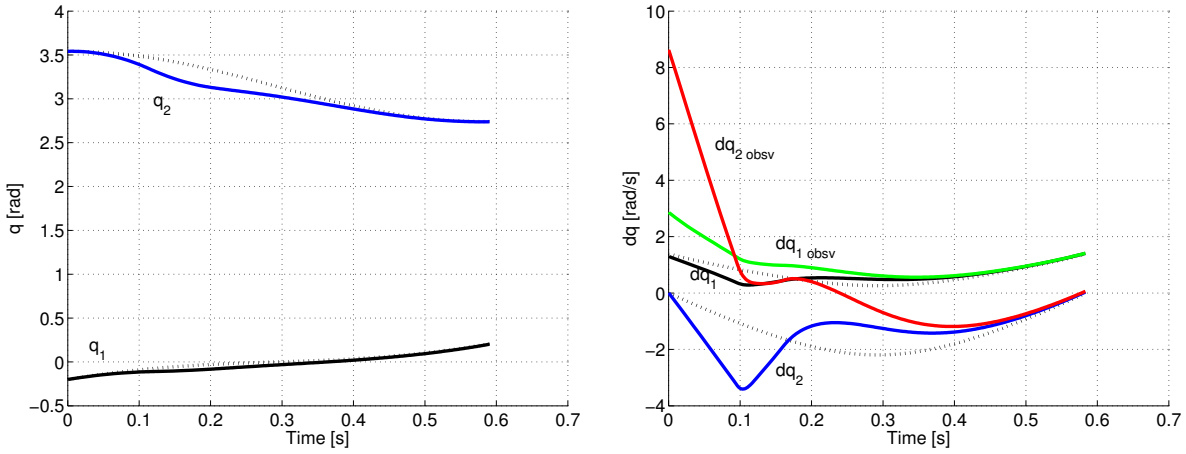

(a) (b)

Figure 6.3. (a) Directly or indirectly measured angular positions q_1, q_2. (b) Observed and real angular velocities $\dot{q}_1$, $\dot{q}_2$ for $k_2 = 10$ and $k_4 = 10$ and references (dotted line).

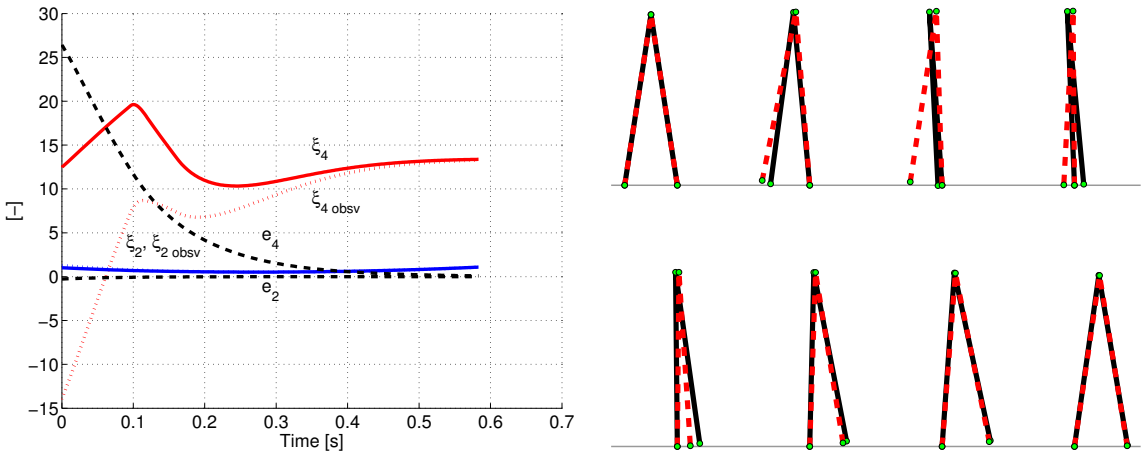

(a) (b)

Figure 6.4. (a) Convergence of estimates $\widehat{\xi}_{2,4}$ to real values of $\xi_{2,4}$ and a time response of errors of estimates $e_{2,4}$. (b) The animation of the single step with sampling time 0.08 s. The dashed line is the reference system, the full line represents "real" Acrobot.

function could be computed from accessible measurements only. As a consequence, the changed linearizing function p is used to minimize the observer error whereas remaining three linear coordinates $\xi_{2,3,4}$ are estimated using the high gain observer because they depend on unmeasured Acrobot states. To do so, define

$$\eta_1(q_2) = p - q_1, \tag{6.19}$$

depending only on angular position q_2 measurement. Remaining linearizing functions η_2, η_3, η_4 are based on the original linearizing function σ defined in (3.22) and its time derivatives

$$\eta_2 = \sigma, \quad \eta_3 = \dot{\sigma}, \quad \eta_4 = \ddot{\sigma}. \tag{6.20}$$

Taking time derivative of (6.19) gives $\dot{\eta}_1 = \dot{p} - \dot{q}_1$ and by (3.28) Acrobot dynamics in the alternative partial exact linearized form is as follows

$$\begin{aligned} \dot{\eta}_1 &= d_{11}^{-1}(q_2)\,\eta_2 - \dot{q}_1, \\ \dot{\eta}_2 &= \eta_3, \\ \dot{\eta}_3 &= \eta_4, \\ \dot{\eta}_4 &= \beta(\eta) + \alpha(\eta_1, \eta_3)\,\tau_2. \end{aligned} \tag{6.21}$$

Recall that $\eta_1, \eta_2, \eta_3, \eta_4$ are given by (6.19), (6.20) The new form (6.21) facilitates the high gain observer design. By virtue of Acrobot measurable outputs q_2 and $\dot{q}_1$, the new linearizing coordinate η_1 is measurable. Only for completeness, the angular velocity $\dot{q}_1$ is measurable using a gyroscope and the angular position q_2 is measurable using e.g. a rotary resolver. Then, the high gain observer for Acrobot takes the following form

$$\begin{aligned} \dot{\hat{\eta}}_1 &= -L_1(\eta_1 - \hat{\eta}_1) + d_{11}^{-1}(q_2)\,\hat{\eta}_2 - \dot{q}_1, \\ \dot{\hat{\eta}}_2 &= -L_2(\eta_1 - \hat{\eta}_1) + \hat{\eta}_3, \\ \dot{\hat{\eta}}_3 &= -L_3(\eta_1 - \hat{\eta}_1) + \hat{\eta}_4, \\ \dot{\hat{\eta}}_4 &= -L_4(\eta_1 - \hat{\eta}_1) + \beta(\hat{\eta}) + \alpha(\eta_1, \hat{\eta}_3)\,\tau_2. \end{aligned} \tag{6.22}$$

Denoting the observer error as $e = \hat{\eta} - \eta$, one has

$$\begin{aligned} \dot{e}_1 &= L_1 e_1 + d_{11}^{-1}(q_2)\,e_2, \\ \dot{e}_2 &= L_2 e_1 + e_3, \\ \dot{e}_3 &= L_3 e_1 + e_4, \\ \dot{e}_4 &= L_4 e_1 + \beta(\hat{\eta}) - \beta(\eta) + (\alpha(\eta_1, \hat{\eta}_3) - \alpha(\eta_1, \eta_3))\,\tau_2. \end{aligned} \tag{6.23}$$

Now, gains $L_{1,2,3,4}$ can be designed using standard high-gain techniques, namely, take any $\widetilde{L}_{1,2,3,4}$ such that the following matrix

$$\begin{bmatrix} \widetilde{L}_1 & 1 & 0 & 0 \\ \widetilde{L}_2 & 0 & 1 & 0 \\ \widetilde{L}_3 & 0 & 0 & 1 \\ \widetilde{L}_4 & 0 & 0 & 0 \end{bmatrix} \tag{6.24}$$

is Hurwitz and define

$$L_1 = \Theta\widetilde{L}_1, \quad L_2 = \Theta^2\widetilde{L}_2, \quad L_3 = \Theta^3\widetilde{L}_3, \quad L_4 = \Theta^4\widetilde{L}_4. \tag{6.25}$$

It is proved in [5] that system (6.23), (6.24), (6.25) is exponentially stable for Θ large enough. Therefore $e(t) = \widehat{\eta}(t) - \eta(t) \to 0$, i.e. $\widehat{\eta}(t) \to \eta(t)$, as $t \to \infty$ and therefore (6.22) is the exponential observer for (6.21).

Summarizing, Acrobot dynamics in the partial exact linearized form together with the high gain observer have the following form

$$\begin{aligned} \dot{\xi}_1 &= d_{11}(q_2)^{-1}\hat{\eta}_2, \\ \dot{\xi}_2 &= \hat{\eta}_3, \\ \dot{\xi}_3 &= \hat{\eta}_4, \\ \dot{\xi}_4 &= \alpha(q,\dot{q})\tau_2 + \beta(q,\dot{q}) = w, \\ \dot{\hat{\eta}}_1 &= -L_1(\eta_1 - \hat{\eta}_1) + d_{11}^{-1}(q_2)\,\hat{\eta}_2 - \dot{q}_1, \\ \dot{\hat{\eta}}_2 &= -L_2(\eta_1 - \hat{\eta}_1) + \hat{\eta}_3, \\ \dot{\hat{\eta}}_3 &= -L_3(\eta_1 - \hat{\eta}_1) + \hat{\eta}_4, \\ \dot{\hat{\eta}}_4 &= -L_4(\eta_1 - \hat{\eta}_1) + \beta(\hat{\eta}) + \alpha(\eta_1, \hat{\eta}_3)\,\tau_2. \end{aligned} \tag{6.26}$$

Simulation

To demonstrate the usability of the presented high gain observer and its straightforward combination with a state feedback controller, the exponential tracking of the pseudo-passive reference trajectory is considered here. One can see a quality of the feedback tracking in Figures 6.5a, b, especially in Figure 6.5a one can see a time response of the estimated angular position q_1. Furthermore, the angular position q_2 is measured while in Figure 6.5b one can see a time response of the estimated angular velocity $\dot{q}_2$. The angular velocity $\dot{q}_1$ is measured. In Figure 6.6a one can see a time response of errors of estimates $e_{2,3,4}$.

The observer gain L is given by (6.25), where $\widetilde{L} = -10^4 \cdot [0.0046, 0.0791, 0.6026, 1.7160]$, and "amplifying" parameter $\Theta = 20$. Initial errors of the observer are approximately 20% of real values of ξ_2, ξ_3, ξ_4. For the sake of comparison with feedback tracking with the reduced observer shown in the previous subsection, the used feedback controller with feedback gain and initial conditions of the reference and the real step are taken the same.

Finally, Figure 6.6b shows the animation of Acrobot walking during one step with the observed angular position q_1 and angular velocity $\dot{q}_2$ using the high gain observer.

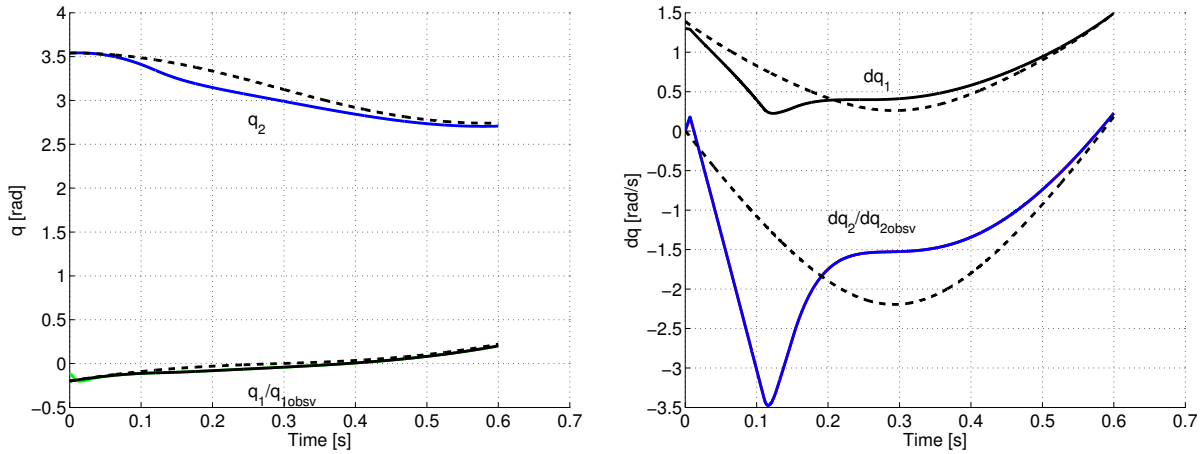

(a) (b)

Figure 6.5. Observed and measured angular positions q_1, q_2 (a) and angular velocities $\dot{q}_1$, $\dot{q}_2$ (b) for high gain observer and references (dotted line) during a feedback tracking of the pseudo-passive reference trajectory during one step.

6.1.3 High gain observer for 4-link

In [12] the high gain observer for 4-link was introduced. This observer is based on the original high gain observer for Acrobot and by virtue of embedding method it is simply extended and used in an application of feedback tracking of a reference trajectory without the underactuated angle q_1 measurement. In contrast to the original high gain observer for Acrobot, angular position and velocity are measured in actuated links of 4-link in order to transform "old" coordinates in (2.7) into "new" coordinates defined in (3.36). In the case of the first link, i.e. the not actuated link, the angular velocity $\dot{q}_1$ is measured only.

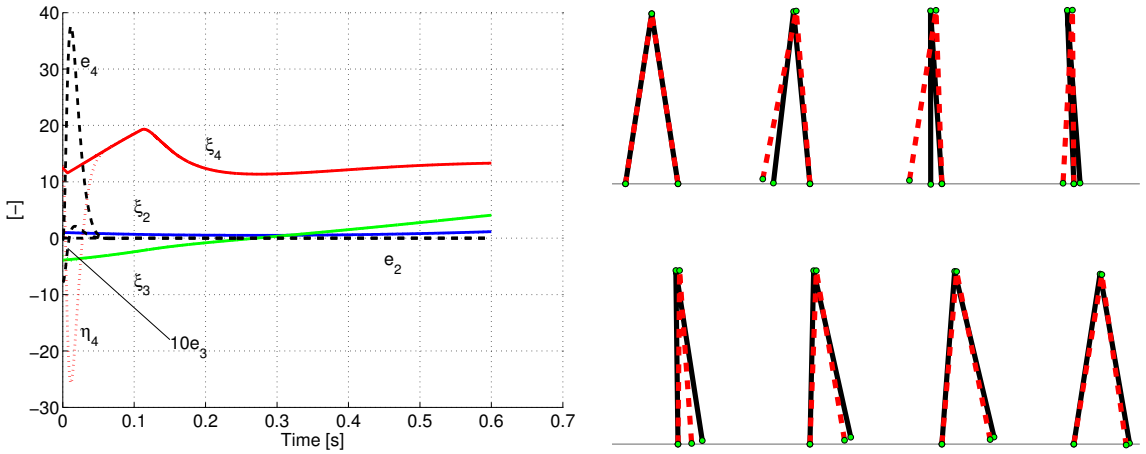

(a) (b)

Figure 6.6. (a) Convergence of estimates $\eta_{2,3,4}$ to real values of $\xi_{2,3,4}$ and a time response of errors of estimates $e_{2,3,4}$. (b) The animation of the single step with sampling time 0.08 s. The dashed line is the reference system, the full line represents the "real" Acrobot.

6.2 Chapter conclusion

Two algorithms how to observe any state of Acrobot based on the knowledge of position variables only or on the knowledge of one angular position variable and one angular velocity variable were provided. Both observers can be combined with the current state feedback approach presented in the previous chapter in order to provide Acrobot reference trajectory tracking using measurement feedback.

Chapter 7

Underactuated walking hybrid stability

In this chapter a stability analysis of Acrobot walking is done using a method of Poincaré sections. Acrobot or 4-link walking consists of a periodic change of a swing phase and a double support phase. Therefore, it is not possible to determine the walking stability without taking the double support phase and the impact into the account. The swing phase of the walking is consecutively controlled using tracking method presented in the previous chapter. Each tracking method is distributively verified by the method of Poincaré sections whether it is able to stabilize not only the swing phase of the step but whole walking including the swing phase, the impact and switch of legs. The stability analysis is done only for Acrobot, nevertheless, by virtue of the embedding method, its extension for 4-link is straightforward. Results of stability analysis by method of Poincaré sections are demonstrated by simulations of Acrobot walking during approximately 150 steps. It demonstrates the ability of Acrobot walking control to make a priory unlimited number of steps.

7.1 Method of Poincaré sections

The walking features the so-called limit cycle resulting from time-continuous phase, impact detection and reinitialization rules. To determine the stability of such hybrid nonlinear system with impulse effects, the method of Poincaré sections is used here. The same idea of stability determination of a biped walking is done e.g. in [129, 130].

The application of the method of Poincaré sections is straightforward. Roughly speaking, a solution $\phi(t, x)$ of a system is sampled according to usually event-based or time-based rule and then the stability of an equilibrium point of the sampled system is evaluated. The event-based or time-based rule is in the literature usually called Poincaré

section $\mathcal{S}$, which is determined by crossing a plane being transversal to a trajectory of the system solution $\phi(t, x)$. The correspondence between two subsequent crossing of $\mathcal{S}$ by the trajectory of the system solution $\phi(t, x)$ is called in the literature as the Poincaré return map $\mathcal{P}$, $\mathcal{P} : \mathcal{S} \to \mathcal{S}$. In another words, the Poincaré return map $\mathcal{P}$ is a mapping from an initial point $x \in \mathcal{S}$ to the intersection of the surface $\mathcal{S}$ with the solution $\phi(t, x)$, i.e. $\mathcal{P}(x) := \phi(t, x)$.

In our case, the Poincaré section is defined at the middle of the step time $\frac{T}{2}$, where T is total step time. The Poincaré return map is defined by the Poincaré section $\mathcal{S}$ and it represents the evolution of Acrobot swing phase from this point until the end of the step through the impact phase including change of legs and Acrobot swing phase in the next step until it intersects the Poincaré section $\mathcal{S}$ in the middle of the next step.

A point $x^* \in \mathcal{S}$ is called a fixed point of the Poincaré map if $\mathcal{P}(x^*) = x^*$. The known cyclic motion of coordinates $q, \dot{q}$ gives a unique fixed point $x^* = (q_1(\frac{T}{2}),\ q_2(\frac{T}{2}),\ \dot{q}_1(\frac{T}{2}),\ \dot{q}_2(\frac{T}{2}))$ which depends on used feedback controller. By definition, the Poincaré return map

$$x[k+1] = \mathcal{P}(x[k]) \tag{7.1}$$

is a discrete-time system on the Poincaré section $\mathcal{S}$. Define $\delta x^z[k] = x^z[k] - x^*$ the Poincaré return map linearized about the fixed-point x^*, then it gives rise to a linearized system

$$\delta x^z[k+1] = A^z \delta x^z[k], \tag{7.2}$$

where the (4x4) square matrix A^z is the Jacobian of the Poincaré map and it is computed as follows

$$A^z = [A_1^z \ \ A_2^z \ \ A_3^z \ \ A_4^z]_{4\text{x}4}\,, \tag{7.3}$$

where

$$A_i^z = \frac{P(x^* + \Delta x_i^z) - P(x^* - \Delta x_i^z)}{2\,\Delta x_i^z}, \quad i = 1, 2, 3, 4, \tag{7.4}$$

and $\Delta x_i^z = \Delta q_{1,2}$ for $i = 1, 2$ and $\Delta x_i^z = \Delta \dot{q}_{1,2}$ for $i = 3, 4$. A fixed-point x^* of the Poincaré return map is locally exponentially stable if, and only if, the eigenvalues of A^z lie inside the unit circle. For more details see e.g. [130].

The calculation of the matrix A^z requires eight evaluations of the Poincaré return map $\mathcal{P}$, two evaluations for each coordinate. Each evaluation of the Poincaré return map is composed of the integration of the swing phase from $t = \frac{T}{2}$ to the collision with the ground, the calculation of the influence of the impact on angular velocities including their relabeling due to switching the swing and the stance leg and relabeling of angular positions and the integration of the swing phase until $t = \frac{T}{2}$.

7.2 Stability analysis

The stability analysis of Acrobot walking using the method of Poincaré sections is done here. Acrobot is controlled using tracking methods presented in Chapter 5. If eigenvalues of matrix A^z defined in (7.3) lie inside the unit circle, the corresponding tracking method is stable. This analysis is performed in the sequel for each of tracking methods presented in Sections 5.2-5.6 of Chapter 5.

Stability analysis - LMI design

To track the multi-step walking reference trajectory by Acrobot using the LMI design described in Section 5.2, the feedback gain $K = -10^5 \cdot [5.2958,\ 2.9152,\ 0.4415,\ 0.0145]$ is used. The corresponding matrix A^z has the following form

$$A^z = \begin{bmatrix} -0.6072 & 0.0549 & -0.1692 & 0.0121 \\ 0.0157 & 0.0857 & -0.0319 & -0.0156 \\ 2.5882 & -0.2576 & 0.7308 & -0.0478 \\ 3.9368 & -1.2556 & 1.4751 & 0.0795 \end{bmatrix}$$

and its eigenvalues are as follows

$$\mathrm{eig}(A^z) = [0.2174,\ 0.0689,\ 0.0037,\ -0.0011]\,,$$

therefore, Acrobot walking controlled by the LMI method is stable according to the Poincaré test of stability.

Figures 7.1a, b show phase-plane plots of variables q_1 and q_2. The convergence towards a periodic motion is clearly seen from simulations of approximately 150 steps.

Stability analysis - Analytical design

To track the multi-step walking reference trajectory for Acrobot using the analytical design described in Section 5.3, the feedback gain $\widetilde{K} = -(9, 6, 12, 8)$ is used together with the "amplifying" parameter $\Theta = 15$. The corresponding matrix A^z has the following form

$$A^z = \begin{bmatrix} -0.3046 & 0.0660 & -0.1609 & 0.0060 \\ 2.3486 & 0.0524 & 0.4040 & -0.0916 \\ 2.7134 & -0.4604 & 1.2364 & -0.0649 \\ -0.8721 & -2.4579 & 3.5321 & 0.2259 \end{bmatrix}$$

and its eigenvalues are as follows

$$\mathrm{eig}(A^z) = [0.6456,\ 0.5514,\ 0.0153,\ -0.0021]\,.$$

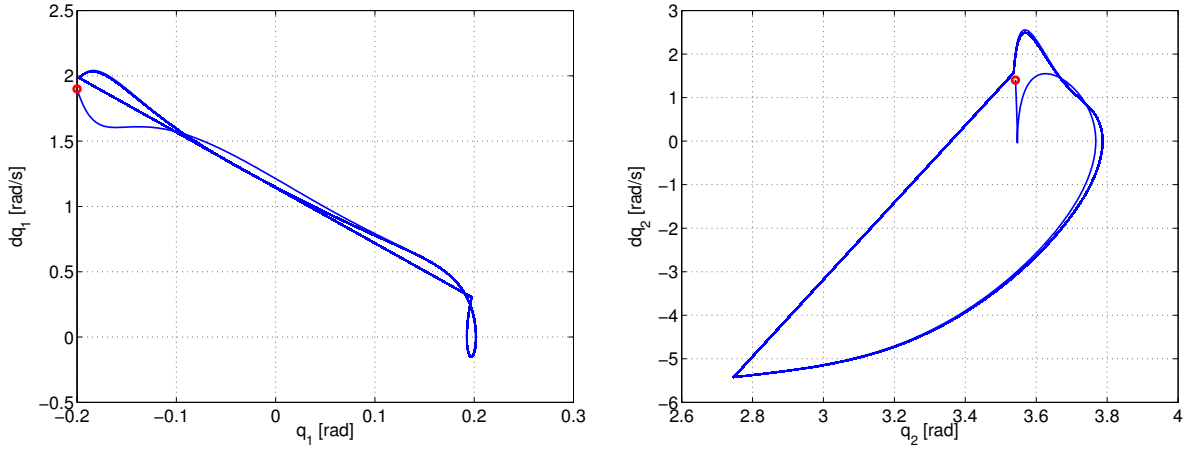

(a) (b)

Figure 7.1. Phase-plane plots of the LMI design for (a) q_1, (b) q_2. The initial state is represented by a red circle.

One can see that the Poincaré test of stability is fulfilled, therefore, Acrobot walking controlled using the analytical design approach is stable.

Figures 7.2a, b show phase-plane plots of variables q_1 and q_2. The convergence towards a periodic motion is clearly seen from simulations of approximately 150 steps.

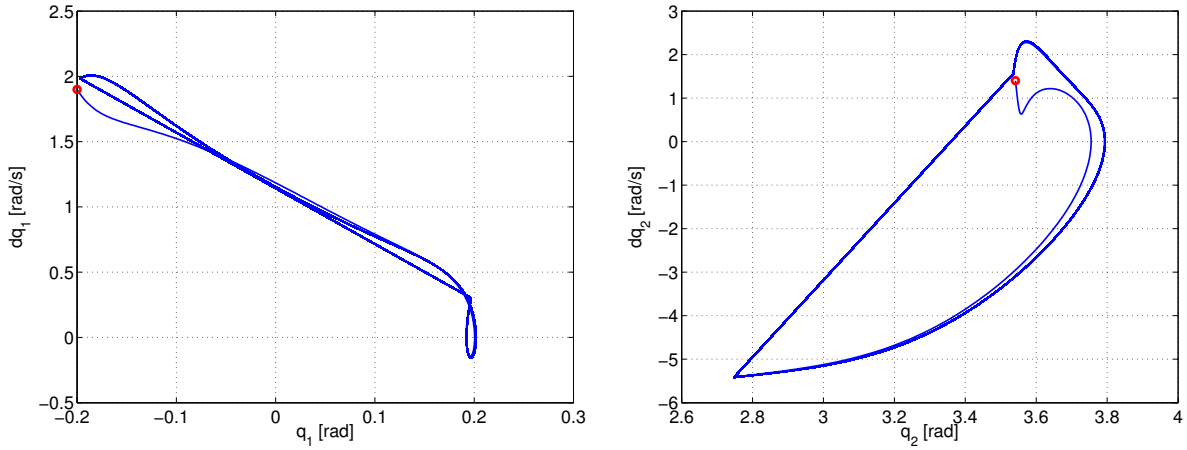

(a) (b)

Figure 7.2. Phase-plane plots of (a) q_1, (b) q_2. Acrobot walking is controlled using the analytical approach. The initial state is represented by a red circle.

Stability analysis - Extended analytical design

The advantage of the extended analytical approach, presented in Section 5.4, consists in a time varying state and a feedback transformation which enable to design a fundamental matrix of the error dynamics in an explicit form. Moreover, a product of that fundamental matrix at the end of the single support walking phase, i.e. at the end of the step, by the Jacobian of the impact map enables directly prove a stability of the multi-step walking reference trajectory tracking by computing certain 4x4 matrix and determining numerically whether its eigenvalues lie within the unit circle or not. Therefore, the stability proof is done here using an analytical method in contrast to the numerical method used in previous cases.

By virtue of transformation (5.21)-(5.24), the corresponding error dynamics (5.34) has a form enabling to simply solve the matrix exponential, i.e. to find the state transition matrix. Just to remind, equation (5.34) has following form

$$\dot{\bar{e}} = \left(\widetilde{A} + \widetilde{B}K\right)\bar{e} = \begin{pmatrix} 0 & 1 & 0 & 0 \\ 0 & 0 & 1 & 0 \\ 0 & 0 & 0 & 1 \\ K_1 & K_2 & K_3 & K_4 \end{pmatrix} \bar{e}.$$

The solution of (5.34) will be used to determine the analytical proof of the Acrobot walking stability. The stability analysis is based on the eigenvalues of the matrix $e(T^+)$ which is defined below. This matrix corresponds to the error after one step followed by the impact.

$$e(T^+) = \frac{\partial \widetilde{\Phi}^{\xi}_{\mathrm{Imp}}}{\partial \xi}(\xi(T)) \times X^{-1}(T)\Phi(T)X(0)e_0, \tag{7.5}$$

where e_0 is the initial error, $\Phi(T)$ is the solution of differential equation (5.34) and $\widetilde{\Phi}^{\xi}_{\mathrm{Imp}}(\xi(T))$ is a matrix realizing influence of the impact on angular velocities including their relabeling due to switching the swing and the stance leg and relabeling of angular positions in ξ coordinates. And $X(0)$ and $X(T)$ defined in 5.29 are evaluated at the beginning or at the end of the step, respectively. The impact matrix $\widetilde{\Phi}_{\mathrm{Imp}}(q(T))$ initially developed in $q, \dot{q}$ coordinates, see Section 2.2, is extended by the transformation $\mathcal{T}$ expressed in (3.31) related with transformation from $q, \dot{q}$ coordinates to ξ coordinates obtained in [30].

For the sake of an easier and compact notation the transformation $\mathcal{T}$ is represented

as follows

$$\begin{bmatrix} \mathcal{T}_1 \\ \mathcal{T}_3 \\ \mathcal{T}_2 \\ \mathcal{T}_4 \end{bmatrix} = \begin{bmatrix} p(q_1, q_2) \\ \theta_4 g \sin q_1 + \theta_5 g \sin(q_1 + q_2) \\ \Phi_2(q_1, q_2) \begin{bmatrix} \dot{q}_1 \\ \dot{q}_2 \end{bmatrix} \end{bmatrix},$$

where p is given by (3.22) and $\Phi_2(q)$ is defined in (3.35).

In Section 2.2 impact matrix $\widetilde{\Phi}_{\mathrm{Imp}}(q(T))$ (2.39) was developed realizing the influence of the impact on angular velocities including their relabeling and relabeling of angular positions in q coordinates. The impact matrix has the following meaning

$$\left[q_1^+ \; q_2^+ \; \dot{q}_1^+ \; \dot{q}_2^+\right]^{\mathrm{T}} = \widetilde{\Phi}_{\mathrm{Imp}}(q(T)) \left[q_1^- \; q_2^- \; \dot{q}_1^- \; \dot{q}_2^-\right]^{\mathrm{T}}, \tag{7.6}$$

where $\dot{q}_1^-$, $\dot{q}_2^-$ are velocities "just before" the impact, while $\dot{q}_1^+$, $\dot{q}_2^+$ are velocities "just after" the impact and relabeling. Angular positions do not change during the impact, therefore q_1^+, q_2^+ denote angular positions after relabeling only.

Its Jacobian $\frac{\partial \widetilde{\Phi}_{\mathrm{Imp}}(q(T))}{\partial(q,\dot{q})}$ is as follows

$$\frac{\partial \widetilde{\Phi}_{\mathrm{Imp}}(q(T))}{\partial(q, \dot{q})} = \begin{bmatrix} -1 & -1 & 0 & 0 \\ 0 & -1 & 0 & 0 \\ \left[\frac{\partial \bar{\bar{\Phi}}_{\mathrm{Imp}}}{\partial q_1} \; \frac{\partial \bar{\bar{\Phi}}_{\mathrm{Imp}}}{\partial q_2}\right] \dot{q} \; \bar{\bar{\Phi}}_{\mathrm{Imp}} \end{bmatrix}, \tag{7.7}$$

where, $\bar{\bar{\Phi}}_{\mathrm{Imp}}$ represents adapted solution of (2.36). Only the first and the second column and row of (2.36) are taken into the account, moreover in contrast to $\bar{\Phi}_{\mathrm{Imp}}$, the second row is subtracted from the first row of the sub-matrix. This adaptation is done according to the definition of the impact matrix (2.39).

Nevertheless, in order to express the Jacobian of the impact matrix in ξ coordinates, it is necessary to permute the second and the third component of the Jacobian of the transformation $\mathcal{T}$ originally expressed in equation (3.31). Therefore, denote as T_r a matrix permuting the second and the third component, than the Jacobian of the transformation $\mathcal{T}$ is as follows

$$T_r \frac{\partial \mathcal{T}}{\partial(q, \dot{q})} T_r^{-1} = \begin{bmatrix} \Phi_1(q) & 0 \\ \Phi_3(q, \dot{q}) & \Phi_2(q) \end{bmatrix}, \tag{7.8}$$

where $\Phi_1(q)$ is defined in (3.34), $\Phi_2(q)$ is defined in (3.35) and $\Phi_3(q, \dot{q})$ is a certain (2×2) matrix of smooth functions.

The final form of equation (7.5) is as follows

$$e(T^+) = \frac{\partial \mathcal{T}}{\partial(q, \dot{q})} \frac{\partial \widetilde{\Phi}_{\mathrm{Imp}}(q(T))}{\partial(q, \dot{q})} \left(\frac{\partial \mathcal{T}}{\partial(q, \dot{q})}\right)^{-1} \times X^{-1}(T)\, \Phi(T)\, X(0)\, e_0, \tag{7.9}$$

where the first three therms express the impact matrix $\widetilde{\Phi}^{\xi}_{\mathrm{Imp}}(\xi(T))$ in ξ coordinates.

Substituting (7.8), (7.7) in (7.9) the equation for computing eigenvalues of the matrix $e(T^+)$ is as follows

$$e(T^+) = T_r \begin{bmatrix} \Phi_1 & 0 \\ \Phi_3 & \Phi_2 \end{bmatrix} \begin{bmatrix} -1 & -1 & 0 & 0 \\ 0 & -1 & 0 & 0 \\ \left[\frac{\partial \bar{\bar{\Phi}}_{\mathrm{Imp}}}{\partial q_1} \; \frac{\partial \bar{\bar{\Phi}}_{\mathrm{Imp}}}{\partial q_2}\right] \dot{q} & & \bar{\bar{\Phi}}_{\mathrm{Imp}} & \end{bmatrix} \begin{bmatrix} \Phi_1^{-1} & 0 \\ -\Phi_3 \Phi_1^{-1} \Phi_2^{-1} & \Phi_2^{-1} \end{bmatrix} T_r^{-1} \times \tag{7.10}$$

$$X^{-1}(T)\, \Phi(T)\, X(0)\, e_0.$$

To analyze the stability of Acrobot walking it is necessary to compute eigenvalues of the matrix $e(T^+)$. Matrices $X(T)$ and $X(0)$ defined in (5.29) are evaluated at the end and at the beginning of the step, respectively, using values of reference functions $\mu_{1,2,3}(t)$ and its time derivative. Matrices $\frac{\partial \Phi_{Imp_{q,\dot{q}}}}{\partial(q,\dot{q})}$ and $\frac{\partial \mathcal{T}}{\partial(q,\dot{q})}$ are evaluated at the end of the step as well. Feedback gains for the system (5.31) have to be chosen so that the closed-loop system (5.34) is stable.

For feedback gains $K = -10^6 \cdot [1.2150, 0.1688, 0.0079, 0.0002]$ the degree of eigenvalues of the matrix $e(T^+)$ is less than 10^{-3}, therefore, using this feedback approach Acrobot walking is stable and it converges to the stable walking cycle. This proof of the Acrobot walking stability is equivalent to the stability proof by Poincaré sections. The Poincaré test gives eigenvalues, indeed, inside the unit circle.

Figures 7.3a, b show phase-plane plots of variables q_1 and q_2. The convergence towards a periodic motion is clearly seen from simulations of approximately 150 steps.

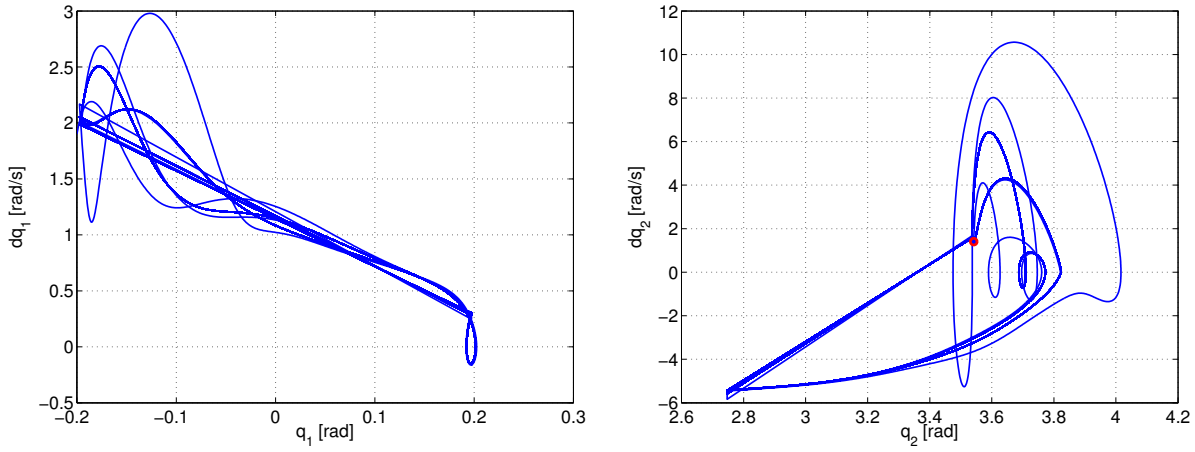

(a) (b)

Figure 7.3. Phase-plane plots for (a) q_1, (b) q_2. Acrobot walking is controlled using the extended analytical approach. The initial state is represented by a red circle.

Stability analysis - Approximate analytical design

To track the multi-step walking reference trajectory by Acrobot using the approximate analytical tracking technique described in Section 5.5, the feedback gain $K = -10^5 \times [5.2958, 2.9152, 0.4415, 0.0145]$ is used. The corresponding matrix A^z has the following form

$$A^z = \begin{bmatrix} 0.0358 & -0.0042 & 0.0027 & -0.0002 \\ 0.3112 & -0.0395 & 0.0265 & -0.0020 \\ 1.8303 & -0.1626 & 0.0755 & -0.0055 \\ 24.9280 & -2.2151 & 1.0107 & -0.0733 \end{bmatrix}$$

and its eigenvalues are as follows

$$\text{eig}(A^z) = [-0.0126,\ 0.0092,\ 0.0001,\ 0.0017]\,.$$

One can see that the Poincaré test of stability is fulfilled, therefore, Acrobot walking controlled using the approximate analytical design approach is stable.

Figures 7.4a, b show phase-plane plots of variables q_1 and q_2. The convergence towards a periodic motion is clearly seen from simulations of approximately 150 steps.

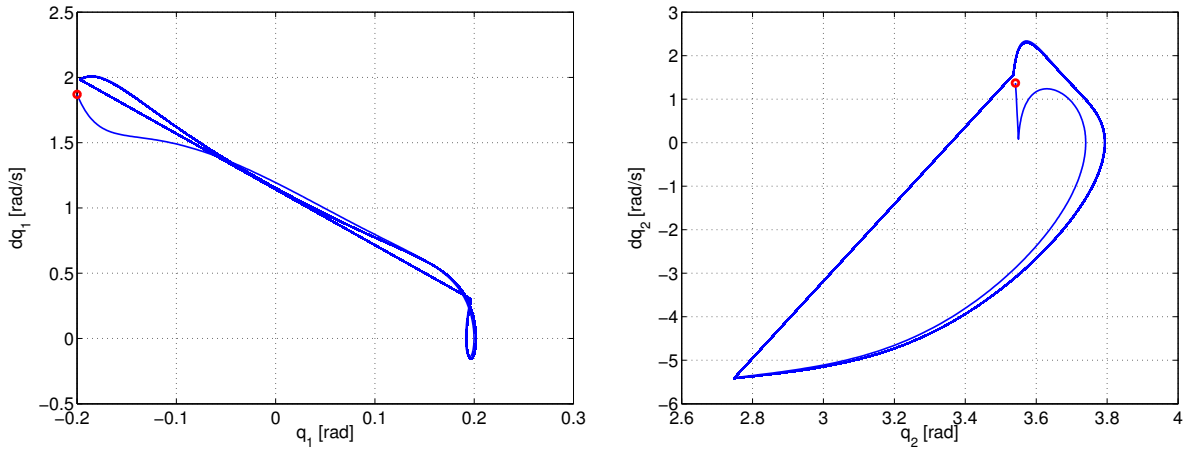

(a) (b)

Figure 7.4. Phase-plane plots for (a) q_1, (b) q_2. Acrobot walking is controlled using the approximate analytical approach. The initial state is represented by a red circle.

Stability analysis - Yet another analytical design

To track the multi-step walking reference trajectory by Acrobot using the yet another analytical design described in Section 5.6, the feedback gain $K = [-16, -32, -24, -8]$

is used together with the "amplifying" parameter $\Theta = 15$. The corresponding matrix A^z has the following form

$$A^z = \begin{bmatrix} 0.0358 & -0.0042 & 0.0027 & -0.0002 \\ 0.3112 & -0.0395 & 0.0265 & -0.0020 \\ 1.8303 & -0.1626 & 0.0755 & -0.0055 \\ 24.9280 & -2.2151 & 1.0107 & -0.0733 \end{bmatrix}$$

and its eigenvalues are as follows

$$\text{eig}(A^z) = [-0.0126,\ 0.0092,\ 0.0001,\ 0.0017]\,.$$

One can see that the Poincaré test of stability is fulfilled, therefore, Acrobot walking controlled using the yet another analytical design approach is stable.

Figures 7.5a, b show phase-plane plots of variables q_1 and q_2. The convergence towards a periodic motion is clearly seen from simulations of approximately 150 steps.

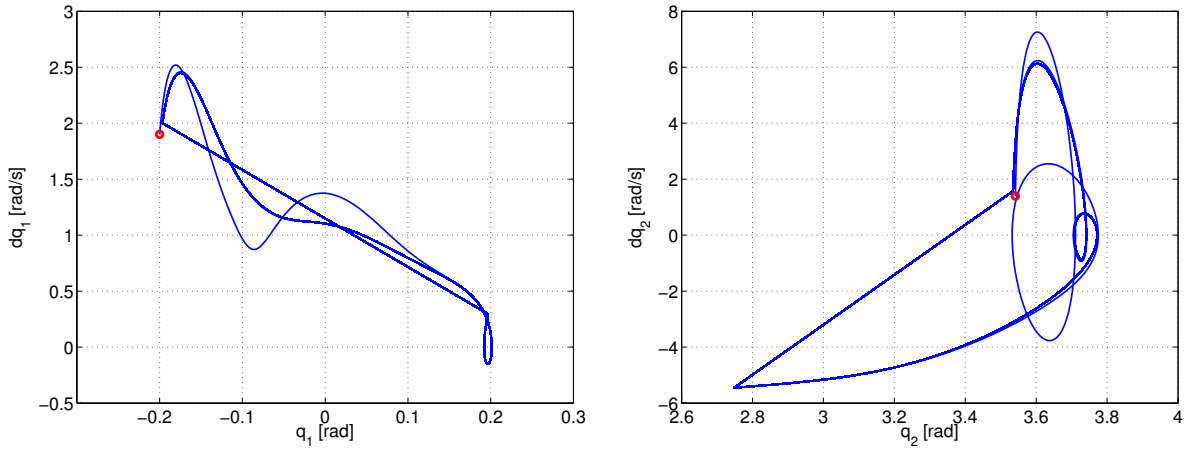

(a) (b)

Figure 7.5. Phase-plane plots for (a) q_1, (b) q_2. Acrobot walking is controlled using the yet another analytical approach. The initial state is represented by a red circle.

7.3 Chapter conclusion

The chapter deals with the stability analysis of Acrobot walking controlled by techniques presented in Chapter 5. The walking includes time-continuous phase, impact detection and re-initialization rules. Therefore, the stability analysis was done using the method of Poincaré sections. In the case of the extended analytical approach which allows to

transform the Acrobot error dynamics into a linear form, the stability test was performed using a fundamental matrix of the transformed error dynamics.

Chapter 8

Conclusions and outlooks

8.1 Summary

This thesis was devoted to the study of the novel methods of underactuated walking robot control using nonlinear control methods in order to improve the existing approaches. Some new theoretical properties of underactuated walking robot control were developed. These methods depend crucially on partial feedback linearization techniques. In particular, new feedback controllers, state observers and reference trajectories were developed based on the partial linear form of Acrobot as the representative of a class of underactuated walking robots. More specifically, few state feedback controllers were developed based on either a robust approach or on the more or less deeper knowledge of the reference Acrobot model. Two observers to estimate any state of Acrobot based on particular knowledge of angular positions and velocities were developed. The newly developed multi-step reference trajectory keep a relation between angular velocities at the end and at the beginning of the step via the impact model and, therefore, the multi-step reference trajectory minimizes initial errors at the beginning of the new step. The main contributions of the thesis are the novel techniques ensuring a movement of Acrobot in a way resembling a human walk. In contrast to another control methods based on a numerical approach, the novel tracking techniques use the feedback controller to track the carefully designed reference trajectory. By virtue of this, Acrobot can make practically unlimited number of steps. Moreover, these methods are simpler when extended to more complicated walking structures. Finally, the so-called embedding method was suggested to extend Acrobot results to more general planar walking models.

8.2 Future research outlooks

Besides the numerical simulation, verification of theoretical concepts will be done on an existing simple laboratory model of 4-link mechanical system with four actuators, imitating legs with a hip and knees without a body or even a torso. A description of that real laboratory model can be found in [13].

The future research related to real mechanical models of the underactuated walking robots will be also devoted to another aspects of observers for their precision and dependence on output noise measurements. Probably a sensor fusion problem will be necessary to solve. Furthermore, the impact model and its accuracy is connected with measurement of model states. Actually, these two problems are closely related as it is an important issue how to estimate the time of the impact, which heavily depends on accuracy of the measurements and the estimation precision of state variables as well as the accuracy of the impact model.

Fulfillment of Stated Goals and Objectives

Structured according to their formulations on page xi, the goals and objectives fulfillment can be summarized as follows:

1. This goal was achieved in Chapter 2. The basic approaches of obtaining mathematical models of walking robots were repeated there and they were used to find mathematical models of the swing phase and the double phase of Acrobot and 4-link.

2. This goal was obtained in Section 4.2.1 and in Chapters 5 and 6. Namely, in Section 4.2.1 a new reference trajectory taking into the account the impact effect to minimize initial errors during tracking was developed. In Chapter 5 new state feedback controllers to track a given reference trajectory based on partially linear form of Acrobot were obtained to improve the existing tracking approaches. Finally, two observers for Acrobot were developed in Chapter 6 to observe the unmeasured states of Acrobot.

3. This goal was fulfilled in Chapter 7, where the stability of the newly developed tracking algorithms was proved. It was shown there that Acrobot can make a priori unlimited number of steps by virtue of tracking of the new reference trajectory using the newly developed feedback controllers.

4. This goal was achieved in Sections 3.2, 4.1.2, 4.2.2. Namely, the partial feedback linearization of 4-link was obtained in Sections 3.2 where the so-called embedding method was introduced. Based on that, two reference trajectories for 4-link and their tracking were developed in Sections 4.1.2, 4.2.2. and 5.7. Finally, the high gain observer for 4-link is obtained using the mentioned embedding method in Section 6.1.3.

Bibliography

[1] M.C. Aclan and M.C. Ramos. Bipedal robot locomotion using multivariable control. In *Proceedings of the IEEE Region 10 Conference (TENCON'09)*, pages 1–6, Jan 2009.

[2] Ja. Alvarez-Gallegos, Jq. Alvarez-Gallegos, and H.G. Gonzalez-Hernandez. Analysis of the dynamics of an underactuated robot: the forced Pendubot. In *Proceedings of the 36th IEEE Conference on Decision and Control*, volume 2, pages 1494–1499, Dec 1997.

[3] M. Anderle and S. Čelikovský. Analytical design of the acrobot exponential tracking with application to its walking. In *Proceedings of the IEEE International Conference on Control and Automation*, pages 163–168, 2009.

[4] M. Anderle and S. Čelikovský. Position feedback tracking of the acrobot walking-like trajectory based on the reduced velocity observer. In *Preprints of the 8th IFAC Symposium on Nonlinear Control Systems*, pages 1011–1016, Bologna, Italy, 2010. IFAC.

[5] M. Anderle and S. Čelikovský. Position feedback tracking of the acrobot walking-like trajectory based on the reduced velocity observer. In *Proceedings of the 9th International Conference on Process Control*, Kouty nad Desnou, Czech Republic, 2010.

[6] M. Anderle and S. Čelikovský. Sustainable acrobot walking based on the swing phase exponentially stable tracking. In *Proceedings of the ASME 2010 Dynamic Systems and Control Conference*, Cambridge, Massachusetts, USA, 2010. ASME.

[7] M. Anderle and S. Čelikovský. Feedback design for the acrobot walking-like trajectory tracking and computational test of its exponential stability. In *Proceedings of the IEEE Multi-Conference on Systems and Control*, pages 1026–1031, Denver, Colorado, 2011.

[8] M. Anderle and S. Čelikovský. Stability analysis of the acrobot walking with observed geometry. In *Preprints of the 18th World Congress IFAC*, Milan, Italy, 2011.

[9] M. Anderle and S. Čelikovský. Approximate feedback linearization of the acrobot tracking error dynamics with application to its walking-like trajectory tracking. In *Proceedings of the 20th Mediterranean Conference on Control & Automation*, pages 1007–1012, Barcelona, ES, July 2012.

[10] M. Anderle and S. Čelikovský. Acrobot stable walking in hybrid systems notation. In *Proceedings of the 16th International Conference on Computer Modelling and Simulation, UKSim-AMSS*, pages 199–204, Cambridge, GB, March 2014.

[11] M. Anderle and S. Čelikovský. Cyclic walking-like trajectory design and tracking in mechanical chain with impacts. In *Proceedings of the XXIth Congreso ACCA*, pages 341–346, Santiago de Chile, CL, November 2014.

[12] M. Anderle and S. Čelikovský. High gain observer for embedded Acrobot. In *Preprints of the 19th World Congress IFAC*, pages 2818–2823, Cape Town, South Africa, August 2014.

[13] M. Anderle, S. Čelikovský, and K. Dolinský. Simple model of underactuated walking robot. In *Proceedings of the 10th Asian Control Conference*, pages 341–346, Kota Kinabalu, Malaysia, May 2015.

[14] M. Anderle, S. Čelikovský, D. Henrion, and J. Zikmund. LMI based design for the acrobot walking. In *Preprints of the 9th IFAC Symposium on Robot Control*, pages 595–600, Gifu, Japan, 2009.

[15] M. Anderle, S. Čelikovský, D. Henrion, and J. Zikmund. Advanced LMI based analysis and design for acrobot walking. *International Journal of Control*, 83(8):1641–1652, 2010.

[16] Aristotle. *The complete works of Aristotle: the revised Oxford translation*. Princeton University Press, 41 William Street, Princeton, New Jersey, USA, 08540-5237, 1984.

[17] O. Begovich, Edgar N. Sanchez, and M. Maldonado. Takagi-sugeno fuzzy scheme for real-time trajectory tracking of an underactuated robot. *IEEE Transactions on Control Systems Technology*, 10(1):14–20, Jan 2002.

[18] M.D. Berkemeier and R.S. Fearing. Tracking fast inverted trajectories of the underactuated acrobot. *IEEE Transactions on Robotics and Automation*, 15(4):740–750, Aug 1999.

[19] K. Berns. The walking machine catalogue, jun 2007.

[20] G. Bornard and H. Hammouri. A high gain observer for a class of uniformly observable systems. In *Proceedings of the 30th IEEE Conference on Decision and Control*, pages 1494–1496 vol.2, Dec 1991.

[21] S.A. Bortoff and M.W. Spong. Pseudolinearization of the acrobot using spline functions. In *Proceedings of the 31st IEEE Conference on Decision and Control*, pages 593–598 vol.1, 1992.

[22] T. Boukhobza and J.-P. Barbot. High order sliding modes observer. In *Proceedings of the 37th IEEE Conference on Decision and Control*, volume 2, pages 1912–1917 vol.2, Dec 1998.

[23] R.M. Brach. Rigid body collisions. *Transaction of the ASME, Journal of Applied Mechanics*, 56:133–138, 1989.

[24] B. Brogliato. *Nonsmooth Mechanics: Models, Dynamics and Control*. London: Springer Verlag, 1996.

[25] M. Buhler and D.E. Koditschek. Analysis of a simplified hopping robot. In *Proceedings of the IEEE International Conference on Robotics and Automation*, pages 817–819 vol.2, Apr 1988.

[26] M. Buhler, D.E. Koditschek, and Peter J. Kindlmann. A family of robot control strategies for intermittent dynamical environments. *IEEE Control Systems Magazine*, 10(2):16–22, Feb 1990.

[27] L. Cambrini, C. Chevallereau, C.H. Moog, and R. Stojic. Stable trajectory tracking for biped robots. In *Proceedings of the 39th IEEE Conference on Decision and Control*, 2000.

[28] S. Čelikovský, M. Anderle, and C. Moog. Embedding the acrobot into a general underactuated n-link with application to novel walking design. In *Proceedings of the Europen Control Conference*, pages 682–689, Zurich, Switzerland, 2013.

[29] S. Čelikovský and J. Zikmund. Composite control of the n-link chained mechanical system. In *Proceedings of the 16th International Conference on Process Control*, volume 130, pages 1–6, Strbské Pleso, Slovakia, 2007.

[30] S. Čelikovský, J. Zikmund, and C. Moog. Partial exact linearization design for the acrobot walking. In *Proceedings of the American Control Conference*, pages 874–879, Seattle, USA, 2008.

[31] N. Chaillet, G. Abba, and E. Ostertag. Double dynamic modelling and computed-torque control of a biped robot. In *Proceedings of the IEEE/RSJ/GI International Conference on Intelligent Robots and Systems, 'Advanced Robotic Systems and the Real World'*, volume 2, pages 1149–1155, Sep 1994.

[32] C. Chevallereau and Y. Aoustin. Optimal reference trajectories for walking and running of a biped robot. *Robotica*, 19:557–569, 9 2001.

[33] C. Chevallereau, A. Formal'sky, and B. Perrin. Control of a walking robot with feet following a reference trajectory derived from ballistic motion. In *Proceedings of the IEEE International Conference on Robotics and Automation*, volume 2, pages 1094–1099, Apr 1997.

[34] Ch. Chevallereau, G. Bessonnet, G. Abba, and Y. Aoustin. *Bipedal Robots: Modeling, Design and Walking Synthesis*. Wiley-ISTE, 2009.

[35] S.H. Collins, M. Wisse, and A. Ruina. A three-dimensional passive-dynamic walking robot with two legs and knees. *The International Journal of Robotics Research*, 20(7):607–615, 2001.

[36] Honda Corporation. Asimo's homepage, 2007.

[37] M.A. Diftler, J.S. Mehling, M.E. Abdallah, N.A. Radford, L.B. Bridgwater, A.M. Sanders, R.S. Askew, D.M. Linn, J.D. Yamokoski, F.A. Permenter, B.K. Hargrave, R. Piatt, R.T. Savely, and R.O. Ambrose. Robonaut 2 - the first humanoid robot in space. In *Proceedings of the IEEE International Conference on Robotics and Automation (ICRA'11)*, pages 2178 –2183, may 2011.

[38] D. Djoudi, C. Chevallereau, and Y. Aoustin. Optimal reference motions for walking of a biped robot. In *Proceedings of the IEEE International Conference on Robotics and Automation*, pages 2002–2007, April 2005.

[39] I. Fantoni and R. Lozano. *Non-linear control of underactuated mechanical systems*. Heidelberg: Springer Verlag, 2002.

[40] I. Fantoni, R. Lozano, and M.W. Spong. Passivity based control of the pendubot. In *Proceedings of the American Control Conference*, volume 1, pages 268–272, 1999.

[41] Charles FranĂ§ois and Claude Samson. A new approach to the control of the planar one-legged hopper. *The International Journal of Robotics Research*, 17(11):1150–1166, 1998.

[42] J. Furusho and M. Masubuchi. Control of a dynamical biped locomotion system for steady walking. *Journal of Dynamic Systems, Measurement, and Control*, 108(2):111–118, 1986.

[43] K. Furuta, M. Yamakita, and S. Kobayashi. Swing up control of inverted pendulum. In *Proceedings of International Conference on Industrial Electronics, Control and Instrumentation*, pages 2193–2198 vol.3, Oct 1991.

[44] M. Garcia, A. Chatterjee, and Ruina A. Efficiency, speed, and scaling of two-dimensional passive-dynamic walking. *Dynamics and Stability of Systems*, 15(2):75–99, 2000.

[45] M. Garcia, A. Chatterjee, and A. Ruina. Speed, efficiency, and stability of small-slope 2d passive dynamic bipedal walking. In *Proceedings of the IEEE International Conference on Robotics and Automation*, volume 3, pages 2351–2356, May 1998.

[46] J.P. Gauthier, H. Hammouri, and S. Othman. A simple observer for nonlinear systems applications to bioreactors. *IEEE Transactions on Automatic Control*, 37(6):875–880, Jun 1992.

[47] A. Goswami, B. Espiau, and A. Keramane. Limit cycles and their stability in a passive bipedal gait. In *Proceedings of the IEEE International Conference on Robotics and Automation*, pages 246–251 vol.1, Minneapolis, MN, USA, 1996.

[48] W. Greiner. *Classical mechanics: system of particles and hamiltonian dynamics*. Berlin: Springer Verlag, 2003.

[49] J.W. Grizzle, G. Abba, and F. Plestan. Asymptotically stable walking for biped robots: analysis via systems with impulse effects. *IEEE Transactions on Automatic Control*, 46(1):51–64, Jan 2001.

[50] J.W. Grizzle, J. Hurst, B. Morris, Hae-Won Park, and K. Sreenath. Mabel, a new robotic bipedal walker and runner. In *Proceedings of the American Control Conference*, pages 2030–2036, june 2009.

[51] J.W. Grizzle, C.H. Moog, and C. Chevallereau. Nonlinear control of mechanical systems with an unactuated cyclic variable. *IEEE Transactions on Automatic Control*, 50(5):559–576, may 2005.

[52] M. Hardt, K. Kreutz-Delgado, and J.W. Helton. Optimal biped walking with a complete dynamical model. In *Proceedings of the 38th IEEE Conference on Decision and Control*, volume 3, pages 2999–3004, 1999.

[53] S. Hashimoto et al. Humanoid robots in waseda university—hadaly-2 and wabian. *Auton. Robots*, 12(1):25–38, 2002.

[54] H. Hemami and B.F. Wyman. Modeling and control of constrained dynamic systems with application to biped locomotion in the frontal plane. *IEEE Transactions on Automatic Control*, 24(4):526–535, Aug 1979.

[55] K. Hirai, M. Hirose, Y. Haikawa, and T. Takenaka. The development of honda humanoid robot. In *Proceedings of the IEEE International Conference on Robotics and Automation*, volume 2, pages 1321–1326, may 1998.

[56] Y. Hurmuzlu and D.B. Marghitu. Rigid Body Collisions of Planar Kinematic Chains With Multiple Contact Points. *The International Journal of Robotics Research*, 13(1):82–92, 1994.

[57] Yildirim Hurmuzlu. Dynamics of bipedal gait part i: Objective functions and the contact event of a planar five-link biped. *Journal of Applied Mechanics*, 60:331–336, 1998.

[58] Yildirim Hurmuzlu. Dynamics of bipedal gait part ii: Stability analysis of a planar five-link biped. *Journal of Applied Mechanics*, 60:343, 1998.

[59] A. Isidori. *Nonlinear Control Systems*. New York: Springer Verlag, 1996.

[60] S. Kajita and K. Tani. Experimental study of biped dynamic walking in the linear inverted pendulum mode. In *Proceedings of the IEEE International Conference on Robotics and Automation*, volume 3, pages 2885–2891, May 1995.

[61] S. Kajita and K. Tani. Experimental study of biped dynamic walking. *IEEE Control Systems Magazine*, 16(1):13–19, feb 1996.

[62] S. Kajita, T. Yamaura, and A. Kobayashi. Dynamic walking control of a biped robot along a potential energy conserving orbit. *IEEE Transactions on Robotics and Automation*, 8(4):431–438, aug 1992.

[63] R.E. Kalman. A new approach to linear filtering and prediction problem. *Journal Of Basic Engineering, ASME Transactions, Ser. D*, 82:35–45, 1960.

[64] R.E. Kalman and R.S. Bucy. New results in linear filtering and prediction theory. *Journal Of Basic Engineering, ASME Transactions, Ser. D*, 83:95–108, 1961.

[65] K. Kaneko, F. Kanehiro, M. Morisawa, K. Akachi, G. Miyamori, A. Hayashi, and N. Kanehira. Humanoid robot HRP-4 - humanoid robotics platform with

lightweight and slim body. In *Proceedings of the IEEE/RSJ International Conference on Intelligent Robots and Systems (IROS'11)*, pages 4400–4407, Sept 2011.

[66] R. Katoh and M. Mori. Control method of biped locomotion giving asymptotic stability of trajectory. *Automatica*, 20(4):405–414, 1984.

[67] J.B. Keller. Impact with friction. *Transaction of the ASME, Journal of Applied Mechanics*, 53:1–4, 1986.

[68] H. K. Khalil. *Nonlinear Systems*. Prentice Hall, 2001.

[69] A.J. Krener. Approximate linearization by state feedback and coordinate change. *Systems and Control Letters*, 5(3):181–185, 1984.

[70] V.R. Kumar and K.J. Waldron. *A review of research on walking vehicles*. MIT Press, Cambridge, Mass, 1989.

[71] A.D. Kuo. Stabilization of lateral motion in passive dynamic walking. *The International Journal of Robotics Research*, 18(9):917–930, 1999.

[72] V. Lebastard, Y. Aoustin, and F. Plestan. Observer-based control of a biped robot. In *Proceedings of the Fourth International Workshop on Robot Motion and Control*, pages 67–72, June 2004.

[73] V. Lebastard, Y. Aoustin, and F. Plestan. Step-by-step sliding mode observer for control of a walking biped robot by using only actuated variables measurement. In *IEEE/RSJ International Conference on Intelligent Robots and Systems*, pages 559–564, Aug 2005.

[74] V. Lebastard, Y. Aoustin, and F. Plestan. Finite time observer for absolute orientation estimation of a five-link walking biped robot. In *Proceedings of the American Control Conference*, pages 2522–2527, June 2006.

[75] V. Lebastard, Y. Aoustin, and F. Plestan. Observer-based control of a walking biped robot without orientation measurement. *Robotica*, 24:385–400, May 2006.

[76] V. Lebastard, Y. Aoustin, F. Plestan, and L. Fridman. Absolute orientation estimation based on high order sliding mode observer for a five link walking biped robot. In *International Workshop on Variable Structure Systems*, pages 373–378, June 2006.

[77] R.A. Liston and R.S. Mosher. A versatile walking truck. In *Transportation Engineering Conference*, London, 1968. Institution of Civil Engineers.

[78] Yang Liu and Hongnian Yu. A survey of underactuated mechanical systems. *IET Control Theory Applications*, 7(7):921–935, May 2013.

[79] D.G. Luenberger. Observing the state of a linear system. *IEEE Transactions on Military Electronics*, 8(2):74–80, 1964.

[80] D.G. Luenberger. An introduction to observers. *IEEE Transactions on Automatic Control*, 16(6):596–602, 1971.

[81] D. Maalouf, C. Moog, Y. Aoustin, and S. Li. Maximum feedback linearization with internal stability of 2-dof underactuated mechanical systems. In *Proceedings of the 18th IFAC World Congress*, pages 8132–8137, Milan, Italy, 2012.

[82] N. Manamani, N.N. Gauthier, and N.K. M'Sirdi. Sliding mode control for a pneumatic robot leg. In *Proceedings of the European Control Conference*, pages 2743–2748, July 1997.

[83] R. Marino and P. Tomei. *Nonlinear control design: Geometric, Adaptive and Robust*. Prentice Hall, New York, 1995.

[84] T.G. McGee and M.W. Spong. Trajectory planning and control of a novel walking biped. In *Proceedings of the IEEE International Conference on Control Applications*, pages 1099–1104, 2001.

[85] T. McGeer. Passive dynamic walking. *The International Journal of Robotics Research*, 9(2):62–82, 1990.

[86] T. McGeer. Passive walking with knees. In *Proceedings of the IEEE International Conference on Robotics and Automation*, pages 1640–1645 vol.3, Cincinnati, OH , USA, 1990.

[87] P. Micheau, M. A. Roux, and P. Bourassa. Self-tuned trajectory control of a biped walking robot. In *Proceedings of the International Conference on Climbing and Walking Robot CLAWAR*, pages 527–534, 2003.

[88] E.A. Misawa and J.K. Hedrick. Nonlinear observers - a state-of-the-art survey. *Journal of Dynamic systems Measurement and Control, Transactions of the ASME*, 111(3):344 – 352, Sept 1989.

[89] R.M. Murray and J. Hauser. A case study in approximate linearization: the acrobot example. In *Proceedings of the American Control Conference*, pages 874–879, San Diego, USA, 1990.

[90] J. Nakanishi, T. Fukuda, and D.E. Koditschek. Preliminary studies of a second generation brachiation robot controller. In *Proceedings of the IEEE International Conference on Robotics and Automation*, volume 3, pages 2050–2056 vol.3, Apr 1997.

[91] J. Nakanishi, T. Fukuda, and D.E. Koditschek. A brachiating robot controller. *IEEE Transactions on Robotics and Automation*, 16(2):109–123, Apr 2000.

[92] M. Nikkhah, H. Ashrafiuon, and F. Fahimi. Robust control of underactuated bipeds using sliding modes. *Robotica*, 25:367–374, May 2007.

[93] Kenzo Nonami, RanjitKumar Barai, Addie Irawan, and MohdRazali Daud. Historical and modern perspective of walking robots. In *Hydraulically Actuated Hexapod Robots*, volume 66 of *Intelligent Systems, Control and Automation: Science and Engineering*, pages 19–40.

[94] Y. Ogura, H. Aikawa, K. Shimomura, A. Morishima, Hun ok Lim, and A. Takanishi. Development of a new humanoid robot wabian-2. In *Proceedings of the IEEE International Conference on Robotics and Automation*, pages 76–81, May 2006.

[95] R. Olfati-Saber. *Nonlinear Control of underactuated mechanical systems with application to robotics and aerospace vehicles.* PhD thesis, Massachusetts Institute of Technology, 2001.

[96] R. Olfati-Saber. Normal forms for underactuated mechanical systems with symmetry. *IEEE Transactions on Automatic Control*, 47(2):305–308, Feb 2002.

[97] K. Ono, R. Takahashi, A. Imadu, and T. Shimada. Self-excitation control for biped walking mechanism. In *Proceedings of the IEEE/RSJ International Conference on Intelligent Robots and Systems*, volume 2, pages 1143–1148, 2000.

[98] K. Ono, K. Yamamoto, and A. Imadu. Control of giant swing motion of a two-link underactuated horizontal bar robot. In *Proceedings of the IEEE/RSJ International Conference on Intelligent Robots and Systems*, volume 3, pages 1676–1683 vol.3, 2000.

[99] J.H. Park and K.D. Kim. Biped robot walking using gravity-compensated inverted pendulum mode and computed torque control. In *Proceedings of the IEEE International Conference on Robotics and Automation*, volume 4, pages 3528–3533, May 1998.

[100] J. Pratt and G. Pratt. Intuitive control of a planar bipedal walking robot. In *Proceedings of the IEEE International Conference on Robotics and Automation*, volume 3, pages 2014–2021, May 1998.

[101] J.E. Pratt, M.C. Chew, A. Torres, P. Dilworth, and G.A. Pratt. Virtual Model Control: An Intuitive Approach for Bipedal Locomotion. *The International Journal of Robotics Research*, 20(2):129–143, 2001.

[102] M. Raibert, S. Tzafestas, and C. Tzafestas. Comparative simulation study of three control techniques applied to a biped robot. In *Proceedings of the International Conference on Systems, Man and Cybernetics, 'Systems Engineering in the Service of Humans'*, pages 494–502 vol.1, Oct 1993.

[103] Marc H. Raibert. *Legged Robots That Balance*. Massachusetts Institute of Technology, Cambridge, MA, USA, 1986.

[104] M. Reyhanoglu, A. van der Schaft, N.H. McClamroch, and I. Kolmanovsky. Dynamics and control of a class of underactuated mechanical systems. *IEEE Transactions on Automatic Control*, 44(9):1663–1671, Sep 1999.

[105] M.E. Rosheim. *Robot Evolution: The Development of Anthrobotics*. Wiley-Interscience, November 1994.

[106] L.A. Rygg. Draft of the first quadruped walking machine: The mechanical horse, February 1893.

[107] F. Saito, T. Fukuda, and F. Arai. Swing and locomotion control for two-link brachiation robot. In *Proceedings of the IEEE International Conference on Robotics and Automation*, pages 719–724 vol.2, May 1993.

[108] F. Saito, T. Fukuda, and F. Arai. Swing and locomotion control for a two-link brachiation robot. *IEEE Control Systems*, 14(1):5–12, Feb 1994.

[109] A. Sano and J. Furusho. Realization of natural dynamic walking using the angular momentum information. In *Proceedings of the IEEE International Conference on Robotics and Automation*, pages 1476–1481 vol.3, Cincinnaty, OH, May 1990.

[110] U. Saranli, W.J. Schwind, and D.E. Koditschek.

[111] Manuel F. Silva and J.A. Tenreiro Machado. A historical perspective of legged robots. *Journal of Vibration and Control*, 13(9-10):1447–1486, 2007.

[112] S. Song and K.J. Waldron. *Machines That Walk: The Adaptive Suspension Vehicle*. The MIT Press; First edition, Cambridge, Mass, 1988.

[113] M. W. Spong, S. Hutchinson, and M. Vidyasagar. *Robot Modeling and Control*. John Wiley & Sons, Inc., 2005.

[114] M. W. Spong and M. Vidyasagar. *Robot Dynamics and Control*. John Wiley & Sons, Inc., 1989.

[115] Mark Spong. Underactuated mechanical systems. In Bruno Siciliano and Kimon Valavanis, editors, *Control Problems in Robotics and Automation*, volume 230 of *Lecture Notes in Control and Information Sciences*, pages 135–150. Springer Berlin / Heidelberg, 1998. 10.1007/BFb0015081.

[116] M.W. Spong. The control of underactuated mechanical systems. Plenary Lecture, *The First International Conference on Mechatronics*, Mexico City, 1994.

[117] M.W. Spong. Partial feedback linearization of underactuated mechanical systems. In *Proceedings of the IEEE/RSJ/GI International Conference on Intelligent Robots and Systems '94. 'Advanced Robotic Systems and the Real World'*, volume 1, pages 314–321, 1994.

[118] M.W. Spong. Swing up control of the acrobot. In *Proceedings of the IEEE International Conference on Robotics and Automation*, pages 2356–2361 vol.3, May 1994.

[119] M.W. Spong. The swing up control problem for the acrobot. *IEEE Control Systems*, 15(1):49–55, Feb 1995.

[120] M.W. Spong. Energy based control of a class of underactuated mechanical systems. In *IFAC World Congress*, pages 431–435, July 1996.

[121] M.W. Spong and D.J. Block. The pendubot: a mechatronic system for control research and education. In *Proceedings of the 34th IEEE Conference on Decision and Control*, volume 1, pages 555–556, Dec 1995.

[122] M.W. Spong, J.K. Holm, and Dongjun Lee. Passivity-based control of bipedal locomotion. *IEEE Robotics Automation Magazine*, 14(2):30–40, June 2007.

[123] R. Stojic and C. Chevallereau. On the stability of biped with point foot-ground contact. In *Proceedings of the IEEE International Conference on Robotics and Automation*, volume 4, pages 3340–3345, 2000.

[124] B. Thuilot, A. Goswami, and B. Espiau. Bifurcation and chaos in a simple passive bipedal gait. In *Proceedings of the IEEE International Conference o Robotics and Automation*, volume 1, pages 792–798, Apr 1997.

[125] D.J. Todd. *Walking Machines: An Introduction to Legged Robots*. Chapman & Hall, August 1985.

[126] R.Q. Van Der Linde. Active leg compliance for passive walking. In *Proceedings of the IEEE International Conference on Robotics and Automation*, volume 3, pages 2339–2344, May 1998.

[127] M. Vukobratovic, B. Borovac, D. Surla, and D. Stokic. *Biped Locomotion: Dynamics, Stability, Control and Application*. Springer-Verlag, Berlin, April 1990.

[128] Miomir Vukobratovic and Davor Juricic. Contribution to the synthesis of biped gait. *IEEE Transactions on Biomedical Engineering*, BME-16(1):1–6, Jan 1969.

[129] Ting Wang and Christine Chevallereau. Stability analysis and time-varying walking control for an under-actuated planar biped robot. *Robotics and Autonomous Systems*, 59(6):444 – 456, 2011.

[130] E.R. Westervelt, J.W. Grizzle, C. Chevallereau, J.H. Choi, and B. Morris. *Feedback Control of Dynamic Bipedal Robot Locomotion*. CRC Press, Berlin, June 2007.

[131] E.R. Westervelt, J.W. Grizzle, and D.E. Koditschek. Hybrid zero dynamics of planar biped walkers. *IEEE Transactions on Automatic Control*, 48(1):42–56, Jan 2003.

[132] M. Wiklund, A. Kristenson, and K.J. Åström. A new strategy for swinging up an inverted pendulum. In *Preprints of the IFAC World Congress*, pages 191–196, Sydney, Australia, 1993.

[133] J. Zikmund. *Analyse et commande des systèmes mécaniques sous-actionnés aves application aux robots à pattes*. PhD thesis, Thèse de Doctorat en Cotutelle, L École Centrale do Nantes et l Universitè de Nantes, N° ED 366-356, 2008.

[134] J. Zikmund. Composite control of the n-link chained mechanical systems. *Kybernetika*, 44(5):664–684, 2008.

[135] J. Zikmund and C.H. Moog. The structure of 2-body mechanical systems. In *Proceedings of the IEEE Conference on Decision and Control*, pages 6464–6469, San Diego, USA, 2006.

[136] J. Zikmund, S. Čelikovský, and C.H. Moog. Nonlinear control design for the acrobot. In *Preprints of the 3rd IFAC Symposium on Systems Structure Control*, Foz do Iguassu, Brazil, 2007.

Curriculum Vitae

Milan Anderle was born in České Budějovice, Czechoslovakia, in 1984. He received his Ing. degree (equivalent to M.Sc.) in study program cybernetics and measurement at Faculty of Electrical Engineering, Czech Technical University in Prague in 2008. During finishing his master thesis, from November 2007 to August 2008, he was employed in the Centre for Applied Cybernetics, CTU. He defended his master thesis focused on electronic circuit design for precise position measurement using capacitance sensors. He started his Ph.D. study at the same university in September 2008. The topic of his research is "Modelling and Control of Walking Robots". His research interests include nonlinear control systems, mathematical modelling, numerical simulations and applications of input shapers for control of multibody systems. Since 2009 he has been employed in the Institute of Information Theory and Automation of the Czech Academy of Sciences. He was member of research teams of the projects: "New concepts in the theory of signals shapers with time delay" supported by the Czech Science Foundation during 2013-2015 and "Advanced methods for complex systems analysis and control" supported by the Czech Science Foundation during 2012-2014.

Research results of Milan Anderle were presented at several international conferences, e.g. IFAC World Congress (IFAC 2011, IFAC 2014), IFAC Symposiums (SYROCO 2009, NOLCOS 2010), IEEE conference (MSC 2011) or European Control Conferences (ECC 2013, ECC 2014). In addition, his results were published in the impacted journal *International Journal of Control*.

List of Author's Publications

Publications related to the thesis

Publications in Journals with impact factor

M. Anderle, S. Čelikovský, D. Henrion, J. Zikmund. Advanced LMI based analysis and design for Acrobot walking. *International Journal of Control. 2010, vol. 83, no. 8, p. 1641-1652. ISSN 0020-7179.* (IF = 0.848)
Contribution: M. Anderle - 25%, S. Čelikovský - 25%, D. Henrion - 25%, J. Zikmund - 25%
Cited by:

> X. Xin, T. Yamasaki. Energy-Based Swing-Up Control for a Remotely Driven Acrobot: Theoretical and Experimental Results. *IEEE Transactions on Control Systems Technology. 2012, vol. 20, no. 4, p. 1048-1056.*

Publications indexed in Web of Science

S. Čelikovský, M. Anderle and C. H. Moog. Embedding the generalized Acrobot into the n-link with an unactuated cyclic variable and its application to walking design. *Proceedings of the European Control Conference 2013 (ECC)*, Zurich, CH, July 2013.
Contribution: 33%

M. Anderle, S. Čelikovský and H. Ibarra. Virtual constraints for the underactuated walking design: comparison of two approaches. *Proceedings of the 9th Asian Control Conference 2013 (ASCC)*, Istanbul, TR, June 2013.
Contribution: 34%

M. Anderle and S. Čelikovský. Sustainable Acrobot Walking Based on the Swing Phase Exponentially Stable Tracking. *Proceedings of the ASME 2010 Dynamic Systems and Control Conference*, Cambridge, MA, September 2010.
Contribution: 50%

M. Anderle and S. Čelikovský. Analytical design of the Acrobot exponential tracking with application to its walking. *Proceedings of the 7th IEEE International Conference on Control and Automation*, Christchurch, New Zealand, December 2009.
Contribution: 50%
Cited by:

> T. Wang, C. Chevallereau. Stability analysis and time-varying walking control for an under-actuated planar biped robot. *Robotics and autonomous systems. 2011, vol. 59, no. 6, p. 444-456.*
>
> AC. Zhang, JH. She, XZ. Lai, M. Wu. Motion planning and tracking control for an Acrobot based on a rewinding approach. *Automatica. 2013, vol. 49, no. 1, p. 278-284.*

Other publications

M. Anderle and S. Čelikovský and K. Dolinský. Simple model of underactuated walking robot. *Proceedings of the 10th Asian Control Conference (ASCC)*, Kota Kinabalu, Sabah, MY, May 2015.
Contribution: 34%

M. Anderle, S. Čelikovský. Cyclic walking-like trajectory design and tracking in mechanical chain with impacts. *Proceedings of the XXIst Congreso de la Asociación Chilena de Control Automático (ACCA)*, Santiago de Chile, CL, November 2014.
Contribution: 50%

M. Anderle and S. Čelikovský. High gain observer for embedded Acrobot. *Preprints of the 19th World Congress IFAC*, Cape Town, South Africa, August 2014.
Contribution: 50%

M. Anderle and S. Čelikovský. Acrobot stable walking in Hybrid systems notation. *Proceedings of the 16th International Conference on Computer Modelling and Simulation (UKSim-AMSS)*, Cambridge, GB, March 2014.
Contribution: 50%

M. Anderle and S. Čelikovský. Approximate feedback linearization of the Acrobot tracking error dynamics with application to its walking-like trajectory tracking. *Proceedings of the 20th Mediterranean Conference on Control & Automation (MED)*, Barcelona, ES, July 2012.
Contribution: 50%

M. Anderle and S. Čelikovský. Feedback design for the Acrobot walking-like trajectory tracking and computational test of its exponential stability. *Proceedings of the IEEE International Symposium on Computer-Aided Control System Design (CACSD)*, Denver Colorado, US, September 2011.
Contribution: 50%

M. Anderle and S. Čelikovský. Stability analysis of the Acrobot walking with observed geometry. *Preprints of the 18th IFAC World Congress*, Milano, Italy, September 2011.
Contribution: 50%

M. Anderle and S. Čelikovský. Position feedback tracking of the Acrobot walking-like trajectory based on the reduced velocity observer. *Preprints of the 8th IFAC Symposium on Nonlinear Control Systems*, Bologna, Italy, August 2010.
Contribution: 50%

M. Anderle and S. Čelikovský. Comparison of nonlinear observers for underactuated mechanical systems. *Proceedings of the 9th International Conference Process Control*, Kouty nad Desnou, Czech Republic, June 2010.
Contribution: 50%

M. Anderle, S. Čelikovský, D. Henrion, J. Zikmund. LMI based design for the Acrobot walking. *Preprints of the 9th IFAC Symposium on Robot Control*, Gifu, Japan, September 2009.
Contribution: 25%

M. Anderle and S. Čelikovský. Analytical and LMI based design for the Acrobot tracking with application to robot walking. *Proceedings of the 10th International PhD Workshop on Systems and Control*, Hluboká nad Vltavou, Czech Republic, September 2009.
Contribution: 50%

M. Anderle and S. Čelikovský. Nonlinear techniques for the Acrobot tracking with application to robot walking. *4emes Journées Nationales de la Robotique Humanoide*, Nantes, France, May 2009.
Contribution: 50%

Publications unrelated to the thesis

Publications indexed in Web of Science

T. Vyhlídal, M. Hromčík, V. Kučera and M. Anderle. Double Oscillatory Mode Compensation by Inverse Signal Shaper with Distributed Delays. *Proceedings of the European Control Conference 2014 (ECC)*, Strasbourg, France, June 2014.
Contribution: 25%

T. Vyhlídal, M. Hromčík, V. Kučera and M. Anderle. Zero vibration derivative shaper with distributed delay for both feed-forward and feedback interconnections. *Proceedings of the 6th International Symposium on Communications, Control and Signal Processing (ISCCSP)*, Athens, Greece, May 2014.
Contribution: 25%

Other publications

M. Anderle, P. Augusta, B. Rehák. Simulace regulace systémů s rozloženými parametry v simulinku. *Preprints of the Technical Computing Prague 2008*, Praha, Czech Republic, November 2008.
Contribution: 34%

M. Anderle, P. Augusta, O. Holub. Simulace systémů s rozprostřenými parametry v simulinku. *Preprints of the Technical Computing Prague 2007*, Praha, Czech Republic, November 2007.
Contribution: 34%